NASA TECHNICAL NOTE

NASA TN D-5620

c. 1

NASA TN D-5620

PRELIMINARY SURVEYS OF THE WALL BOUNDARY LAYER IN A MACH 6 AXISYMMETRIC TUNNEL

by Robert A. Jones and William V. Feller

Langley Research Center

Langley Station, Hampton, Va.

NATIONAL AERONAUTICS AND SPACE ADMINISTRATION • WASHINGTON, D. C. • FEBRUARY 1970

1. Report No. NASA TN D-5620	2. Government Accession No.	3. Recipient's Catalog No.
4. Title and Subtitle PRELIMINARY SURVEYS OF THE WALL BOUNDARY LAYER IN A MACH 6 AXISYMMETRIC TUNNEL		5. Report Date February 1970
		6. Performing Organization Code
7. Author(s) Robert A. Jones and William V. Feller		8. Performing Organization Report No. L-6697
		10. Work Unit No. 129-01-20-07-23
9. Performing Organization Name and Address NASA Langley Research Center Hampton, Va. 23365		11. Contract or Grant No.
		13. Type of Report and Period Covered Technical Note
12. Sponsoring Agency Name and Address National Aeronautics and Space Administration Washington, D.C. 20546		14. Sponsoring Agency Code
15. Supplementary Notes		

16. Abstract

Total-temperature and total-pressure distributions were measured in the boundary layer on the wall of a straight pipe test section at four different locations up to about 100 boundary-layer thicknesses downstream of the nozzle exit. The free-stream Mach number was approximately 6, the ratio of wall temperature to total temperature was about 0.68, and the momentum-thickness Reynolds number varied from 8×10^3 to 80×10^3. Values of the local pitot pressure, Mach number, velocity, and temperature in the boundary layer are tabulated along with the integral properties of the boundary layer. Low-frequency temperature and pressure fluctuations were observed in the wall boundary layer, and corresponding temperature fluctuations were found near the wall of the stagnation chamber.

17. Key Words Suggested by Author(s) Turbulent boundary layer; Temperature and pressure survey		18. Distribution Statement Unclassified – Unlimited	
19. Security Classif. (of this report) Unclassified	20. Security Classif. (of this page) Unclassified	21. No. of Pages 70	22. Price* $3.00

*For sale by the Clearinghouse for Federal Scientific and Technical Information
Springfield, Virginia 22151

PRELIMINARY SURVEYS OF THE WALL BOUNDARY LAYER IN A MACH 6 AXISYMMETRIC TUNNEL

By Robert A. Jones and William V. Feller
Langley Research Center

SUMMARY

Total-temperature and total-pressure distributions were measured in the boundary layer on the wall of a straight pipe test section at four different locations up to about 100 boundary-layer thicknesses downstream of the nozzle exit. The free-stream Mach number was approximately 6, the ratio of wall temperature to total temperature was about 0.68, and the momentum-thickness Reynolds number varied from 8×10^3 to 80×10^3. Values of the local pitot pressure, Mach number, velocity, and temperature in the boundary layer are tabulated along with the integral properties of the boundary layer. Low-frequency temperature and pressure fluctuations were observed in the wall boundary layer, and corresponding temperature fluctuations were found near the wall of the stagnation chamber.

INTRODUCTION

It has occasionally been assumed that if the local pressure gradient is zero or very small at the measuring station, then the characteristics of a tunnel-wall boundary layer will correspond to those on a flat plate at some equivalent-length Reynolds number. Recently, however, there have been some indications that this correspondence is not realized. (See refs. 1 to 4.) The available flat-plate data generally scatter around a linear relation between total temperature and velocity whereas this relation for tunnel-wall data is usually more nearly quadratic than linear. (See ref. 4.) A critical examination of the differences between flat-plate and tunnel-wall boundary layers is needed to identify the sources of these differences. At the present time there is a scarcity of detailed data for turbulent boundary layers for hypersonic speeds and large ranges of flow length and unit Reynolds numbers. Most of the available tunnel-wall data were obtained at positions very near the nozzle exit with little variation in downstream distance and little definition of possible effects of upstream pressure gradient and stagnation-chamber flow conditions.

The Mach 6 high Reynolds number tunnel at the Langley Research Center was designed to allow detailed investigations of the tunnel-wall boundary layer. The tunnel is provided with a gradually expanding nozzle 2.44 meters long followed by a 4-meter-long straight pipe section of 30.5-cm diameter. At the design operating conditions, boundary-layer data can be obtained at equivalent-length Reynolds numbers from 5×10^6 to 1.2×10^9. At the time of the present investigation, the construction of this facility was only partially completed. A temporary air heating and pipe system that allowed operation only at the lower end of the design Reynolds number range was used.

As a first step in a program of detailed studies of the turbulent wall boundary layer, a series of total-pressure and total-temperature surveys were made at four stations along the 4-meter straight pipe test section, and some measurements were also made in the stagnation chamber. The free-stream Mach number was approximately 6, the ratio of wall temperature to total temperature was about 0.68, and the effective-length Reynolds number varied from 14×10^6 to 240×10^6. The purpose of this paper is to present the results of this first step of the investigation which includes some temperature profiles in the stagnation chamber and estimates of possible downstream effects of nonuniformities in these profiles.

SYMBOLS

A_m	constant in equation (10)
C_f	skin-friction coefficient
M	Mach number
m	constant in equation (10)
n	exponent in power-law velocity relation, equation (1)
p	pressure
r	radius of test section
R	Reynolds number
T	temperature
T'	magnitude of temperature fluctuation

$\overline{T}$	temperature parameter, $\frac{T_{t,l} - T_w}{T_{t,e} - T_w}$
u	velocity
x	length from nozzle throat
y	distance measured normal to wall
γ	ratio of specific heats
δ	boundary-layer thickness based on pitot surveys
δ^*	displacement thickness
θ	momentum thickness
μ	viscosity
ρ	density

Subscripts:

e	edge of boundary layer
eq	equivalent conditions
l	local position
p	probe
sc	stagnation chamber
t	total conditions behind normal shock
x	based on x
w	wall
θ	based on momentum thickness

∞	free stream
$\mathcal{C}$	center line
2	behind normal shock

APPARATUS

Wind Tunnel

All data reported herein were obtained in the Mach 6 high Reynolds number tunnel at the Langley Research Center. This facility was designed to provide for studies of turbulent boundary layers over a large range of Reynolds numbers. The nozzle is axisymmetric and contoured with a maximum flow turning angle of only 0.105 radian to reduce the longitudinal pressure gradients. The 2.44-meter-long nozzle is followed by a 4-meter-long straight pipe section of 30.5-cm diameter. Although the facility was designed for operation at stagnation pressures up to 2200 N/cm^2, construction of the air piping and controls was not complete at the time of this study. Therefore, these data were taken by using a temporary air supply and air heating system. Consequently, stagnation conditions were limited to a maximum pressure of 483 N/cm^2 and a maximum temperature of about 500° K.

A photograph of the tunnel is presented in figure 1, and a sketch showing the stagnation-chamber arrangement and various measuring stations is given in figure 2. The stagnation chamber is of conventional design with a liner and a diffusing cone followed by four fine-mesh screens. Four access ports were located at station -30 (approximately 0.76 meter upstream of the nozzle minimum area, station zero) in the pressure vessel. These ports were used for fixed total-pressure and total-temperature probes as well as for making total-temperature surveys across the stagnation chamber.

The nozzle was designed by the method given in reference 5. A correction to the inviscid coordinates to account for the boundary-layer displacement thickness was used. This displacement thickness was based on stagnation conditions of 2070 N/cm^2 and 556° K. The design Mach numbers along the nozzle are given in table I.

The 4-meter-long straight pipe portion of the tunnel was made in four interchangeable sections with lengths of 0.457, 0.761, 1.22, and 1.525 meters. The 1.525-meter-long section incorporated the boundary-layer survey apparatus and could be positioned to allow surveys at intervals over the 4-meter length.

Boundary-Layer Survey Mechanism

A photograph of the section containing the boundary-layer survey apparatus is shown in figure 3. Access ports in this section can be used to locate the survey mechanism and boundary-layer probes at x-intervals of about 35 cm. The traversing mechanism was driven by a remotely controlled stepping-type motor. A digital readout system (reading to 2.5 μm) was used to record the rake position. The boundary-layer probes were mounted on a strut which extended across the test section so that measurements could be made on the opposite wall. Figure 4 shows the total-pressure rake on this strut mounted in the test section. The strut was electrically insulated from the tunnel so that a small battery-powered light could be used to indicate the position at which the probe made contact with the wall. By using this system and by allowing the probe strut to heat for about 1 minute before taking data to minimize thermal expansion errors, the y-position of the probes is believed to be known to an accuracy of 50 μm.

A sharp 0.32-cm-thick strut which held both a total-temperature probe and a pitot-pressure probe in the free stream 10 cm from the wall was located at the measuring station. (See fig. 4.) In addition, static-pressure orifices were located along the entire length of the nozzle and 4-meter pipe section.

Boundary-Layer Rakes

Two boundary-layer rakes were used: one to measure total pressure, the other to measure total temperature. Sketches of these two rakes are given in figures 5 and 6. The total-pressure rake is also shown in the photograph of figure 4. This total-pressure rake contained two probes about 2.41 cm apart. The probe nearer the wall (probe 1) was made from 0.508-mm-diameter tube flattened at the tip to have a height of 0.33 mm, and the other probe (probe 2) was made from 1.52-mm-diameter tube flattened to 0.46 mm at the tip. Both pressure probes were connected to pressure transducers by 46-cm lengths of steel tube with an inside diameter of 0.10 mm. These transducers had variable-capacitance-type sensing units with seven ranges from 1 mm mercury full scale to 1000 mm mercury full scale and were therefore capable of providing accurate measurements for a wide range of pressures. The output of the transducers was recorded on magnetic tape for all rake survey data.

The total-temperature rake also contained two probes about 2.05 cm apart. Details of the probe construction are shown in figure 6. These probes were made by welding together chromel-alumel wires (0.13-mm in diameter) to make a small loop at the end of a 1.57-mm-diameter swaged thermocouple wire. The thermocouple junction was then hammered flat to give a high ratio of surface area to cross-sectional area in order to reduce the effects of conduction along the wire. The 1.57-mm swaged wire was placed in a tube with an outside diameter of 3.15 mm and had four slots as shown in figure 6. Then a shield with an inside diameter of 3.15 mm was spotwelded to the 3.15-mm tube; slots were left open at the rear of the shield to make an aspirating probe. The entrance of the shield was flattened to reduce the sampling height. The ratio of exhaust area to entrance area was 0.15 for probe 1 and 0.17 for probe 2. Thermocouple outputs also were recorded on magnetic tape. The free-stream total-temperature probe was similar to the boundary-layer probes except that the entrance was not flattened.

Stagnation-Chamber Probes

Two total-temperature probes were used in the stagnation chamber. One was fixed at a position 0.64 cm from the center line of the chamber; the other was movable in the y-direction. Both probes were at station -30 (about 76 cm ahead of the throat of the nozzle). Both were "bare wire" thermocouples made from 0.076-mm-diameter chromel-alumel wire. The small thermocouple wire was butt-welded together and then welded across the ends of 0.76-mm-diameter thermocouple wires which protruded about 6.4 mm from the end of a 6.4-mm-diameter support tube. (See sketch.) The small thermocouple loop was always positioned transverse to the flow.

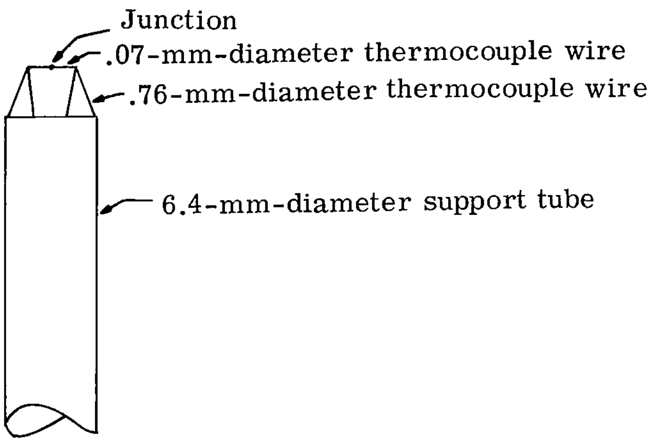

TEST TECHNIQUE

At the low stagnation pressures of these tests, the tunnel exhausted into a vacuum sphere. The vacuum capacity limited the running time to a maximum of 6 minutes. Pumping time between runs was approximately 30 minutes. With the temporary heater and pipe system used in these tests, there were about 61 meters of 15.2-cm high-pressure pipe between the heater and the tunnel. A bypass valve was located about 6 meters upstream of the stagnation chamber so that the system could be preheated to this point. Approximately 1 hour was required to preheat the system up to the bypass valve. Between runs the preheat flow was again turned on in order to keep this upstream part of the system hot. The last 6 meters of pipe from the bypass valve to the stagnation chamber and the stagnation chamber itself were preheated by making a run at maximum temperature and pressure at the start of each day. Between runs the last 6 meters of pipe and the stagnation chamber cooled somewhat. Heat loss to these cooler sections presumably would account for the observed increase in mean total temperature with time during each run.

No data were recorded during the first minute of a run to allow the stagnation temperature to level off and to allow the strut holding the probe to warm up in order to minimize its change in length due to thermal expansion during the run. After this 1-minute period the probe was moved to the wall as indicated by the contact circuit and light. The output of the probe nearest the wall and the output of the fixed probe (located in the free stream 10 cm from the wall) were monitored visually on a strip-chart recorder. When it was apparent that the probe output had reached its equilibrium value, data were recorded for an interval of about 2 seconds. These data were recorded on magnetic tape by means of an analog-to-digital conversion system at a rate of 20 points per second. The y-position was manually put into the digital system at each probe position. An average of the output value over the 2-second interval was used in reducing the data. The boundary-layer total temperatures and total pressures were always referenced to the measured free-stream values of the fixed probe located 10 cm from the wall in order to minimize any effects of varying free-stream pressure or temperature with running time. Temperature recovery factors were applied to both the fixed free-stream total-temperature probe and the boundary-layer total-temperature probes as discussed in more detail in a subsequent section.

RESULTS AND DISCUSSION

Free-Stream Conditions

The free-stream Mach number of the straight pipe test section as determined by pitot-pressure surveys made in the central core (20-cm in diameter) of the flow is shown in figure 7 for four stations and several stagnation pressures. These data are for positions well outside the boundary layer except for the lowest Reynolds number and the station farthest downstream. These calibrations were made at essentially the same stagnation temperature conditions as the boundary-layer surveys. The bars indicate the variation of Mach number across this 20-cm core. There is a gradual reduction in Mach number with increasing distance from the end of the nozzle. Presumably, this reduction results from a gradual compression of the flow caused by the increasing thickness of the boundary layer with distance. Measured wall static pressures along the straight pipe section are shown in figure 8. These data indicate a gradual reduction in Mach number (as can be seen by the Mach number scale on the right-hand side of the figure) with distance, similar to that shown by the free-stream pitot surveys. The pressure gradient along the wall (a parameter to be used later), as determined by measuring the slope of the straight line faired through the data for $p_{sc} = 79\ \text{N/cm}^2$ in figure 8, was

$$\frac{d\left(\frac{p_w}{p_{sc}}\right)}{dx} = 1.18 \times 10^{-8}\ \text{meter}^{-1}$$

Probe Temperature Recovery

The two total-temperature probes on the boundary-layer rake and the fixed free-stream total-temperature probe were calibrated in the free stream over a large range of Reynolds numbers. The temperature recovery factor $T_p/T_{t,sc}$ was taken as the ratio of the indicated probe temperature to the temperature of the thermocouple in the center of the stagnation chamber. Variations of this recovery ratio were indicated by the probes for different locations in the free stream, and very small variations occurred for the two boundary-layer probes at the same location. Some of these data are plotted against the Reynolds number behind the normal shock and based on probe height $(R_{p,2})$ in figure 9. The faired line in this figure was used in the data reduction of all total-temperature data. Data in tables II to V for values of $R_{p,2}$ less than 400 were obtained by extrapolation of this faired line beyond the data points as indicated in figure 9.

Boundary-Layer Pressure and Temperature Fluctuations

During the course of the investigation it was noticed on the visual monitor that for certain distances from the wall in the boundary layer, both the total temperature and the total pressure fluctuated at a rather low frequency. These fluctuations were observed over the entire length of the straight pipe section surveyed. They disappeared completely as the probe approached the tunnel wall or moved into the free stream outside the boundary layer. No fluctuations were observed in the wall static-pressure measurements. Careful tests were made which eliminated the possibility that these fluctuations were due to mechanical vibrations or to any upstream influence of unsteady flow conditions in the diffuser section.

To study these fluctuations more carefully, a boundary-layer rake having both a total-temperature probe and a total-pressure probe was used. This rake was made from the existing total-temperature rake by replacing probe 1 with a pitot tube. The two probes were about 2.0 cm apart with the total-pressure probe located nearer the wall. The outputs of these probes were recorded on a strip-chart recorder. A sample of the simultaneous traces of the probe outputs at station 172 is shown in figure 10 for stagnation conditions of 505° K and 355 N/cm^2. The total-pressure probe was located at $y = 1.3$ cm, and the total-temperature probe was located at $y = 3.3$ cm. In general, all the survey data showed fluctuations present in the boundary layer at frequencies of 1 to 20 hertz. As indicated in figure 10, the maximum temperature fluctuation was about 11° K or 2.5 percent, and the maximum pressure fluctuation was about 5 mm of mercury or 1.8 percent. Correlation between data from identical probes at this separation distance was good; however, correlation between the temperature and pressure fluctuations shown in figure 10 is poor. The parts of the boundary layer where these pressure fluctuations were observed are indicated qualitatively in figure 11 for the survey data taken at station 94. In general, the y-region where this phenomenon was observed grew larger with larger pressure levels. Data for the other survey stations were similar, that is, an apparent increase in the y-region with an increase in distance, as well as with an increase in pressure.

A qualitative check was made of the frequency range of these fluctuations by inserting a 0.076-mm-diameter hot wire into the boundary layer. The low frequencies were also observed in the hot-wire output. It is believed that the very low frequencies were not associated with any hypersonic turbulent boundary-layer phenomenon but were originating elsewhere.

Stagnation-Chamber Surveys

In an attempt to identify the source of the low-frequency temperature and pressure fluctuations observed in the test-section boundary layer, some preliminary surveys were made of the total-temperature distribution in the stagnation chamber. Detailed results from these surveys are presented because of possible effects on the development of the test-section tunnel-wall boundary layer. These possible effects are discussed in more detail subsequently. The surveys were made upstream of the converging section of the nozzle at station -30. (See fig. 2.) One thermocouple probe was held fixed near the center line ($y = 25.4$ cm) of the stagnation chamber for use as a reference while a second thermocouple probe was moved from the edge of the liner to the center line. The stagnation conditions were as follows: pressure, 355 N/cm^2; temperature, 505° K; velocity, 1.5 m/sec. The thin liner (fig. 2) was used to insulate the flow from the thick case of the pressure vessel. This liner was preheated before these tests by making a run at maximum temperature and pressure in the same manner as for all the other tests. The results of this survey are shown in figure 12. The total temperature T_t and the magnitude of the fluctuations in total temperature T_t' were both uniform from the center line ($y = 25.4$ cm) to a position 2.0 cm from the liner. In this region the time-averaged total temperature was 505° K, and the maximum fluctuations were 0.5 percent, or 2.2° K peak to peak. The frequency of these fluctuations was in the range of 1 to 20 hertz. However in the region very near the liner ($y < 2.0$ cm), a rather large decrease in mean temperature and large low-frequency fluctuations (also of about 1 to 20 hertz) were measured. The maximum amplitude of the fluctuations occurred about 0.63 cm from the edge of the liner and was 17 percent, or 77° K peak to peak in magnitude.

The thickness of a turbulent boundary layer on the liner at the survey station was estimated to be about 0.5 cm based on the conditions in the central part of the stagnation chamber and the length of the liner. A comparison of this small thickness with the thickness of the temperature deficient layer and the presence of the low-frequency fluctuations suggest that a large-scale mixing phenomenon between the "cold" outer portion of the turbulent pipe flow entering the stagnation chamber and its higher temperature core may be responsible for the nonuniform temperature distribution near the liner.

The stagnation chamber of this facility is typical of many hypersonic blowdown facilities; therefore, it is believed that other high Mach number tunnels may have similar stagnation-chamber flow conditions. Very few total-temperature distributions in stagnation chambers have been published for high Mach number tunnels. However, data for one other facility, the NOL Boundary Layer Channel, which was built especially for boundary-layer studies along the tunnel wall, exhibit a similar temperature deficiency near the wall of the stagnation chamber. (See ref. 6.)

An approximate mass-flow calculation, based on a uniform velocity of 1.5 m/sec (calculated velocity in the stagnation chamber) and the measured mean temperature profile, indicates that this temperature deficient layer in the stagnation chamber could influence approximately half of the test-section boundary layer at station 172, or 4.35 m downstream of the nozzle throat. Since turbulent mixing should not occur outside the dynamic or velocity boundary layer in the entrance section of the nozzle, it is believed that the nozzle boundary layer was growing in a layer of air with a lower total temperature than the central core of the flow. The boundary layer eventually swallows the entire layer of cold air and continues to grow in a uniform total-temperature stream, but a considerable downstream distance could be required for the boundary layer to recover to the temperature distribution appropriate to the core of the flow.

It is believed that the cold layer of air along the liner can be eliminated by heating the entire stagnation chamber, nozzle throat section, and upstream connecting pipe to a temperature equal to the desired total temperature. The Mach 6 high Reynolds number tunnel at the Langley Research Center is presently being equipped with electric strip heaters and insulation which should eliminate this cold layer.

Boundary-Layer Surveys

Total-pressure surveys.- Total-pressure surveys were made with the two-probe boundary-layer rake shown in figure 5. The pitot-pressure data for station 94 are shown in figure 11. Two tests were made for each pressure level, and in some cases more than two were made. Data for different runs are indicated by different symbols in the figure. Flagged symbols indicate data for the outer probe (probe 2) of the two on the rake. There are a considerable number of data points in the region where the y/r location of the two probes overlap. The local total pressure in the boundary layer is nondimensionalized by the measured free-stream total pressure of the fixed probe to eliminate any effect of small changes in pressure level with time. As mentioned previously, total-pressure fluctuations with a maximum magnitude of 2.5 percent were observed in the middle part of the boundary layer. These fluctuations are believed to account for part of the scatter in the data for this part of the boundary layer.

Small variations in total pressure with y/r were apparant at the edge of the boundary layer. In addition, the total pressure at the edge was not exactly equal to the free-stream total pressure measured with the fixed probe. Since these data were to be used in conjunction with the measured total-temperature distributions which were made subsequently and were not taken at the same y/r locations, the data were faired. The faired values were used for further calculations; examples are shown by the solid lines in figure 11. The edge of the boundary layer δ was taken to be the y/r location at which no further variation with y/r occurred for the faired lines. Values of δ determined in this manner are listed in table VI for all stations and pressure levels. For all data reduction, the level of the pressure $p_{t,\infty}$ was corrected to make the ratio $p_{t,l}/p_{t,\infty}$ equal to 1 at the edge of the boundary layer.

Mach number.- The Mach number at the edge of the boundary layer was determined from the ratio of the faired, measured pitot pressure to the simultaneous stagnation-chamber pressure. A plot of this edge Mach number with length along the test section is shown in figure 13 for all stations and four pressure levels. The edge Mach number generally decreases with both an increase in flow length or a decrease in pressure level. This value of edge Mach number was used to determine the free-stream static pressure p_∞ at each station and pressure level. By assuming that the static pressure remained constant across the boundary layer, the ratio $p_\infty/p_{t,l}$ was calculated for each y/r location at which total-temperature data were available. The local Mach number in the boundary layer was then calculated from the values of $p_\infty/p_{t,l}$. The local Mach numbers for station 94 are plotted against y/r in figure 14. Also, a complete tabulation of the boundary-layer survey data is given in tables II to V. In tables II to V the probe numbers indicate the inner probe (probe 1) or the outer probe (probe 2). The values of y/r listed are the positions for which total-temperature data were taken. The values of pressure were read from faired curves at corresponding y/r values.

Total-temperature surveys.- Boundary-layer total-temperature surveys were made with the two-probe rake shown in figure 6. At least one repeat run with total-temperature data taken all the way across the boundary layer was made for each survey at each station. Both the total temperature measured with the fixed probe in the free stream and the local boundary-layer total temperature were corrected with a temperature recovery factor. This correction was obtained by calculating the Reynolds number behind the shock based on the probe height $(R_{p,2})$ and with the local conditions determined by using the actual total pressure and the actual total temperature. With this value of $R_{p,2}$, the correction factor was then obtained from the curve of figure 9. In addition, the free-stream total temperature indicated with the fixed probe was adjusted so that $\frac{T_{t,l}}{T_{t,\infty}} = 1$ at the edge of the boundary layer. Plots of the temperature profiles for station 94 are given in figure 15.

Local velocity and other boundary-layer parameters.- The final total-temperature data obtained in the way previously described were not faired. Instead, all the required boundary-layer parameters, such as the local probe Reynolds number $R_{p,2}$, the local velocity ratio u_l/u_e, and the local temperature parameter $\overline{T} = \frac{T_{t,l} - T_w}{T_{t,e} - T_w}$, were computed for each corrected total-temperature data point with $p_\infty/p_{t,l}$. These parameters are listed in tables II to V. Since the surface temperatures at the survey stations were not measured directly, estimated values of T_w had to be used. These values were obtained from a measured initial temperature for the wall applicable at the survey station and a computed variation of surface temperature with time by using a heat-transfer coefficient from the theory of Spalding-Chi (refs. 3 and 7) based on the known R_θ values. The variation of T_w with time over a particular test was usually less than 22° K. The values used in the data reduction are listed for each y/r position in tables II to V.

The variation of the local velocity ratio u_l/u_e (calculated from the measured local pressure and temperature as indicated previously) with distance from the wall y/r is shown in figure 16 for station 94. The value of the reciprocal of the exponent in the power-law velocity relation n where

$$\frac{u_l}{u_e} = \left(\frac{y}{\delta}\right)^{1/n} \tag{1}$$

was determined by measuring the slope of the straight line faired through the data similar to figure 16. These values are listed in table VI and are plotted as a function of x in figure 17. These values of n appear to be in agreement with other data at this Mach number. (See refs. 3 and 4.)

Relation between total temperature and velocity.- Because of possible effects of upstream conditions on nozzle wall boundary layers, it is of interest to compare the present results in terms of the relation between $\overline{T}$ and u_l/u_e with corresponding flat-plate results. The available flat-plate data generally scatter around a linear Crocco relation between total temperature and velocity. (See ref. 4.) This linear flat-plate relation is shown by the straight line in figure 18, whereas the present data for station 94 are plotted as $\overline{T}$ against u_l/u_e. Also shown for comparison is the quadratic relation $\overline{T} = \left(\frac{u_l}{u_e}\right)^2$. The relation between total temperature and velocity for the tunnel-wall boundary layer appears to be more nearly quadratic than linear. It has occasionally been assumed that if the local pressure gradient is zero or very small at the measuring station, the characteristics of the tunnel-wall boundary layer will correspond to those on a flat plate at some equivalent-length Reynolds number. Obviously, in terms of the $\overline{\overline{T}}$ variation with u_l/u_e, the present tunnel-wall data do not correspond to those on a flat plate. These apparent differences in flat-plate and tunnel-wall boundary-layer profiles have been noted previously. (See refs. 1 to 4.) Very few of the previous tunnel-wall data have covered any range of flow length downstream of the nozzle exit. A change in temperature profile with downstream distance can be seen in figure 19 which compares the temperature-velocity profiles for the different stations at the highest Reynolds number. The profiles for stations farther downstream appear to be nearer the linear relation than the upstream profiles, particularly in the inner region of the boundary layer. The quadratic temperature-velocity relation is apparently typical of the outer position of tunnel-wall boundary layers (ref. 4) and presumably is caused by the upstream history of the flow, such as the pressure gradient in the nozzle. If this condition exists, the present data indicate that a very long flow length (about 60 boundary-layer thicknesses) is required for the temperature-velocity profile to begin to recover toward a flat-plate type.

The present investigation has revealed another mechanism which may account partly for this quadratic temperature-velocity relation in the nozzle wall boundary layer. This mechanism is the temperature deficiency found in the stagnation-chamber flow near the liner. This temperature deficiency is shown in figure 12 and was discussed previously. It is believed that the cold layer of air may have persisted downstream so that the boundary layer developed within a layer of air at a total temperature generally below that of the central core of the flow. The net effect would be to reduce the total temperatures within the boundary layer and presumably reduce $\overline{\overline{T}}$ below the level of that of a boundary layer developing in a uniform total-temperature flow.

Studies made at the Lewis Research Center (ref. 8) of the thermal and velocity boundary-layer behavior in the converging inlet section of a nozzle indicated that although both boundary layers initially had about the same thickness, the velocity boundary-layer thickness diminished appreciably as the throat was approached, whereas the thermal boundary-layer thickness did not. This result is another indication that in the region just downstream of the throat, the velocity boundary layer would develop within a relatively thick thermal boundary layer that would tend to have the same effect as the cold thermal layer found in the stagnation chamber of the present investigation. Since both types of phenomena may be typical of high Mach number facilities, further investigations of their possible effects on the downstream tunnel-wall boundary layer are required.

Integral and Other Related Parameters

Values of the integral parameters θ, δ^*, $R_{e,\theta}$, $R_{e,x}$, and $(R_{e,x})_{eq}$ are given in table VI for each station and pressure level. The axisymmetric values of the momentum thickness and displacement thickness were calculated by using the following two equations and the measured boundary-layer properties (ref. 9, p. 394):

$$\theta = \int_0^{\delta} \frac{\rho u}{\rho_e u_e}\left(1 - \frac{u}{u_e}\right)\left(1 - \frac{y}{r}\right)dy \tag{2}$$

$$\delta^* = \int_0^{\delta}\left(1 - \frac{\rho u}{\rho_e u_e}\right)\left(1 - \frac{y}{r}\right)dy \tag{3}$$

Skin friction.- Skin friction was not measured directly in these tests; therefore, in order to determine the skin friction and the magnitude of the effects of pressure gradient on it, the momentum thickness was used. The variation of θ with x is shown in figure 20, and the variation of $R_{e,\theta}$ with $R_{e,x}$ is shown in figure 21. The data of figure 21 for the highest pressures have not been faired since the actual value of pressure was somewhat different at each station, higher at the first station and lower at the last. This variation in pressure level for the highest pressures was the result of the pressure limit of the instrumentation used. The highest pitot pressure that could be measured was 1000 mm Hg, and since the Mach number decreased as x increased, the maximum stagnation pressure for which the free-stream pitot pressure was lower than 1000 mm Hg decreased with increasing x. The lines faired through these data for the three lower pressures are almost linear for the first three stations; however, they have considerable curvature between the last two stations. The second derivative is negative in this region for the higher pressure data, as would be expected. However, it is positive for the lower two pressures. It is believed that this behavior at the last station is associated with the larger increase in wall static pressure in this region which was measured for the lower pressure levels. (See fig. 8.) Additional surveys are needed for stations between 172 and 215.

By using the slope of the momentum thickness from figure 20 and the flat-plate momentum equation

$$C_f = 2\frac{d\theta}{dx} \tag{4}$$

the following values are determined for skin friction at station 94:

p_{sc}, N/cm^2	C_f
45	0.00082
79	.00070
217	.00095

Since for a flat plate

$$C_f = 2\,\frac{d\theta}{dx} = 2\,\frac{dR_{e,\theta}}{dR_{e,x}} \tag{5}$$

it should be interesting to compare the values of skin friction obtained from the slope of figure 21. Except for the most downstream station, these data fall very close to the faired straight line which has the slope

$$\frac{dR_{e,\theta}}{dR_{e,x}} = 0.00051$$

and which gives a value of skin-friction coefficient of 0.00102, which is higher than the values determined from equation (4). The accuracy of determining the slope of the momentum thickness is less than is desirable and is probably less than the accuracy of $dR_{e,\theta}/dR_{e,x}$, since $dR_{e,\theta}/dR_{e,x}$ correlates the data of the different pressure levels into one line. Nevertheless, the difference between the two skin-friction coefficients is not negligible. The parameter $dR_{e,\theta}/dR_{e,x}$ includes the change in local properties with distance such as ρ_e and μ_e, and although the pressure gradient is very small $\left(\frac{d}{dx}\left(\frac{p_w}{p_{t,\infty}}\right) = 1.2 \times 10^{-6}\ \text{cm}^{-1}\right.$ from fig. 8 for $\left.p_{sc} = 79\ \text{N/cm}^2\right)$, it should be interesting to evaluate the contribution of pressure gradient to the skin friction.

The complete momentum equation is (ref. 9)

$$\frac{d\theta}{dx} + \theta\left(\frac{\frac{\delta^*}{\theta} + 2}{u_e}\,\frac{du_e}{dx} + \frac{1}{\rho_e}\,\frac{d\rho_e}{dx} + \frac{1}{r}\,\frac{dr}{dx}\right) = \frac{C_f}{2} \tag{6}$$

In terms of the wall pressure gradient (by assuming isentropic flow at the edge of the boundary layer) equation (6) becomes $(dr/dx = 0)$:

$$\frac{d\theta}{dx} + \theta\,\frac{d}{dx}\,\frac{p_w}{p_{t,\infty}}\left[\frac{p_{t,\infty}}{\gamma p_e} - \left(\frac{\delta^*}{\theta} + 2\right)\frac{p_{t,\infty}}{\rho_e u_e^2}\right] = \frac{C_f}{2} \tag{7}$$

Comparing the two terms on the left-hand side of equation (7) by using the experimental data for station 94 and $p_{sc} = 79\ \text{N/cm}^2$ (fig. 20) shows that $\frac{d\theta}{dx} = 0.00034$, and the pressure term is 0.000112 by using the gradient $\frac{d}{dx}\left(\frac{p_w}{p_{t,\infty}}\right) = 1.2 \times 10^{-6}\ \text{cm}^{-1}$ from figure 8. This comparison indicates that the contribution of the wall pressure gradient to C_f is 33 percent of the $d\theta/dx$ term. As a check on this value, equation (7) can be written in terms of the local Mach number gradient at the edge of the boundary layer as

$$\frac{d\theta}{dx} - \theta\,\frac{\gamma M_e\,\frac{dM_e}{dx}}{\left(1 + \frac{\gamma - 1}{2}\,M_e^2\right)^{\frac{2\gamma - 1}{\gamma - 1}}}\left[\frac{p_{t,\infty}}{\gamma p_w} - \left(\frac{\delta^*}{\theta} + 2\right)\frac{p_{t,\infty}}{\rho_e u_e^2}\right] = \frac{C_f}{2} \tag{8}$$

and the second term of this equation can be evaluated by using the data of figure 13, which are based on the measured pitot pressure at the edge of the boundary layer and are thus independently measured values from the wall static pressures. For the same conditions (station 94 and $p_{sc} = 79\ N/cm^2$), dM_e/dx is $-0.0011\ cm^{-1}$, and the contribution to C_f is 0.000110, which is in excellent agreement with the values derived by using the method based on measured wall pressures. From the data of figures 8 and 13, it is apparent that the contribution of the pressure or Mach number gradient for the other pressure levels is also about 30 percent. Therefore, the values of C_f as determined from the complete momentum equations, which are 0.00904 for equation (7) and 0.0090 for equation (8), and a pressure level of $p_{sc} = 79\ N/cm^2$ indicate that even though the pressure gradient is very small at the exit of a nozzle, its effect on tunnel-wall skin friction should not be neglected.

Velocity profile.- The variation of n with $R_{e,\theta}$ is shown in figure 22. In this plot the data for a particular x location are indicated by one type of symbol so that the increase in $R_{e,\theta}$ for a particular symbol is due entirely to an increase in pressure level. In general, there is a trend for n to increase with $R_{e,\theta}$, as has been shown for other data (refs. 3 and 4); however, there is also the trend for n to decrease with an increase in x for a given pressure level. This trend may possibly be due to the boundary-layer profiles trying to adjust to or recover from the upstream pressure-gradient effects.

Equivalent flat-plate Reynolds number.- Although the present data are for conditions where a very weak adverse pressure gradient existed and may have been affected by the upstream history of the flow in the nozzle, it is desirable to consider what the Reynolds number of a fully developed turbulent boundary layer on a flat plate having the same external flow conditions would be in order to give some indication of the magnitude of the Reynolds numbers involved for these tests. Therefore, an equivalent flat-plate Reynolds number $(R_{e,x})_{eq}$ is defined as the value for turbulent flow on a flat plate which, if exposed to the same free-stream conditions, would have the same momentum thickness as the experimentally determined values. The equivalent flat-plate Reynolds number was evaluated by solving the following two relationships for turbulent compressible skin friction on a flat plate:

$$\frac{C_f}{2} = \frac{d\theta}{dx} = \frac{dR_{e,\theta}}{dR_{e,x}} \tag{9}$$

$$\frac{C_f^*}{2} = \frac{C_f}{2}\frac{\rho_e}{\rho^*} = A_m\left(R_{e,\theta}^*\right)^{-1/m} = A_m\left(\frac{u^*}{u_e}\right)^{1/m}\left(R_{e,\theta}\right)^{-1/m} \tag{10}$$

where the asterisk denotes values based on reference temperature conditions T^* taken from reference 10:

$$\frac{T^*}{T_e} = 1 + 0.035M_e^2 + 0.45\left(\frac{T_w}{T_e} - 1\right) \tag{11}$$

and A_m and m are constants taken to be 0.013 and 4, respectively. The solution of equations (9) and (10) for $R_{e,x} = 0$ at $R_{e,\theta} = 0$ is:

$$\left(R_{e,x}\right)_{eq} = \frac{m}{A_m(m + 1)} \frac{\rho_e}{\rho^*}\left(\frac{u_e}{u^*}\right)^{1/m} \left(R_{e,\theta}\right)^{\frac{m+1}{m}} \tag{12}$$

The equivalent flat-plate Reynolds numbers determined in this manner are listed in table VI. For the range of pressures and various lengths from the nozzle throat, these values varied from 14.4×10^6 to 240.1×10^6.

CONCLUSIONS

Measured total-temperature and total-pressure distributions were taken in the boundary layer on the test-section wall at four different locations from the nozzle exit to 4 meters downstream. The free-stream Mach number was approximately 6, the wall-to-total temperature ratio was about 0.68, and the momentum-thickness Reynolds number was varied from 8×10^3 to 80×10^3. The significant results of this study are as follows:

1. For all survey locations and all test conditions, very low-frequency fluctuations (2 to 20 hertz) in both total temperature and total pressure were observed in the tunnel-wall boundary layer. The amplitude of these fluctuations was a maximum of about 2.5 percent in temperature and 1.8 percent in pressure. They disappeared completely as the probe approached very near the wall or moved out into the free stream.

2. Total-temperature surveys across the stagnation chamber upstream on the converging section of the nozzle showed a thin layer of air (about 2-cm thick in a 50.8-cm-diameter section) along the wall which contained relatively large temperature fluctuations at frequencies in the same range as for those in the test section. The amplitude of these fluctuations was a maximum of about 17 percent of the total temperature. In addition to the low-frequency fluctuations, it was found that the average temperature in this layer along the wall was much less than the temperature of the main core of the flow.

3. The relations between total temperature and velocity obtained from the measured boundary-layer profiles were compared with the linear Crocco relation. As is typical of most tunnel-wall boundary-layer data, the present data exhibited a more nearly quadratic-type relation than a linear one. In this respect, the tunnel-wall data did not

correspond to those for a flat plate. However, for data at the position farthest downstream, the relation between total temperature and velocity appeared to be closer to the linear variation than for the upstream stations. Hence, it might be postulated that the quadratic temperature-velocity relation was caused by the upstream history of the flow, such as the pressure gradient in the nozzle. It is considered possible, however, that at least part of the deviation of the temperature-velocity profile from the flat-plate type of relation could have been caused by the cool layer of gas along the wall ahead of the nozzle.

4. Values of momentum thickness were determined from the measured profiles at each station, and the rate of change of momentum thickness with distance was found. The values of skin-friction coefficient were then determined from the complete momentum equation. Although the pressure gradient along the tunnel was very small, the contribution of the pressure-gradient term was approximately 30 percent of the total skin friction.

Langley Research Center,
National Aeronautics and Space Administration,
Langley Station, Hampton, Va., November 6, 1969.

REFERENCES

1. Seiff, Alvin; and Short, Barbara J.: An Investigation of Supersonic Turbulent Boundary Layers on Slender Bodies of Revolution in Free Flight by Use of the Mach-Zender Interferometer and Shadowgraphs. NACA TN 4364, 1958.

2. Rotta, J. C.: Heat Transfer and Temperature Distribution in Turbulent Boundary Layers at Supersonic and Hypersonic Flow. AGARDograph 97, pt. 1, May 1965, pp. 35-63.

3. Bertram, Mitchel H.; and Neal, Luther, Jr.: Recent Experiments in Hypersonic Turbulent Boundary Layers. Presented at the AGARD Specialists' Meeting on Recent Developments in Boundary-Layer Research (Naples, Italy), May 10-14, 1965.

4. Bushnell, Dennis M.; Johnson, Charles B.; Harvey, William D.; and Feller, William V.: Comparison of Prediction Methods and Studies of Relaxation in Hypersonic Turbulent Nozzle-Wall Boundary Layers. NASA TN D-5433, 1969.

5. Johnson, Charles B.; Boney, Lillian R.; Ellison, James C.; and Erickson, Wayne, D.: Real-Gas Effects on Hypersonic Nozzle Contours With a Method of Calculation. NASA TN D-1622, 1963.

6. Lee, R. E.; Yanta, W. J.; Leonas, A. C.; and Carner, J. W.: The NOL Boundary Layer Channel. NOLTR 66-185, ASTIA no. AD 646 748, U.S. Navy, Nov. 7, 1966.

7. Spalding, D. B.; and Chi, S. W.: The Drag of a Compressible Turbulent Boundary Layer on a Smooth Flat Plate With and Without Heat Transfer. J. Fluid Mech., vol. 18, pt. 1, Jan. 1964, pp. 117-143.

8. Boldman, Donald R.; Schmidt, James F.; and Gallagher, Anne K.: Laminarization of a Turbulent Boundary Layer as Observed From Heat-Transfer and Boundary-Layer Measurements in Conical Nozzles. NASA TN D-4788, 1968.

9. Howarth, L., ed.: Modern Developments in Fluid Dynamics – High Speed Flow. Vol. I. Clarendon Press (Oxford), 1953.

10. Sommer, Simon C.; and Short, Barbara J.: Free-Flight Measurements of Turbulent-Boundary-Layer Skin Friction in the Presence of Severe Aerodynamic Heating at Mach Numbers From 2.8 to 7.0. NACA TN 3391, 1955.

TABLE I.- DESIGN MACH NUMBER IN NOZZLE

Station	x, cm	M_e
0	0	1.00
2	5.1	1.22
4	10.2	1.44
6	15.2	1.66
8	20.0	1.87
10	25.4	2.08
15	38.1	2.65
23	58.4	3.54
31	78.8	4.29
37	93.9	4.70
50	127.0	5.32
56	142.1	5.54
76	192.9	5.89
89	226.0	5.99

TABLE II.- BOUNDARY-LAYER SURVEY DATA AT STATION 94

(a) p_{sc} = 45 N/cm^2; M_e = 5.866

y/r	M_l	$p_\infty/p_{t,2}$	T_w, °K	$T_{t,e}$, °K	u_l/u_e	$T_{t,l}/T_{t,e}$	$\frac{T_{t,l} - T_w}{T_{t,e} - T_w}$	$R_{p,2}$
Probe 1								
0.004	1.05	0.5004	336.3	455.5	0.4146	0.836	0.375	82
.007	1.30	.3671	336.6	457.6	.4972	.851	.437	100
.014	1.95	.1853	336.9	459.1	.6582	.875	.530	156
.024	2.26	.1420	337.1	459.1	.7160	.887	.575	187
.039	2.53	.1147	337.2	461.7	.7561	.889	.589	219
.072	2.96	.0850	337.5	462.8	.8142	.909	.663	271
.121	3.53	.0607	337.7	463.8	.8713	.929	.740	348
.193	4.37	.0398	337.9	464.9	.9349	.963	.863	483
.262	5.29	.0274	338.1	465.4	.9758	.980	.927	662
.333	5.83	.0226	338.3	465.4	.9872	.976	.913	794
.004	1.05	.5004	327.7	442.5	.4129	.829	.342	86
.008	1.54	.2799	328.2	445.1	.5598	.850	.427	125
.017	2.06	.1682	328.6	447.7	.6783	.876	.533	172
.033	2.43	.1237	328.8	448.7	.7407	.885	.568	215
.054	2.74	.0986	329.0	450.3	.7844	.895	.610	253
.087	3.13	.0763	329.3	451.3	.8314	.911	.672	303
.159	3.95	.0485	329.5	452.9	.9054	.945	.796	426
.217	4.71	.0344	329.7	453.4	.9522	.970	.891	562
.289	5.56	.0248	329.9	454.4	.9833	.981	.929	746
.348	5.86	.0224	330.1	455.0	.9889	.978	.921	820
.391	5.87	.0223	330.4	456.0	.9905	.981	.931	818
Probe 2								
0.135	3.69	0.0557	186.8	455.5	0.8858	0.937	0.894	632
.138	3.72	.0547	187.0	457.6	.8900	.942	.901	634
.145	3.81	.0523	187.2	459.1	.8965	.944	.906	655
.155	3.92	.0493	187.3	459.1	.9065	.951	.917	683
.170	4.09	.0455	187.3	461.7	.9167	.953	.921	727
.203	4.50	.0376	187.5	462.8	.9423	.966	.944	845
.252	5.17	.0287	187.6	463.8	.9723	.980	.966	1063
.325	5.80	.0229	187.7	464.9	.9966	.996	.994	1278
.393	5.87	.0223	187.8	465.4	1.0023	1.005	1.008	1292
.464	5.87	.0223	187.9	465.4	1.0017	1.003	1.006	1294
.135	3.69	.0557	182.0	442.5	.8865	.939	.896	653
.139	3.74	.0542	182.3	445.1	.8913	.942	.902	661
.148	3.84	.0515	182.5	447.7	.8988	.945	.907	684
.164	4.02	.0470	182.7	448.7	.9123	.952	.919	732
.185	4.27	.0418	182.8	450.3	.9282	.959	.930	802
.218	4.71	.0344	182.9	451.3	.9519	.969	.948	942
.290	5.57	.0248	183.1	452.9	.9867	.987	.978	1239
.348	5.86	.0224	183.2	453.4	.9996	1.000	.999	1336
.420	5.87	.0223	183.3	454.4	1.0030	1.006	1.010	1326
.479	5.87	.0223	183.4	455.0	1.0024	1.005	1.008	1326
.522	5.87	.0223	183.6	456.0	1.0051	1.010	1.017	1315

TABLE II.- BOUNDARY-LAYER SURVEY DATA AT STATION 94 – Continued

(b) p_{sc} = 79 N/cm^2; M_e = 5.871

y/r	M_l	$p_\infty/p_{t,2}$	T_w, °K	$T_{t,e}$, °K	u_l/u_e	$T_{t,l}/T_{t,e}$	$\frac{T_{t,l} - T_w}{T_{t,e} - T_w}$	$R_{p,2}$
Probe 1								
0.004	1.10	0.4703	338.1	456.4	0.4288	0.827	0.334	149
.008	1.76	.2234	338.8	458.5	.6114	.855	.444	243
.013	2.05	.1699	339.2	460.1	.6755	.874	.520	287
.019	2.21	.1476	339.8	460.6	.7060	.881	.545	316
.024	2.31	.1355	340.2	461.1	.7239	.885	.561	335
.029	2.42	.1248	340.3	462.7	.7395	.886	.568	356
.041	2.63	.1064	340.6	462.7	.7732	.899	.618	396
.081	3.20	.0734	340.9	463.8	.8434	.925	.718	521
.104	3.52	.0609	341.2	464.3	.8740	.936	.760	600
.139	3.99	.0478	341.4	464.8	.9100	.951	.814	727
.173	4.45	.0385	341.7	465.8	.9380	.962	.859	866
.191	4.72	.0344	342.8	465.8	.9525	.970	.888	951
.004	1.10	.4703	329.3	441.3	.4298	.831	.335	155
.008	1.68	.2409	330.1	443.9	.5936	.851	.418	240
.023	2.29	.1388	330.4	445.5	.7167	.878	.528	346
.036	2.55	.1131	331.1	448.1	.7589	.890	.580	397
.049	2.75	.0978	331.4	449.7	.7886	.902	.627	438
.057	2.87	.0900	331.8	450.7	.8063	.911	.664	462
.092	3.35	.0672	332.1	452.3	.8577	.929	.734	575
.125	3.80	.0525	332.4	453.3	.8955	.943	.785	697
.171	4.42	.0390	332.7	454.4	.9340	.957	.838	889
.207	4.95	.0313	333.0	454.9	.9606	.971	.890	1066
.242	5.35	.0268	333.3	455.4	.9760	.977	.915	1216
.275	5.66	.0239	333.5	456.4	.9875	.984	.942	1332
.344	5.86	.0224	333.8	457.5	.9895	.980	.925	1420
Probe 2								
0.135	3.93	0.0490	187.8	456.4	0.9027	0.941	0.900	1223
.139	4.00	.0475	188.2	458.5	.9069	.943	.903	1247
.144	4.06	.0461	188.5	460.1	.9115	.946	.908	1273
.150	4.14	.0443	188.8	460.6	.9172	.949	.913	1309
.155	4.21	.0430	189.0	461.1	.9220	.952	.919	1336
.160	4.27	.0417	189.1	462.7	.9241	.950	.915	1373
.172	4.45	.0386	189.2	462.7	.9359	.958	.930	1454
.212	5.02	.0304	189.4	463.8	.9605	.966	.942	1780
.235	5.28	.0275	189.5	464.3	.9714	.972	.952	1937
.270	5.63	.0242	189.7	464.8	.9854	.982	.969	2143
.304	5.78	.0230	189.8	465.8	.9923	.989	.981	2225
.322	5.82	.0227	190.4	465.8	.9980	.998	.997	2231
.135	3.93	.0490	183.0	441.3	.9019	.940	.897	1275
.139	3.99	.0478	183.4	443.9	.9057	.942	.901	1292
.154	4.19	.0434	183.6	445.5	.9187	.947	.910	1391
.167	4.38	.0398	183.9	448.1	.9297	.952	.918	1483
.180	4.56	.0368	184.1	449.7	.9386	.955	.923	1577
.188	4.68	.0349	184.3	450.7	.9456	.959	.931	1639
.223	5.14	.0290	184.5	452.3	.9655	.968	.946	1912
.256	5.50	.0254	184.7	453.3	.9787	.975	.958	2131
.302	5.77	.0230	184.8	454.4	.9903	.985	.974	2297
.338	5.85	.0225	185.0	454.9	.9968	.995	.991	2322
.373	5.87	.0223	185.2	455.4	.9966	.993	.989	2335
.406	5.87	.0223	185.3	456.4	.9998	1.000	1.000	2312
.475	5.87	.0223	185.4	457.5	1.0000	1.000	1.000	2307

TABLE II.- BOUNDARY-LAYER SURVEY DATA AT STATION 94 – Continued

(c) p_{sc} = 217 N/cm^2; M_e = 5.953

y/r	M_l	$p_\infty/p_{t,2}$	T_w, °K	$T_{t,e}$, °K	u_l/u_e	$T_{t,l}/T_{t,e}$	$\frac{T_{t,l} - T_w}{T_{t,e} - T_w}$	$R_{p,2}$
				Probe 1				
0.004	1.75	0.2259	333.5	480.1	0.5909	0.808	0.373	601
.005	1.93	.1883	334.8	482.7	.6359	.828	.438	664
.013	2.33	.1341	335.9	484.3	.7171	.867	.565	811
.045	3.07	.0791	336.8	486.2	.8246	.911	.711	1167
.112	4.10	.0451	337.8	487.6	.9101	.941	.809	1809
.177	5.05	.0300	338.9	488.9	.9574	.960	.871	2539
.244	5.85	.0224	339.9	490.0	.9896	.984	.946	3222
.278	5.95	.0217	340.7	491.0	.9968	.994	.980	3273
.349	5.95	.0217	341.6	492.2	.9934	.987	.957	3294
.415	5.95	.0217	342.4	492.6	.9998	1.000	.999	3241
.004	1.77	.2206	341.4	487.6	.5984	.816	.387	593
.009	2.18	.1518	342.6	489.7	.6898	.857	.524	737
.014	2.35	.1314	343.7	491.8	.7235	.873	.578	802
.019	2.50	.1169	344.4	493.4	.7479	.881	.606	867
.029	2.75	.0980	345.3	494.5	.7858	.899	.667	973
.037	2.93	.0869	346.2	496.1	.8117	.914	.716	1051
.072	3.51	.0613	347.2	496.6	.8708	.935	.783	1368
.105	4.00	.0474	347.9	497.7	.9047	.941	.805	1690
.125	4.30	.0412	348.5	498.2	.9235	.950	.832	1892
.154	4.73	.0341	349.2	499.3	.9449	.957	.857	2214
.173	5.00	.0306	349.9	499.8	.9601	.969	.897	2404
.205	5.44	.0259	350.5	499.8	.9757	.975	.917	2781
.278	5.95	.0217	351.2	500.9	.9959	.992	.973	3204
				Probe 2				
0.135	4.45	0.0386	185.3	480.1	0.9237	0.937	0.897	3545
.136	4.47	.0381	186.0	482.7	.9281	.943	.908	3534
.144	4.59	.0363	186.6	484.3	.9335	.945	.911	3673
.176	5.05	.0301	187.1	486.2	.9568	.960	.935	4279
.243	5.84	.0225	187.7	487.6	.9959	.996	.994	5392
.308	5.95	.0217	188.3	488.9	1.0008	1.002	1.003	5527
.375	5.95	.0217	188.9	490.0	1.0072	1.014	1.023	5431
.409	5.95	.0217	189.3	491.0	1.0095	1.019	1.031	5388
.480	5.95	.0217	189.8	492.2	1.0117	1.023	1.038	5346
.546	5.95	.0217	190.2	492.6	1.0181	1.036	1.059	5262
.135	4.45	.0385	189.7	487.6	.9279	.945	.910	3447
.140	4.53	.0372	190.3	489.7	.9304	.943	.907	3550
.145	4.60	.0361	190.9	491.8	.9351	.947	.914	3612
.150	4.68	.0350	191.4	493.4	.9377	.947	.913	3710
.160	4.81	.0330	191.9	494.5	.9442	.950	.918	3891
.168	4.94	.0314	192.3	496.1	.9555	.964	.941	3993
.203	5.42	.0261	192.9	496.6	.9797	.984	.974	4639
.236	5.80	.0229	193.3	497.7	.9933	.993	.989	5201
.256	5.91	.0220	193.6	498.2	1.0025	1.007	1.011	5307
.285	5.95	.0217	194.0	499.3	1.0073	1.015	1.024	5308
.304	5.95	.0217	194.4	499.8	1.0068	1.014	1.022	5311
.336	5.95	.0217	194.7	499.8	1.0062	1.012	1.020	5317
.409	5.95	.0217	195.1	500.9	1.0085	1.017	1.028	5276

TABLE II.- BOUNDARY-LAYER SURVEY DATA AT STATION 94 – Concluded

(d) p_{sc} = 424 N/cm^2; M_e = 5.978

y/r	M_l	$p_\infty/p_{t,2}$	T_w, °K	$T_{t,e}$, °K	u_l/u_e	$T_{t,l}/T_{t,e}$	$\frac{T_{t,l} - T_w}{T_{t,e} - T_w}$	$R_{p,2}$
Probe 1								
0.004	1.85	0.2049	354.9	509.5	0.6092	0.803	0.352	1 143
.007	2.13	.1578	357.9	513.9	.6746	.838	.468	1 307
.012	2.38	.1283	359.5	516.1	.7240	.865	.554	1 471
.018	2.57	.1113	362.1	517.2	.7541	.876	.588	1 615
.024	2.74	.0989	363.2	517.2	.7795	.889	.627	1 746
.034	2.99	.0833	364.2	517.7	.8114	.900	.663	1 977
.037	3.03	.0811	365.2	518.3	.8173	.904	.676	2 007
.054	3.32	.0682	366.4	518.3	.8455	.912	.699	2 299
.091	3.90	.0500	367.8	518.3	.8910	.926	.745	2 953
.120	4.37	.0398	368.8	517.2	.9235	.944	.804	3 549
.155	4.92	.0316	369.8	516.6	.9533	.962	.866	4 312
.195	5.50	.0254	370.8	516.1	.9729	.968	.885	5 295
.004	1.85	.2049	348.7	499.2	.6090	.803	.346	1 173
.008	2.17	.1521	351.3	502.4	.6825	.841	.472	1 374
.011	2.34	.1332	353.1	504.1	.7160	.862	.538	1 475
.015	2.49	.1184	354.5	506.3	.7406	.870	.566	1 590
.021	2.65	.1053	356.2	507.4	.7656	.881	.601	1 715
.027	2.84	.0923	357.6	508.4	.7929	.894	.644	1 870
.035	3.00	.0831	358.9	509.0	.8146	.906	.683	2 004
.046	3.19	.0737	360.1	509.0	.8331	.908	.686	2 209
.073	3.60	.0583	361.3	509.3	.8711	.923	.734	2 645
.107	4.16	.0439	362.2	509.5	.9109	.938	.786	3 329
.144	4.76	.0337	363.1	509.5	.9447	.956	.846	4 152
.174	5.23	.0281	363.9	509.0	.9648	.966	.881	4 904
.207	5.63	.0242	364.8	508.4	.9826	.981	.932	5 535
.240	5.90	.0221	365.4	508.4	.9906	.985	.945	6 007
Probe 2								
0.135	4.61	0.0360	197.2	509.5	0.9318	0.941	0.904	6 722
.138	4.66	.0352	198.8	513.9	.9330	.940	.902	6 800
.143	4.74	.0340	199.7	516.1	.9406	.949	.916	6 911
.149	4.84	.0326	201.2	517.2	.9452	.951	.920	7 142
.155	4.93	.0315	201.8	517.2	.9533	.962	.937	7 266
.165	5.10	.0294	202.3	517.7	.9545	.953	.923	7 819
.168	5.14	.0290	202.9	518.3	.9595	.960	.935	7 841
.185	5.38	.0265	203.5	518.3	.9700	.968	.947	8 453
.222	5.77	.0230	204.4	518.3	.9862	.981	.969	9 485
.252	5.94	.0218	204.9	517.2	.9980	.997	.996	9 850
.286	5.98	.0215	205.5	516.6	1.0009	1.002	1.003	9 915
.326	5.98	.0215	206.0	516.1	.9960	.992	.987	10 043
.135	4.61	.0360	193.7	499.2	.9320	.942	.905	6 885
.139	4.67	.0351	195.2	502.4	.9368	.947	.913	6 952
.142	4.72	.0343	196.2	504.1	.9427	.955	.926	6 996
.146	4.79	.0333	196.9	506.3	.9416	.947	.913	7 225
.152	4.88	.0321	197.9	507.4	.9452	.948	.915	7 434
.158	4.99	.0308	198.7	508.4	.9552	.962	.937	7 579
.166	5.10	.0294	199.4	509.0	.9606	.965	.942	7 869
.177	5.28	.0275	200.0	509.0	.9662	.966	.944	8 364
.204	5.60	.0245	200.7	509.3	.9819	.981	.968	9 141
.238	5.89	.0222	201.2	509.5	.9950	.994	.990	9 893
.275	5.98	.0215	201.7	509.5	1.0018	1.004	1.006	10 056
.305	5.98	.0215	202.2	509.0	.9979	.996	.993	10 161
.338	5.98	.0215	202.7	508.4	.9996	.999	.999	10 134
.371	5.98	.0215	203.0	508.4	.9979	.996	.993	10 174

TABLE III.- BOUNDARY-LAYER SURVEY DATA AT STATION 124

(a) $p_{sc} = 45\ N/cm^2$; $M_e = 5.764$

y/r	M_l	$p_\infty/p_{t,2}$	T_w, °K	$T_{t,e}$, °K	u_l/u_e	$T_{t,l}/T_{t,e}$	$\frac{T_{t,l} - T_w}{T_{t,e} - T_w}$	$R_{p,2}$
Probe 1								
0.004	1.01	0.5204	330.8	434.7	0.4063	0.843	0.343	93
.010	1.43	.3176	331.3	438.4	.5373	.866	.453	126
.023	2.00	.1774	331.7	441.0	.6732	.887	.543	184
.038	2.24	.1442	331.9	443.1	.7162	.891	.565	213
.052	2.40	.1264	332.1	443.6	.7445	.899	.598	233
.065	2.54	.1136	332.3	445.7	.7656	.903	.620	251
.089	2.79	.0955	332.4	446.2	.7994	.913	.659	283
.123	3.08	.0789	332.6	447.2	.8344	.924	.705	326
.156	3.40	.0653	332.6	447.7	.8679	.939	.761	374
.189	3.75	.0539	332.8	448.8	.8987	.952	.814	433
.240	4.33	.0406	332.9	449.8	.9380	.968	.878	545
.305	5.04	.0302	333.1	450.9	.9701	.979	.921	699
.004	1.01	.5204	328.2	441.0	.4041	.834	.350	92
.017	1.83	.2083	328.8	444.6	.6340	.872	.509	165
.031	2.14	.1573	329.1	446.7	.6955	.881	.550	201
.045	2.32	.1347	329.3	448.3	.7282	.888	.579	223
.083	2.73	.0991	329.6	450.3	.7888	.903	.638	276
.107	2.95	.0855	329.7	450.9	.8183	.916	.687	305
.172	3.56	.0596	330.0	452.4	.8805	.940	.777	399
.204	3.92	.0494	330.1	452.9	.9108	.956	.838	460
.272	4.69	.0348	330.4	454.5	.9546	.972	.899	615
.338	5.34	.0269	330.5	455.0	.9807	.983	.937	765
.423	5.75	.0232	330.6	456.6	.9905	.982	.934	874
.509	5.76	.0231	330.8	457.1	.9934	.987	.952	872
.590	5.76	.0231	330.9	458.1	.9992	.998	.994	857
Probe 2								
0.135	3.19	0.0737	183.8	434.7	0.8474	0.931	0.881	589
.141	3.25	.0712	184.0	438.4	.8547	.936	.890	596
.154	3.38	.0659	184.3	441.0	.8684	.943	.901	627
.169	3.54	.0603	184.4	443.1	.8812	.945	.905	670
.183	3.67	.0560	184.5	443.6	.8945	.953	.920	706
.196	3.82	.0519	184.6	445.7	.9042	.954	.922	749
.220	4.10	.0451	184.7	446.2	.9225	.959	.931	840
.254	4.49	.0379	184.8	447.2	.9451	.969	.948	969
.287	4.86	.0324	184.8	447.7	.9630	.977	.960	1106
.320	5.18	.0285	184.9	448.8	.9768	.984	.973	1225
.371	5.58	.0247	185.0	449.8	.9902	.989	.982	1386
.436	5.76	.0231	185.0	450.9	1.0005	1.001	1.002	1446
.135	3.19	.0737	182.3	441.0	.8462	.928	.878	581
.148	3.32	.0683	182.7	444.6	.8608	.937	.893	607
.162	3.45	.0632	182.8	446.7	.8730	.940	.899	641
.176	3.60	.0582	183.0	448.3	.8860	.945	.907	682
.214	4.04	.0466	183.1	450.3	.9162	.953	.921	814
.238	4.31	.0410	183.2	450.9	.9337	.961	.935	903
.303	5.01	.0305	183.3	452.4	.9689	.978	.963	1152
.335	5.32	.0271	183.4	452.9	.9821	.987	.978	1265
.403	5.71	.0236	183.5	454.5	.9974	.997	.995	1416
.469	5.76	.0231	183.6	455.0	1.0010	1.002	1.004	1430
.554	5.76	.0231	183.7	456.6	1.0031	1.006	1.010	1418
.640	5.76	.0231	183.8	457.1	1.0138	1.028	1.046	1381
.721	5.76	.0231	183.8	458.1	1.0261	1.053	1.088	1339

TABLE III.- BOUNDARY-LAYER SURVEY DATA AT STATION 124 – Continued

(b) p_{sc} = 79 N/cm^2; M_e = 5.830

y/r	M_l	$p_\infty/p_{t,2}$	T_w, °K	$T_{t,e}$, °K	u_l/u_e	$T_{t,l}/T_{t,e}$	$\frac{T_{t,l} - T_w}{T_{t,e} - T_w}$	$R_{p,2}$
				Probe 1				
0.004	1.03	0.5111	326.4	443.7	0.4054	0.821	0.323	153
.010	1.76	.2233	327.2	449.4	.6100	.849	.445	261
.023	2.11	.1610	327.7	452.0	.6845	.868	.520	321
.037	2.31	.1358	328.2	454.6	.7227	.881	.573	356
.052	2.50	.1175	328.6	456.7	.7553	.896	.629	389
.065	2.64	.1060	328.9	457.8	.7760	.902	.652	418
.088	2.88	.0896	329.2	459.3	.8107	.918	.710	469
.121	3.24	.0716	329.6	460.4	.8514	.933	.766	553
.154	3.61	.0581	330.2	461.4	.8863	.948	.818	646
.187	3.96	.0485	330.3	463.0	.9119	.956	.848	747
.237	4.50	.0377	330.6	464.0	.9454	.972	.902	913
.304	5.25	.0278	330.9	464.6	.9774	.984	.943	1188
.373	5.79	.0229	331.3	466.1	.9950	.992	.972	1397
.004	1.03	.5111	329.6	451.5	.4034	.813	.307	152
.017	2.01	.1759	330.6	457.8	.6657	.865	.514	297
.030	2.21	.1471	331.2	461.4	.7058	.877	.564	331
.044	2.41	.1261	331.6	463.0	.7398	.890	.611	365
.057	2.55	.1126	332.1	465.1	.7643	.899	.648	392
.071	2.70	.1013	332.4	466.1	.7883	.913	.696	419
.106	3.07	.0795	332.7	467.2	.8335	.928	.749	502
.138	3.43	.0640	333.2	468.2	.8722	.945	.808	588
.171	3.79	.0527	333.3	468.7	.9006	.953	.838	686
.202	4.12	.0448	333.5	470.3	.9254	.966	.884	776
.277	4.95	.0312	333.9	470.8	.9716	.991	.968	1043
.341	5.62	.0243	334.1	471.9	.9918	.993	.976	1304
.413	5.83	.0226	334.3	472.4	1.0002	1.000	1.001	1379
.483	5.83	.0226	334.6	472.9	1.0039	1.008	1.027	1366
				Probe 2				
0.135	3.39	0.0654	181.3	443.7	0.8674	0.941	0.900	1029
.141	3.46	.0630	181.8	449.4	.8708	.937	.895	1051
.154	3.60	.0582	182.0	452.0	.8817	.938	.897	1116
.168	3.76	.0536	182.3	454.6	.8951	.946	.910	1178
.183	3.92	.0495	182.6	456.7	.9073	.952	.919	1248
.196	4.05	.0463	182.7	457.8	.9144	.951	.918	1320
.219	4.30	.0411	182.9	459.3	.9309	.960	.933	1443
.252	4.67	.0350	183.1	460.4	.9506	.968	.947	1644
.285	5.05	.0301	183.5	461.4	.9691	.980	.966	1854
.318	5.40	.0263	183.5	463.0	.9809	.983	.971	2080
.368	5.77	.0231	183.6	464.0	.9970	.997	.995	2301
.435	5.83	.0226	183.8	464.6	1.0007	1.001	1.002	2328
.504	5.83	.0226	184.0	466.1	1.0051	1.010	1.017	2296
.135	3.39	.0654	183.1	451.5	.8704	.948	.912	999
.148	3.53	.0605	183.6	457.8	.8790	.944	.906	1056
.161	3.68	.0559	184.0	461.4	.8915	.949	.915	1113
.175	3.83	.0516	184.2	463.0	.9025	.952	.920	1183
.188	3.97	.0481	184.5	465.1	.9115	.954	.924	1247
.202	4.12	.0448	184.7	466.1	.9237	.963	.939	1309
.237	4.50	.0377	184.8	467.2	.9429	.967	.945	1515
.269	4.87	.0323	185.1	468.2	.9629	.979	.965	1711
.302	5.23	.0280	185.2	468.7	.9763	.983	.971	1936
.333	5.55	.0249	185.3	470.3	.9889	.991	.985	2128
.408	5.83	.0226	185.5	470.8	1.0072	1.015	1.024	2256
.472	5.83	.0226	185.6	471.9	1.0055	1.011	1.018	2260
.544	5.83	.0226	185.7	472.4	1.0104	1.021	1.034	2232
.614	5.83	.0226	185.9	472.9	1.0234	1.047	1.078	2164

TABLE III.- BOUNDARY-LAYER SURVEY DATA AT STATION 124 – Continued

(c) p_{sc} = 217 N/cm^2; M_e = 5.952

y/r	M_l	$p_\infty/p_{t,2}$	T_w, °K	$T_{t,e}$, °K	u_l/u_e	$T_{t,l}/T_{t,e}$	$\frac{T_{t,l} - T_w}{T_{t,e} - T_w}$	$R_{p,2}$
Probe 1								
0.004	1.50	0.2945	326.8	468.9	0.5302	0.797	0.331	521
.010	2.05	.1698	329.2	475.9	.6615	.840	.483	718
.023	2.37	.1298	331.8	482.3	.7245	.870	.583	834
.036	2.60	.1089	333.3	486.1	.7639	.889	.648	926
.050	2.82	.0936	334.6	488.2	.7953	.904	.694	1022
.063	3.02	.0819	335.7	491.4	.8206	.914	.728	1118
.088	3.36	.0668	336.7	493.0	.8535	.922	.754	1307
.121	3.77	.0532	337.7	495.2	.8864	.931	.782	1561
.154	4.16	.0440	338.7	496.8	.9119	.939	.810	1816
.188	4.55	.0368	339.9	497.9	.9343	.949	.841	2095
.240	5.13	.0291	341.0	499.5	.9602	.961	.878	2549
.305	5.80	.0228	342.0	501.1	.9848	.976	.925	3118
.004	1.50	.2945	339.3	483.4	.5318	.802	.337	498
.016	2.24	.1437	341.7	486.1	.7036	.865	.546	768
.030	2.49	.1180	343.2	488.8	.7504	.891	.633	860
.044	2.72	.1001	344.5	490.9	.7857	.907	.689	956
.057	2.92	.0870	345.4	492.0	.8101	.911	.702	1065
.070	3.11	.0773	346.4	493.6	.8350	.926	.753	1148
.104	3.56	.0594	347.2	494.1	.8769	.939	.795	1409
.137	3.97	.0482	348.0	495.2	.9025	.941	.800	1679
.171	4.36	.0401	348.8	495.7	.9272	.951	.836	1948
.205	4.74	.0340	349.5	496.3	.9469	.960	.866	2230
.270	5.47	.0256	350.2	496.8	.9788	.980	.931	2814
.341	5.93	.0219	350.7	497.3	.9969	.995	.982	3206
.427	5.95	.0217	351.1	497.9	.9956	.991	.970	3235
Probe 2								
0.135	3.94	0.0489	181.5	468.9	0.8878	0.913	0.858	3044
.141	4.01	.0473	182.9	475.9	.8951	.921	.871	3049
.154	4.16	.0439	184.4	482.3	.9099	.935	.894	3150
.167	4.31	.0410	185.2	486.1	.9144	.930	.887	3341
.181	4.46	.0383	185.9	488.2	.9258	.939	.902	3495
.194	4.62	.0357	186.5	491.4	.9370	.949	.918	3646
.219	4.89	.0319	187.0	493.0	.9518	.960	.935	3979
.252	5.26	.0277	187.6	495.2	.9671	.968	.948	4490
.285	5.64	.0242	188.2	496.8	.9833	.981	.969	5031
.319	5.88	.0222	188.8	497.9	.9948	.993	.988	5349
.371	5.95	.0217	189.4	499.5	.9958	.992	.987	5456
.436	5.95	.0217	190.0	501.1	1.0055	1.011	1.018	5316
.135	3.94	.0489	188.5	483.4	.8936	.925	.877	2890
.147	4.08	.0457	189.8	486.1	.9017	.927	.880	3044
.161	4.24	.0423	190.6	488.8	.9165	.941	.903	3182
.175	4.40	.0395	191.4	490.9	.9236	.941	.903	3369
.188	4.55	.0369	191.9	492.0	.9306	.942	.906	3562
.201	4.69	.0347	192.5	493.6	.9426	.955	.927	3698
.235	5.07	.0298	192.9	494.1	.9681	.981	.969	4134
.268	5.45	.0259	193.3	495.2	.9788	.981	.969	4725
.302	5.79	.0230	193.8	495.7	.9934	.994	.990	5213
.336	5.92	.0219	194.2	496.3	.9991	.999	.999	5404
.401	5.95	.0217	194.6	496.8	1.0064	1.013	1.021	5358
.472	5.95	.0217	194.8	497.3	1.0093	1.019	1.031	5316
.558	5.95	.0217	195.1	497.9	1.0143	1.029	1.047	5247

TABLE III.- BOUNDARY-LAYER SURVEY DATA AT STATION 124 – Concluded

(d) p_{sc} = 414 N/cm^2; M_e = 5.821

y/r	M_l	$p_\infty/p_{t,2}$	T_w, °K	$T_{t,e}$, °K	u_l/u_e	$T_{t,l}/T_{t,e}$	$\frac{T_{t,l} - T_w}{T_{t,e} - T_w}$	$R_{p,2}$
Probe 1								
0.004	1.68	0.2425	350.0	497.8	0.5741	0.798	0.319	1 200
.008	2.00	.1777	347.3	503.8	.6548	.842	.491	1 393
.022	2.41	.1254	351.8	507.0	.7359	.877	.599	1 720
.036	2.68	.1026	353.9	508.7	.7791	.896	.660	1 958
.049	2.88	.0896	355.9	510.9	.8042	.903	.680	2 157
.063	3.08	.0791	357.4	511.9	.8268	.911	.704	2 363
.087	3.38	.0659	358.8	513.0	.8549	.916	.719	2 732
.121	3.82	.0520	360.3	513.6	.8927	.933	.775	3 275
.157	4.25	.0421	362.3	514.1	.9238	.949	.828	3 881
.188	4.67	.0350	363.3	514.1	.9460	.959	.859	4 556
.239	5.33	.0270	364.3	514.1	.9750	.974	.911	5 722
.302	5.80	.0229	365.3	513.6	.9892	.980	.930	6 630
.374	5.82	.0227	366.2	513.6	.9931	.986	.952	6 632
.004	1.68	.2425	367.3	496.7	.5822	.821	.311	1 163
.017	2.30	.1367	359.9	498.9	.7212	.880	.570	1 633
.031	2.60	.1090	362.3	499.4	.7719	.904	.649	1 889
.046	2.84	.0924	363.8	500.5	.8027	.911	.673	2 133
.058	3.01	.0826	364.9	501.1	.8233	.917	.696	2 316
.072	3.19	.0739	365.9	501.1	.8402	.918	.697	2 540
.111	3.68	.0558	366.7	501.6	.8861	.936	.764	3 154
.140	4.05	.0463	367.7	501.6	.9105	.942	.784	3 697
.174	4.48	.0380	368.6	501.6	.9353	.952	.820	4 380
.207	4.94	.0314	369.9	501.6	.9606	.969	.882	5 153
.273	5.65	.0241	370.6	501.6	.9881	.984	.940	6 464
.338	5.82	.0227	371.2	501.6	.9981	.996	.986	6 738
.406	5.82	.0227	371.7	501.1	1.0015	1.003	1.012	6 693
Probe 2								
0.135	3.98	0.0479	194.4	497.8	0.8992	0.927	0.880	6 244
.139	4.04	.0466	192.9	503.8	.9064	.936	.896	6 232
.153	4.21	.0429	195.4	507.0	.9197	.945	.910	6 584
.167	4.39	.0396	196.6	508.7	.9304	.950	.919	7 000
.180	4.56	.0367	197.7	510.9	.9388	.953	.923	7 442
.194	4.76	.0338	198.5	511.9	.9478	.956	.928	7 977
.218	5.08	.0297	199.4	513.0	.9593	.957	.930	8 965
.252	5.48	.0256	200.2	513.6	.9842	.985	.975	9 939
.288	5.74	.0233	201.3	514.1	.9986	1.001	1.002	10 611
.319	5.82	.0227	201.9	514.1	.9999	1.000	1.000	10 915
.370	5.82	.0227	202.4	514.1	.9999	1.000	1.000	10 915
.433	5.82	.0227	202.9	513.6	.9993	.999	.998	10 943
.505	5.82	.0227	203.4	513.6	1.0032	1.006	1.011	10 845
.135	3.98	.0479	204.0	496.7	.9023	.933	.887	6 208
.148	4.15	.0442	200.0	498.9	.9171	.946	.910	6 532
.162	4.32	.0408	201.3	499.4	.9313	.958	.930	6 909
.177	4.52	.0374	202.1	500.5	.9384	.956	.926	7 468
.189	4.68	.0348	202.7	501.1	.9466	.959	.931	7 931
.203	4.87	.0322	203.3	501.1	.9561	.964	.940	8 459
.242	5.37	.0266	203.7	501.6	.9798	.982	.969	9 889
.271	5.63	.0242	204.3	501.6	.9892	.987	.978	10 740
.305	5.80	.0228	204.8	501.6	.9953	.991	.985	11 295
.338	5.82	.0227	205.5	501.6	.9984	.997	.995	11 277
.404	5.82	.0227	205.9	501.6	1.0040	1.008	1.014	11 129
.469	5.82	.0227	206.2	501.6	1.0051	1.010	1.017	11 100
.537	5.82	.0227	206.5	501.1	1.0068	1.014	1.023	11 071

TABLE IV.-BOUNDARY-LAYER SURVEY DATA AT STATION 172

(a) $p_{sc} = 45\ N/cm^2$; $M_e = 5.581$

y/r	M_l	$p_\infty/p_{t,2}$	T_w, °K	$T_{t,e}$, °K	u_l/u_e	$T_{t,l}/T_{t,e}$	$\frac{T_{t,l} - T_w}{T_{t,e} - T_w}$	$R_{p,2}$
Probe 1								
0.004	1.02	0.5180	340.2	459.8	0.4048	0.824	0.324	108
.012	1.46	.3070	340.6	461.9	.5435	.853	.441	149
.024	1.81	.2111	340.9	463.4	.6336	.871	.513	189
.038	2.01	.1758	341.1	464.5	.6749	.878	.542	214
.071	2.32	.1348	341.3	465.5	.7324	.891	.593	256
.122	2.59	.1096	341.6	466.1	.7787	.912	.669	292
.188	2.99	.0834	341.7	466.6	.8329	.932	.746	354
.253	3.61	.0581	341.9	467.1	.8930	.951	.819	470
.017	1.66	.2461	337.2	458.7	.5951	.857	.460	174
.033	1.95	.1852	337.7	460.8	.6617	.872	.521	209
.057	2.21	.1478	337.9	462.4	.7107	.881	.559	244
.086	2.42	.1251	338.2	463.4	.7474	.894	.607	271
.155	2.77	.0963	338.4	464.0	.8043	.920	.703	322
.237	3.44	.0638	338.7	464.5	.8751	.939	.776	443
.304	4.08	.0457	338.8	465.5	.9267	.963	.863	574
.404	4.98	.0309	338.9	466.1	.9707	.976	.912	801
.505	5.50	.0254	339.1	466.6	.9890	.982	.935	952
Probe 2								
0.135	2.66	0.1045	189.0	459.8	0.7881	0.914	0.854	512
.143	2.70	.1014	189.2	461.9	.7960	.921	.866	517
.155	2.77	.0965	189.4	463.4	.8071	.927	.876	532
.169	2.86	.0911	189.5	464.5	.8181	.930	.882	554
.202	3.10	.0778	189.6	465.5	.8464	.938	.896	623
.253	3.60	.0583	189.8	466.1	.8917	.949	.915	783
.319	4.21	.0429	189.8	466.6	.9336	.963	.937	1008
.384	4.80	.0331	189.9	467.1	.9632	.973	.954	1253
.148	2.73	.0992	187.3	458.7	.7980	.916	.859	534
.164	2.83	.0928	187.6	460.8	.8129	.925	.874	554
.188	2.99	.0836	187.7	462.4	.8320	.930	.883	597
.217	3.24	.0714	187.9	463.4	.8597	.940	.899	671
.287	3.91	.0495	188.0	464.0	.9142	.955	.924	902
.368	4.65	.0353	188.1	464.5	.9546	.967	.944	1200
.435	5.20	.0284	188.2	465.5	.9800	.981	.967	1435
.535	5.56	.0248	188.3	466.1	.9973	.996	.993	1590
.636	5.58	.0246	188.4	466.6	1.0070	1.014	1.023	1564

TABLE IV.- BOUNDARY-LAYER SURVEY DATA AT STATION 172 – Continued

(b) p_{sc} = 79 N/cm^2; M_e = 5.672

y/r	M_l	$p_\infty/p_{t,2}$	T_w, °K	$T_{t,e}$ °K	u_l/u_e	$T_{t,l}/T_{t,e}$	$\frac{T_{t,l} - T_w}{T_{t,e} - T_w}$	$R_{p,2}$
Probe 1								
0.004	1.10	0.4706	323.8	445.8	0.4274	0.815	0.325	192
.010	1.61	.2591	324.4	447.3	.5802	.851	.458	277
.024	1.98	.1801	324.8	449.4	.6643	.868	.522	350
.039	2.15	.1557	325.3	451.0	.6993	.882	.578	381
.074	2.46	.1208	325.7	452.6	.7568	.905	.661	449
.105	2.68	.1029	326.2	453.6	.7928	.923	.725	499
.172	3.21	.0726	326.5	454.7	.8553	.940	.786	648
.241	3.86	.0509	326.8	456.3	.9114	.960	.860	854
.334	4.74	.0340	327.1	457.3	.9627	.981	.932	1190
.407	5.37	.0266	327.4	458.4	.9852	.986	.949	1477
.504	5.67	.0239	327.8	459.9	1.0001	1.000	1.001	1595
.640	5.67	.0239	328.2	461.0	1.0132	1.027	1.092	1543
.004	1.10	.4706	339.2	465.2	.4263	.811	.301	184
.017	1.87	.1993	340.4	468.3	.6418	.864	.502	310
.031	2.06	.1675	340.9	469.4	.6841	.881	.565	344
.058	2.33	.1340	341.4	471.0	.7361	.901	.642	396
.088	2.56	.1123	341.7	472.0	.7761	.920	.708	444
.137	2.92	.0873	342.1	473.1	.8272	.939	.781	532
.220	3.66	.0563	342.4	473.6	.8996	.961	.860	747
.303	4.45	.0385	342.7	474.1	.9507	.979	.926	1023
.370	5.08	.0297	342.9	474.6	.9752	.983	.938	1285
.437	5.54	.0250	343.2	475.2	.9933	.993	.975	1483
Probe 2								
0.135	2.90	0.0884	179.9	445.8	0.8179	0.923	0.871	959
.141	2.96	.0853	180.2	447.3	.8260	.929	.880	976
.155	3.07	.0796	180.5	449.4	.8392	.934	.890	1022
.170	3.20	.0733	180.7	451.0	.8529	.937	.895	1085
.205	3.52	.0610	181.0	452.6	.8825	.947	.911	1247
.236	3.81	.0522	181.2	453.6	.9064	.956	.927	1407
.303	4.45	.0386	181.4	454.7	.9428	.964	.940	1812
.372	5.10	.0295	181.5	456.3	.9737	.979	.964	2257
.465	5.64	.0241	181.7	457.3	.9985	.998	.997	2644
.538	5.67	.0239	181.9	458.4	1.0029	1.006	1.010	2638
.635	5.67	.0239	182.1	459.9	1.0164	1.033	1.055	2546
.771	5.67	.0239	182.3	461.0	1.0254	1.051	1.085	2487
.135	2.90	.0884	188.5	465.2	.8197	.927	.877	905
.148	3.00	.0827	189.1	468.3	.8328	.933	.887	943
.162	3.12	.0767	189.4	469.4	.8486	.943	.904	989
.189	3.38	.0660	189.7	471.0	.8724	.947	.912	1112
.219	3.65	.0568	189.8	472.0	.8969	.958	.929	1245
.268	4.12	.0449	190.0	473.1	.9280	.965	.942	1510
.351	4.90	.0318	190.2	473.6	.9682	.980	.967	2011
.434	5.53	.0251	190.4	474.1	.9937	.994	.991	2450
.501	5.67	.0239	190.5	474.6	1.0023	1.005	1.008	2535
.568	5.67	.0239	190.7	475.2	1.0135	1.027	1.045	2467

TABLE IV.- BOUNDARY-LAYER SURVEY DATA AT STATION 172 – Continued

(c) p_{sc} = 217 N/cm^2; M_e = 5.748

y/r	M_l	$p_\infty/p_{t,2}$	T_w, °K	$T_{t,e}$, °K	u_l/u_e	$T_{t,l}/T_{t,e}$	$\frac{T_{t,l} - T_w}{T_{t,e} - T_w}$	$R_{p,2}$
Probe 1								
0.004	1.51	0.2889	337.5	485.5	0.5366	0.797	0.333	624
.009	1.85	.2032	339.3	489.8	.6265	.837	.469	751
.023	2.20	.1489	341.0	491.4	.7003	.866	.562	909
.045	2.53	.1144	341.4	494.1	.7619	.897	.666	1067
.070	2.78	.0957	342.3	495.7	.7950	.903	.687	1216
.103	3.05	.0803	343.0	497.4	.8264	.912	.716	1384
.169	3.67	.0562	343.8	499.0	.8823	.927	.767	1826
.239	4.34	.0405	344.7	500.1	.9273	.946	.825	2370
.341	5.27	.0276	345.6	501.1	.9719	.968	.898	3257
.402	5.68	.0238	346.3	502.2	.9833	.970	.903	3730
.501	5.75	.0233	347.2	503.3	.9944	.989	.964	3717
.640	5.75	.0233	347.9	504.4	1.0032	1.006	1.020	3631
.004	1.51	.2889	347.6	493.6	.5365	.796	.312	612
.016	2.07	.1664	350.9	496.8	.6750	.857	.513	834
.030	2.32	.1345	351.7	499.0	.7244	.878	.586	952
.053	2.62	.1077	352.9	501.1	.7750	.903	.673	1091
.088	2.92	.0873	354.2	503.3	.8148	.915	.712	1268
.138	3.37	.0661	355.0	504.9	.8616	.928	.758	1566
.205	4.01	.0472	355.8	506.5	.9060	.935	.780	2068
.321	5.08	.0297	356.7	508.2	.9621	.959	.864	3034
.380	5.58	.0247	357.6	509.2	.9805	.969	.897	3547
.449	5.75	.0233	358.2	510.3	.9956	.991	.971	3643
.550	5.75	.0233	359.0	511.4	.9984	.997	.989	3612
Probe 2								
0.135	3.34	0.0675	187.5	485.5	0.8495	0.908	0.850	2744
.140	3.39	.0655	188.5	489.8	.8545	.910	.854	2778
.154	3.52	.0608	189.4	491.4	.8668	.916	.863	2927
.176	3.74	.0541	189.7	494.1	.8856	.925	.878	3181
.201	3.98	.0480	190.2	495.7	.8991	.924	.877	3530
.234	4.29	.0413	190.6	497.4	.9200	.935	.894	3976
.300	4.89	.0319	191.0	499.0	.9582	.964	.941	4873
.370	5.51	.0253	191.5	500.1	.9848	.981	.969	5918
.472	5.75	.0233	192.0	501.1	1.0022	1.004	1.007	6205
.533	5.75	.0233	192.4	502.2	1.0022	1.004	1.007	6189
.632	5.75	.0233	192.9	503.3	1.0134	1.027	1.044	6015
.771	5.75	.0233	193.3	504.4	1.0156	1.031	1.051	5969
.135	3.34	.0675	193.1	493.6	.8479	.904	.843	2703
.147	3.46	.0629	195.0	496.8	.8605	.912	.854	2822
.161	3.59	.0587	195.4	499.0	.8727	.918	.866	2955
.184	3.81	.0522	196.0	501.1	.8922	.930	.884	3210
.219	4.15	.0443	196.8	503.3	.9130	.935	.893	3679
.269	4.61	.0360	197.2	504.9	.9436	.956	.927	4322
.336	5.22	.0281	197.7	506.5	.9699	.967	.946	5370
.452	5.75	.0233	198.2	508.2	.9997	.999	.999	6140
.511	5.75	.0233	198.6	509.2	1.0052	1.010	1.017	6046
.580	5.75	.0233	199.0	510.3	1.0118	1.024	1.039	5939
.681	5.75	.0233	199.4	511.4	1.0146	1.029	1.048	5887

TABLE IV.- BOUNDARY-LAYER SURVEY DATA AT STATION 172 – Concluded

(d) p_{sc} = 389 N/cm^2; M_e = 5.778

y/r	M_l	$p_\infty/p_{t,2}$	T_w, °K	$T_{t,e}$, °K	u_l/u_e	$T_{t,l}/T_{t,e}$	$\frac{T_{t,l} - T_w}{T_{t,e} - T_w}$	$R_{p,2}$
Probe 1								
0.004	1.67	0.2451	342.1	470.8	0.5789	0.816	0.327	1 222
.011	2.03	.1728	343.6	472.4	.6700	.865	.505	1 466
.025	2.34	.1328	345.1	473.0	.7302	.887	.583	1 737
.038	2.55	.1128	346.1	474.0	.7676	.906	.651	1 921
.071	2.92	.0871	347.6	474.6	.8156	.917	.689	2 331
.104	3.20	.0732	348.6	475.1	.8447	.923	.712	2 668
.173	3.88	.0503	349.9	475.1	.9013	.941	.776	3 611
.238	4.55	.0368	350.8	475.7	.9435	.961	.852	4 694
.305	5.15	.0289	351.7	475.7	.9747	.982	.932	5 736
.378	5.68	.0238	352.4	475.7	.9929	.991	.964	6 789
.443	5.78	.0230	353.3	475.7	1.0035	1.007	1.027	6 883
.564	5.78	.0230	354.3	475.7	1.0088	1.018	1.069	6 797
.004	1.67	.2451	351.6	487.6	.5782	.814	.332	1 175
.016	2.16	.1537	354.9	493.0	.6949	.869	.533	1 513
.029	2.42	.1248	356.6	496.3	.7421	.888	.604	1 718
.056	2.77	.0963	358.2	499.0	.7947	.906	.668	2 050
.089	3.08	.0791	359.8	501.7	.8310	.918	.711	2 360
.139	3.53	.0606	361.1	503.8	.8716	.926	.739	2 912
.206	4.22	.0427	363.7	506.0	.9204	.943	.799	3 871
.272	4.86	.0324	364.8	507.6	.9615	.974	.909	4 815
.338	5.43	.0260	364.8	508.7	.9798	.977	.917	5 881
.405	5.77	.0231	365.9	509.8	.9932	.987	.954	6 469
.471	5.78	.0230	366.9	510.9	1.0013	1.003	1.009	6 359
.525	5.78	.0230	368.1	512.0	1.0024	1.005	1.017	6 326
Probe 2								
0.135	3.49	0.0619	190.0	470.8	0.8729	0.935	0.891	5 198
.142	3.56	.0594	190.9	472.4	.8782	.935	.891	5 363
.156	3.70	.0552	191.7	473.0	.8889	.938	.896	5 683
.169	3.84	.0514	192.3	474.0	.9020	.948	.912	5 965
.202	4.18	.0435	193.1	474.6	.9253	.958	.928	6 826
.235	4.52	.0373	193.7	475.1	.9416	.960	.932	7 813
.304	5.15	.0289	194.4	475.1	.9705	.974	.956	9 703
.369	5.63	.0242	194.9	475.7	.9911	.989	.981	11 232
.436	5.78	.0230	195.4	475.7	1.0026	1.005	1.009	11 551
.509	5.78	.0230	195.8	475.7	1.0079	1.016	1.027	11 408
.574	5.78	.0230	196.3	475.7	1.0079	1.016	1.027	11 408
.695	5.78	.0230	196.8	475.7	1.0143	1.029	1.049	11 237
.135	3.49	.0619	195.3	487.6	.8719	.933	.888	4 998
.147	3.62	.0577	197.2	493.0	.8786	.928	.880	5 276
.160	3.75	.0539	198.1	496.3	.8898	.934	.890	5 514
.187	4.03	.0469	199.0	499.0	.8539	.830	.717	7 138
.220	4.38	.0398	199.9	501.7	.9335	.956	.927	6 934
.270	4.84	.0326	200.6	503.8	.9550	.962	.938	8 202
.337	5.42	.0262	202.0	506.0	.9788	.975	.959	9 873
.403	5.76	.0231	202.7	507.6	1.0032	1.007	1.012	10 617
.469	5.78	.0230	202.7	508.7	1.0003	1.001	1.001	10 727
.536	5.78	.0230	203.3	509.8	1.0075	1.015	1.025	10 522
.602	5.78	.0230	203.9	510.9	1.0113	1.023	1.038	10 402
.656	5.78	.0230	204.5	512.0	1.0119	1.024	1.040	10 363

TABLE V.- BOUNDARY-LAYER SURVEY DATA AT STATION 215

(a) $p_{sc} = 45\ N/cm^2$; $M_e = 5.450$

y/r	M_l	$p_\infty/p_{t,2}$	T_w, °K	$T_{t,e}$, °K	u_l/u_e	$T_{t,l}/T_{t,e}$	$\frac{T_{t,l} - T_w}{T_{t,e} - T_w}$	$R_{p,2}$
Probe 1								
0.004	1.08	0.4806	324.4	452.6	0.4201	0.799	0.291	138
.016	1.45	.3115	324.9	455.3	.5383	.842	.447	175
.032	1.72	.2322	325.3	456.3	.6069	.848	.472	213
.055	1.98	.1812	325.4	458.5	.6630	.858	.510	250
.123	2.33	.1340	325.7	460.1	.7325	.883	.598	302
.342	3.55	.0598	326.1	461.2	.8862	.938	.789	545
.547	4.94	.0313	326.2	462.3	.9647	.960	.863	939
.681	5.41	.0262	326.4	462.8	.9898	.982	.938	1075
.004	1.08	.4806	323.6	458.5	.4181	.791	.291	138
.020	1.53	.2836	324.0	460.7	.5580	.836	.448	186
.036	1.79	.2166	324.3	462.3	.6211	.847	.486	221
.085	2.18	.1520	324.6	463.9	.7020	.868	.559	278
.271	3.06	.0801	325.0	466.1	.8362	.919	.732	429
.570	5.07	.0298	325.3	467.2	.9686	.959	.866	971
Probe 2								
0.135	2.38	0.1289	180.2	452.6	0.7423	0.889	0.815	525
.147	2.43	.1238	180.5	455.3	.7516	.893	.823	535
.163	2.49	.1181	180.7	456.3	.7618	.897	.829	551
.186	2.60	.1093	180.8	458.5	.7781	.903	.840	578
.254	2.95	.0858	181.0	460.1	.8256	.919	.867	686
.473	4.47	.0381	181.1	461.2	.9435	.952	.922	1322
.678	5.40	.0263	181.2	462.3	.9967	.996	.993	1751
.812	5.45	.0258	181.3	462.8	1.0101	1.020	1.033	1726
.135	2.38	.1289	179.8	458.5	.7407	.885	.811	520
.151	2.44	.1225	180.0	460.7	.7523	.890	.820	534
.167	2.51	.1161	180.2	462.3	.7646	.896	.830	550
.216	2.73	.0991	180.3	463.9	.7974	.909	.851	612
.402	3.98	.0479	180.6	466.1	.9159	.945	.910	1076
.701	5.45	.0259	180.7	467.2	.9986	.997	.996	1752

TABLE V.- BOUNDARY-LAYER SURVEY DATA AT STATION 215 – Continued

(b) p_{sc} = 79 N/cm^2; M_e = 5.537

y/r	M_l	$p_\infty/p_{t,2}$	T_w, °K	$T_{t,e}$, °K	u_l/u_e	$T_{t,l}/T_{t,e}$	$\frac{T_{t,l} - T_w}{T_{t,e} - T_w}$	$R_{p,2}$
Probe 1								
0.004	1.05	0.4976	325.9	460.4	0.4102	0.800	0.315	209
.012	1.57	.2713	327.0	464.1	.5686	.842	.465	298
.028	1.92	.1905	327.7	465.2	.6516	.859	.524	375
.055	2.18	.1509	328.2	467.3	.7079	.883	.605	432
.121	2.60	.1090	328.6	468.9	.7820	.915	.715	534
.336	4.04	.0466	329.2	470.5	.9247	.961	.869	1028
.537	5.33	.0270	329.6	472.6	.9901	.991	.971	1610
.671	5.54	.0250	330.0	473.1	1.0058	1.012	1.039	1679
.020	1.80	.2139	328.4	471.5	.6234	.849	.503	344
.036	2.01	.1750	328.9	473.1	.6714	.865	.557	389
.088	2.40	.1270	329.5	475.2	.7462	.896	.660	476
.272	3.60	.0581	330.1	477.4	.8938	.951	.842	841
.563	5.44	.0259	330.8	478.9	.9945	.994	.980	1638
Probe 2								
0.135	2.68	0.1026	181.1	460.4	0.7896	0.908	0.849	960
.143	2.73	.0992	181.7	464.1	.7974	.913	.857	971
.159	2.83	.0925	182.0	465.2	.8123	.921	.870	1016
.186	3.02	.0819	182.3	467.3	.8334	.925	.877	1110
.252	3.47	.0625	182.5	468.9	.8801	.942	.905	1357
.467	4.97	.0310	182.9	470.5	.9688	.970	.952	2421
.668	5.54	.0250	183.1	472.6	1.0086	1.017	1.028	2772
.802	5.54	.0250	183.3	473.1	1.0192	1.039	1.063	2701
.151	2.79	.0954	182.4	471.5	.8044	.914	.860	982
.167	2.89	.0891	182.7	473.1	.8188	.922	.873	1025
.220	3.25	.0710	183.1	475.2	.8559	.928	.883	1221
.403	4.53	.0372	183.4	477.4	.9525	.970	.951	2023
.694	5.54	.0250	183.8	478.9	1.0147	1.030	1.048	2691

TABLE V.- BOUNDARY-LAYER SURVEY DATA AT STATION 215 – Continued

(c) p_{sc} = 217 N/cm^2; M_e = 5.663

y/r	M_l	$p_\infty/p_{t,2}$	T_w, °K	$T_{t,e}$, °K	u_l/u_e	$T_{t,l}/T_{t,e}$	$\frac{T_{t,l} - T_w}{T_{t,e} - T_w}$	$R_{p,2}$
Probe 1								
0.004	1.46	0.3060	342.6	492.3	0.5299	0.812	0.382	628
.013	1.94	.1869	345.1	493.9	.6537	.860	.535	837
.028	2.26	.1416	346.3	495.5	.7181	.883	.611	1000
.053	2.54	.1137	347.8	496.6	.7678	.905	.683	1151
.121	3.04	.0808	348.7	498.2	.8304	.919	.730	1485
.204	3.62	.0578	349.6	498.8	.8846	.936	.786	1926
.372	4.98	.0309	350.4	499.8	.9613	.961	.869	3252
.004	1.46	.3060	334.1	461.0	.5318	.818	.339	674
.022	2.15	.1554	335.6	463.1	.6973	.876	.549	1019
.037	2.38	.1287	336.4	464.7	.7424	.898	.630	1140
.087	2.81	.0940	337.2	465.8	.8062	.919	.705	1420
.272	4.15	.0441	338.3	467.4	.9219	.948	.813	2590
.506	5.66	.0239	339.2	468.5	.9975	.995	.982	4289
.575	5.66	.0239	339.8	469.1	.9964	.993	.974	4295
Probe 2								
0.135	3.14	0.0759	190.3	492.3	0.8336	0.906	0.847	2675
.144	3.20	.0732	191.7	493.9	.8416	.912	.856	2729
.159	3.31	.0687	192.4	495.5	.8514	.914	.859	2858
.184	3.47	.0624	193.2	496.6	.8684	.923	.873	3061
.252	3.97	.0481	193.7	498.2	.9057	.935	.893	3780
.335	4.71	.0345	194.2	498.8	.9542	.965	.943	4966
.503	5.66	.0239	194.7	499.8	1.0011	1.002	1.003	6637
.135	3.14	.0759	185.6	461.0	.8360	.911	.851	2873
.153	3.26	.0705	186.5	463.1	.8483	.915	.858	3026
.168	3.37	.0663	186.9	464.7	.8603	.922	.870	3146
.218	3.71	.0549	187.3	465.8	.8893	.932	.887	3654
.403	5.19	.0285	187.9	467.4	.9767	.979	.964	6291
.637	5.66	.0239	188.5	468.5	1.0140	1.028	1.047	6950
.706	5.66	.0239	188.8	469.1	1.0135	1.027	1.045	6950

TABLE V.- BOUNDARY-LAYER SURVEY DATA AT STATION 215 – Concluded

(d) p_{sc} = 355 N/cm^2; M_e = 5.692

y/r	M_l	$p_\infty/p_{t,2}$	T_w, °K	$T_{t,e}$, °K	u_l/u_e	$T_{t,l}/T_{t,e}$	$\frac{T_{t,l} - T_w}{T_{t,e} - T_w}$	$R_{p,2}$
Probe 1								
0.004	1.45	0.3114	335.1	482.1	0.5249	0.810	0.377	1 007
.012	1.96	.1841	338.0	486.9	.6565	.860	.542	1 356
.027	2.29	.1381	339.7	489.1	.7249	.889	.636	1 613
.052	2.61	.1083	341.4	492.3	.7760	.905	.691	1 896
.119	3.14	.0758	343.2	494.5	.8412	.923	.748	2 470
.202	3.81	.0522	344.8	497.1	.9011	.946	.823	3 284
.368	5.18	.0285	346.8	499.3	.9736	.974	.915	5 529
.539	5.69	.0237	348.5	498.8	.9989	.998	.993	6 391
.004	1.45	.3114	345.4	492.8	.5285	.821	.402	964
.020	2.17	.1529	348.6	497.1	.7019	.880	.600	1 481
.037	2.43	.1238	351.0	499.3	.7509	.903	.672	1 684
.087	2.92	.0874	352.8	502.0	.8192	.922	.739	2 158
.271	4.34	.0405	355.0	504.7	.9366	.962	.871	3 981
.506	5.69	.0237	356.7	506.3	1.0054	1.011	1.036	6 185
Probe 2								
0.135	3.26	0.0707	186.2	482.1	0.8510	0.923	0.874	4 547
.143	3.33	.0678	187.8	486.9	.8582	.926	.879	4 640
.158	3.46	.0630	188.7	489.1	.8726	.935	.895	4 874
.183	3.65	.0567	189.7	492.3	.8886	.940	.903	5 280
.250	4.17	.0438	190.7	494.5	.9255	.955	.928	6 477
.333	4.85	.0325	191.5	497.1	.9666	.981	.969	8 181
.499	5.69	.0237	192.7	499.3	1.0014	1.003	1.005	10 627
.670	5.69	.0237	193.6	498.8	1.0153	1.031	1.050	10 299
.135	3.26	.0707	191.9	492.8	.8527	.926	.879	4 400
.151	3.40	.0651	193.7	497.1	.8674	.934	.891	4 641
.168	3.54	.0603	195.0	499.3	.8811	.941	.904	4 908
.218	3.93	.0491	196.0	502.0	.9121	.954	.925	5 747
.402	5.44	.0260	197.2	504.7	.9897	.992	.987	9 758
.637	5.69	.0237	198.2	506.3	1.0154	1.031	1.051	10 117

TABLE VI.- BOUNDARY-LAYER INTEGRAL PARAMETERS

Station	p_{sc}, N/cm^2	n	θ, cm	δ^*, cm	δ, cm	$R_{e,\theta}$	$R_{e,x}$	$(R_{e,x})_{eq}$
94	424	9.3	0.132	1.39	4.14	45.7×10^3	82.6×10^6	126.5×10^6
	217	8.8	.135	1.47	4.39	25.8	45.6	61.0
	79	7.8	.165	1.81	5.46	13.4	19.4	27.0
	45	7.7	.176	2.01	5.44	8.05	11.0	14.3
124	414	8.4	0.163	1.73	4.79	59.6×10^3	115.5×10^6	172.0×10^6
	217	8.3	.173	1.90	6.08	33.1	60.4	83.1
	79	7.1	.191	2.16	6.37	15.4	25.4	31.4
	45	7.1	.207	2.45	6.74	9.93	15.6	19.0
172	389	8.8	0.208	2.22	6.32	77.2×10^3	162.0×10^6	236.4×10^6
	217	8.4	.234	2.37	6.91	47.0	88.0	124.4
	79	7.3	.235	2.80	7.36	20.2	37.4	43.2
	45	6.7	.273	3.08	8.54	13.7	21.8	26.1
215	355	8.8	0.234	2.58	7.28	79.7×10^3	186.3×10^6	237.8×10^6
	217	8.4	.256	2.73	7.53	56.6	120.5	155.1
	79	6.8	.302	3.32	9.11	26.5	47.9	58.1
	45	6.0	.368	3.81	10.69	19.7	29.1	39.3

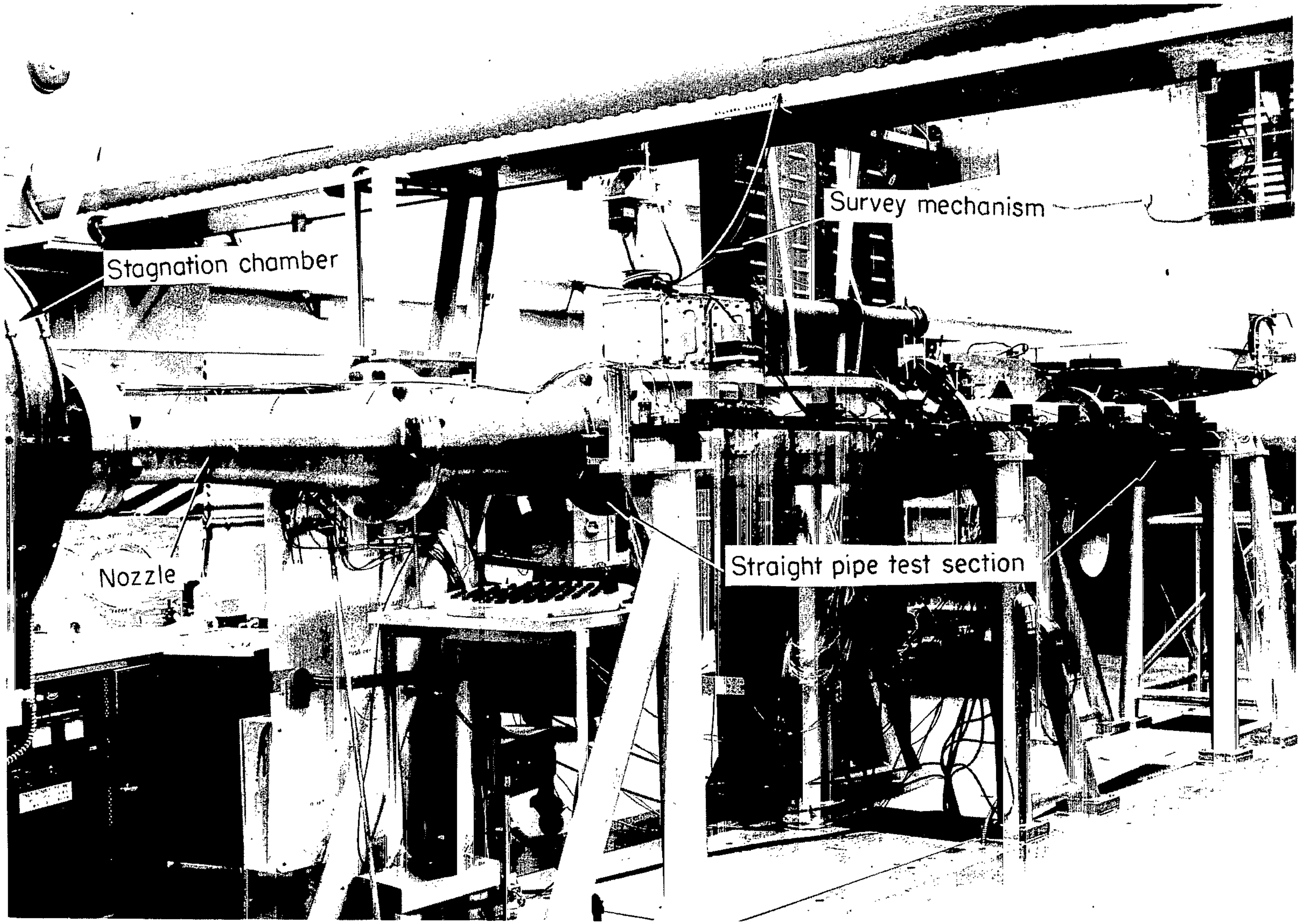

Figure 1.- Mach 6 high Reynolds number tunnel at the Langley Research Center.

L-68-8625

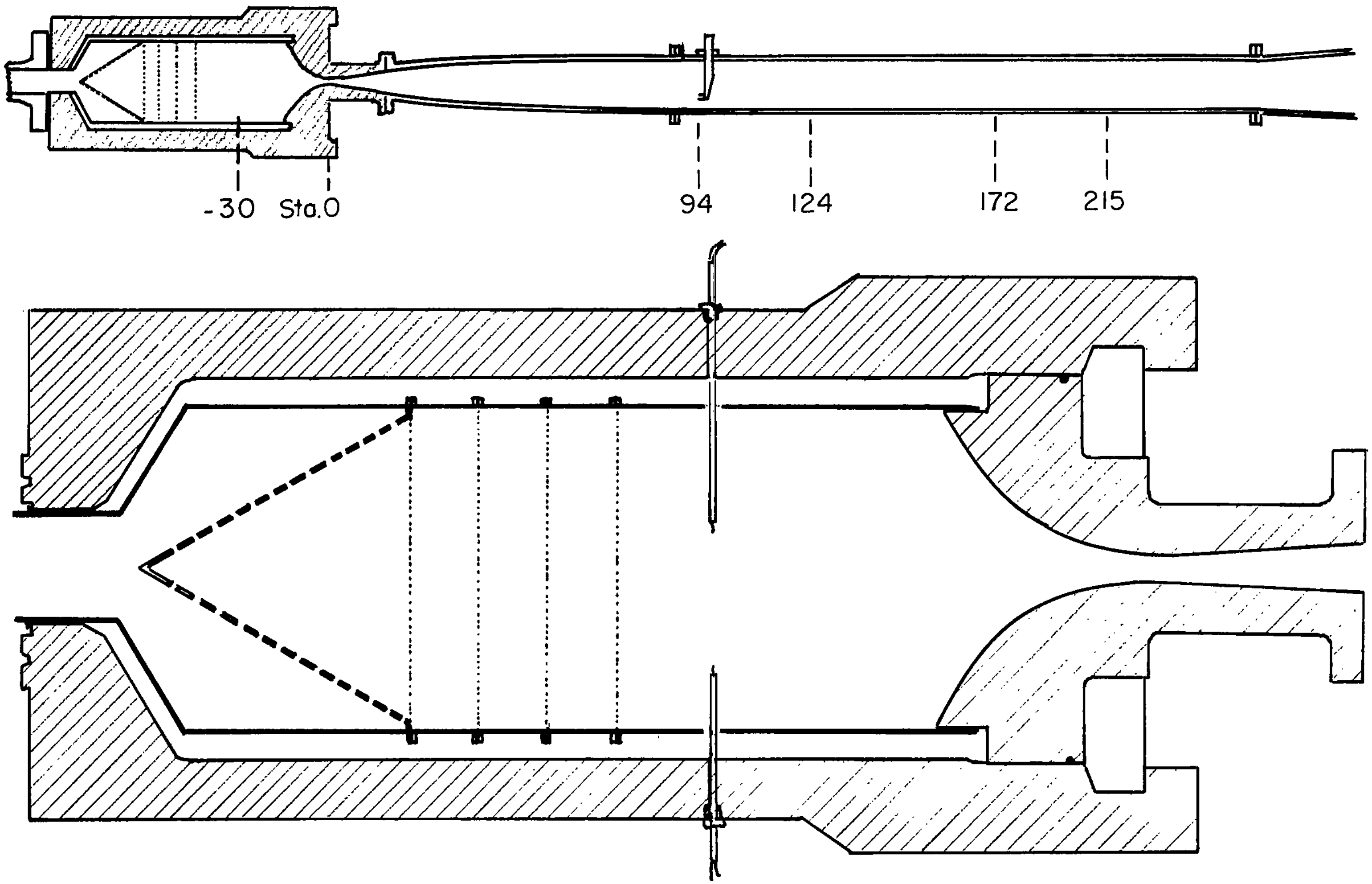

Figure 2.- Sketch of facility.

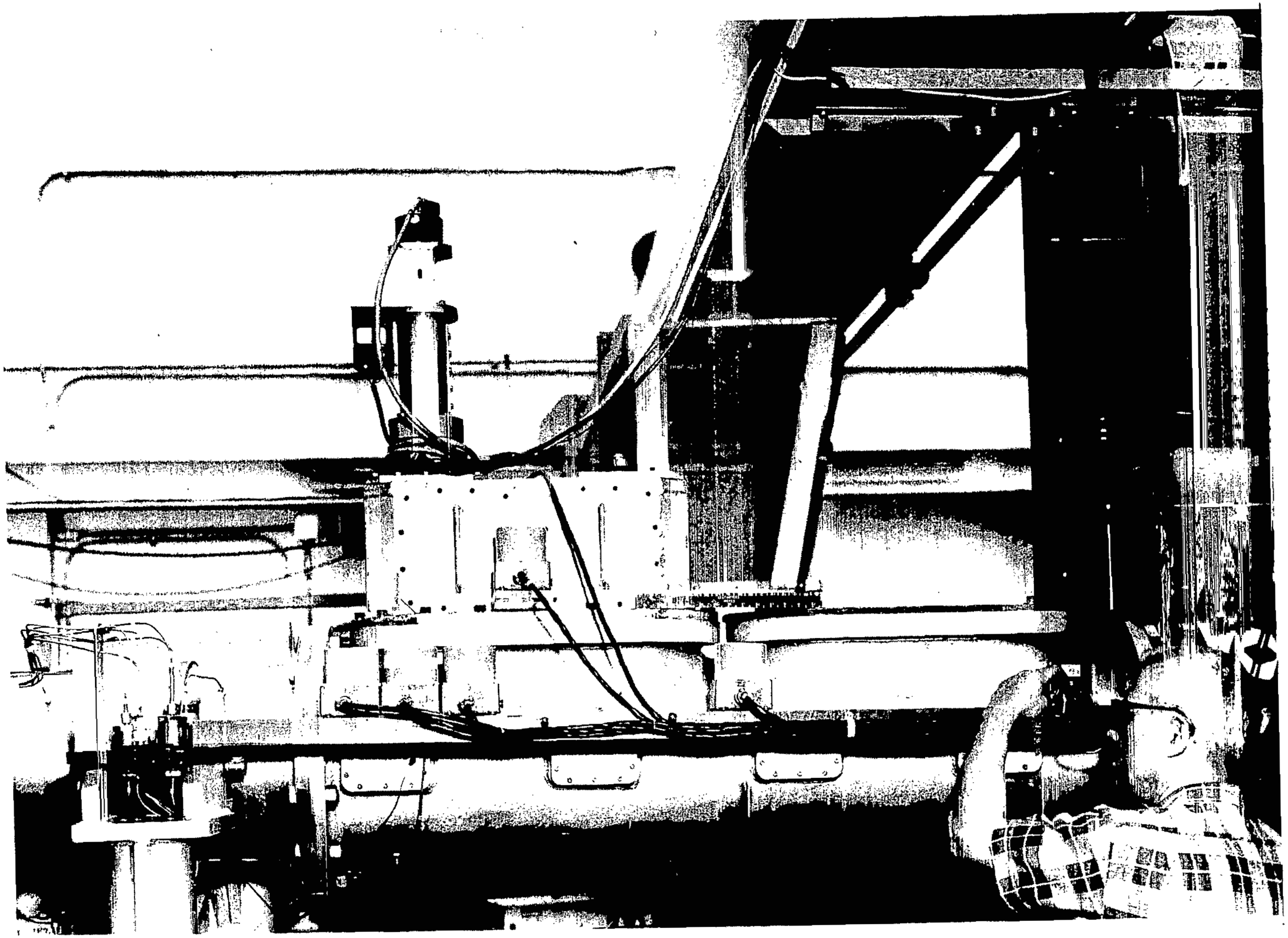

L-68-8624

Figure 3.- Boundary-layer survey section.

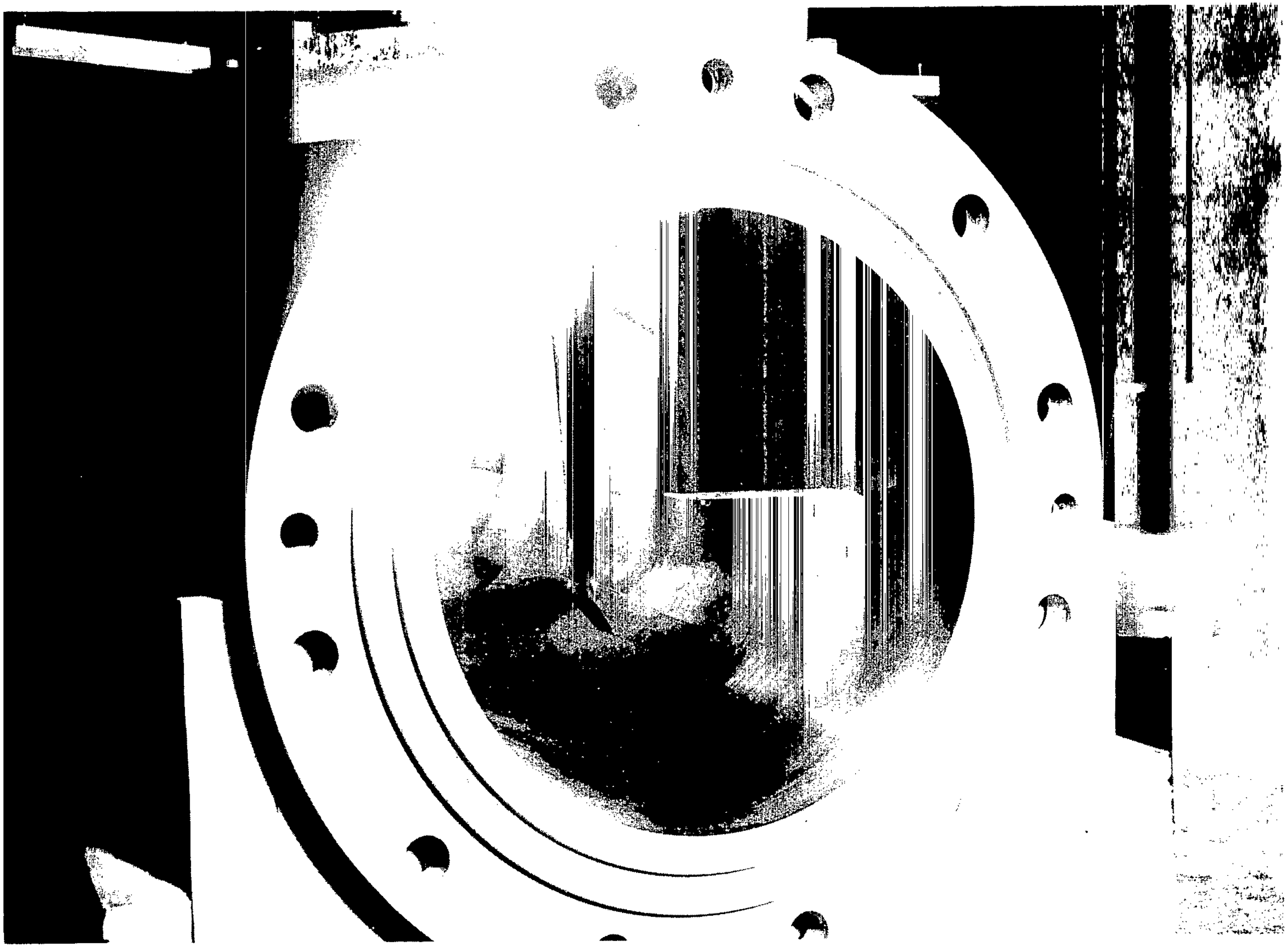

Figure 4.- Total-pressure rake.

L-68-8215

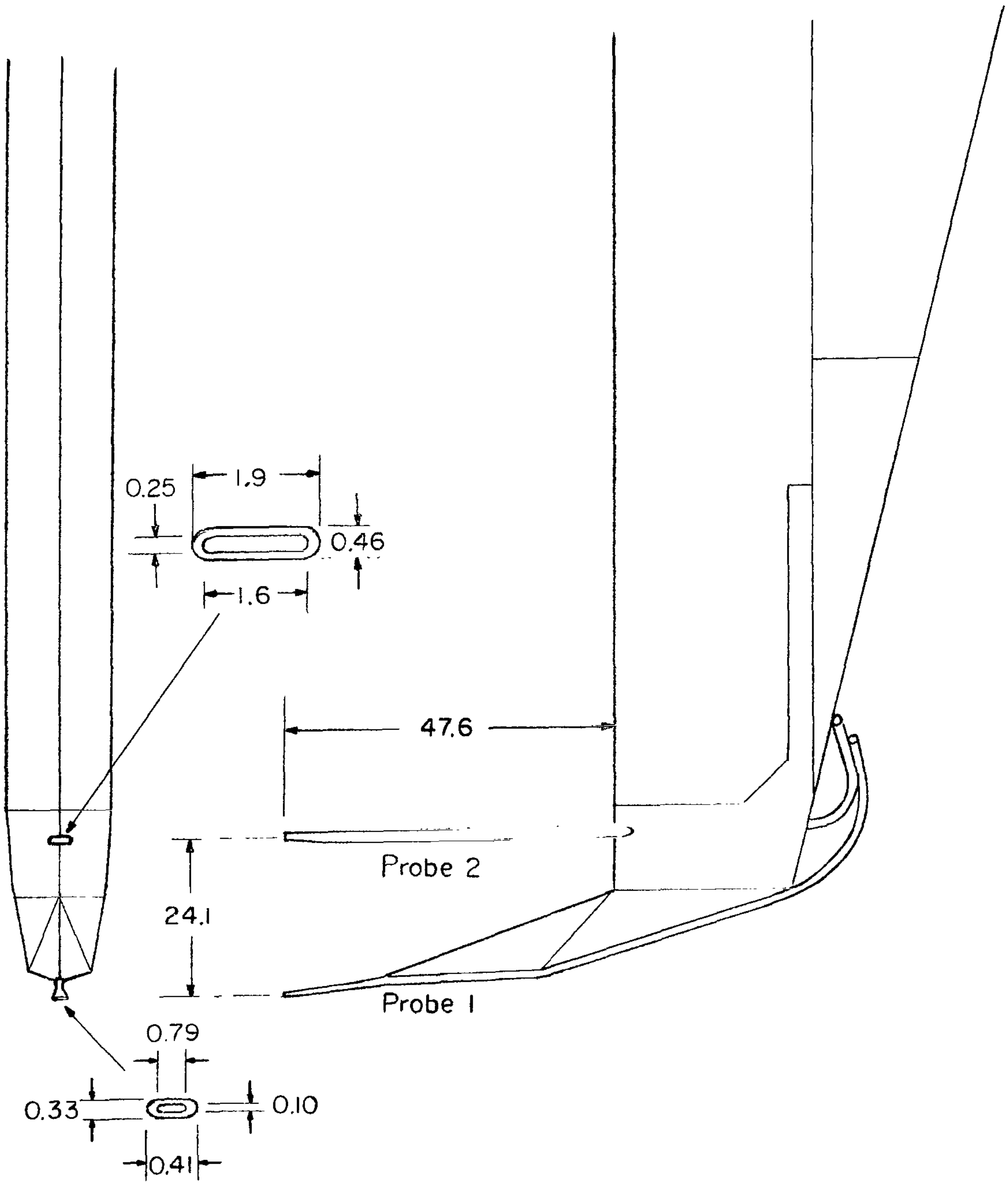

Figure 5.- Boundary-layer rake with total-pressure probes. (Dimensions are in millimeters)

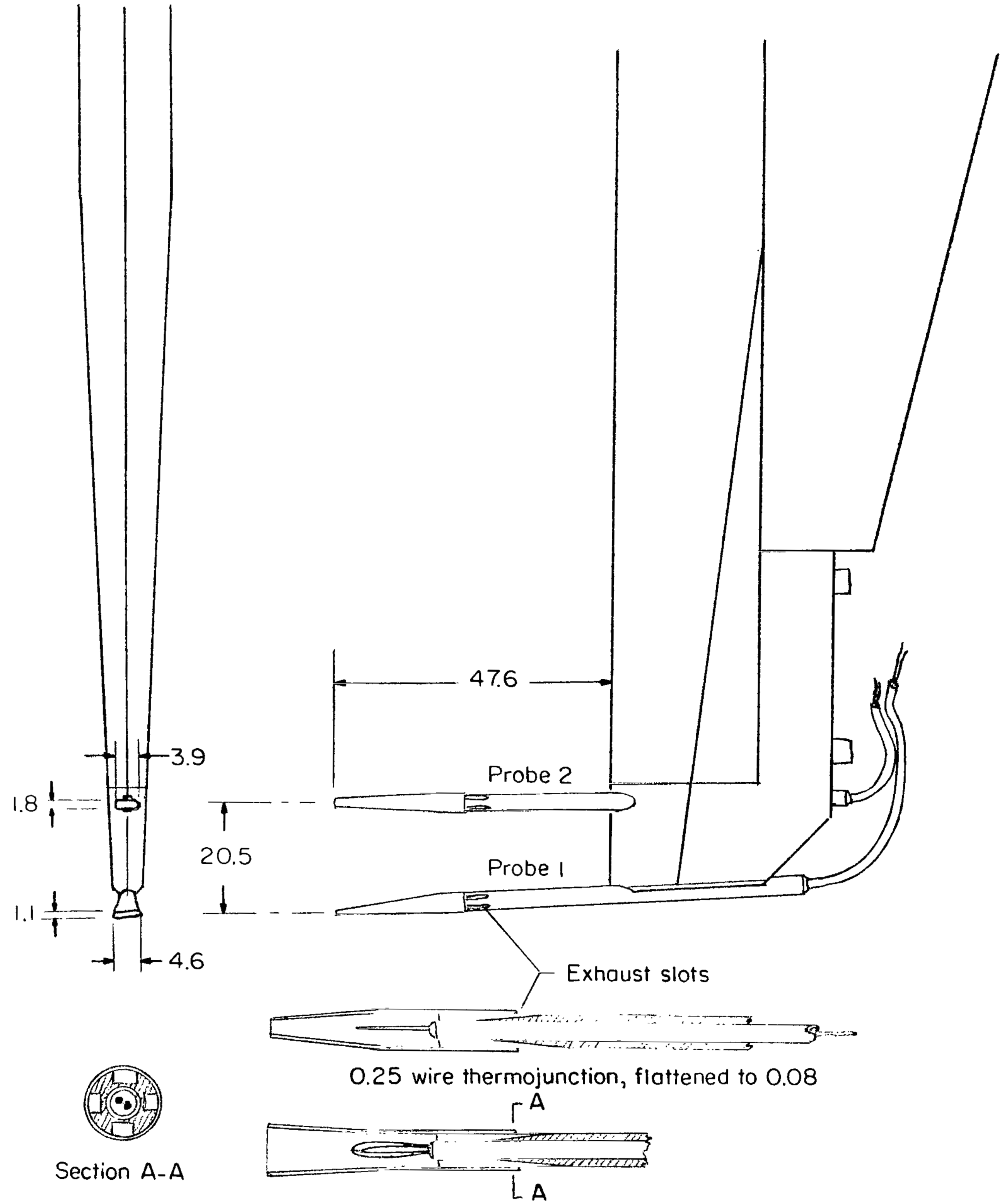

Figure 6.- Boundary-layer rake with total-temperature probes. (Dimensions are in millimeters.)

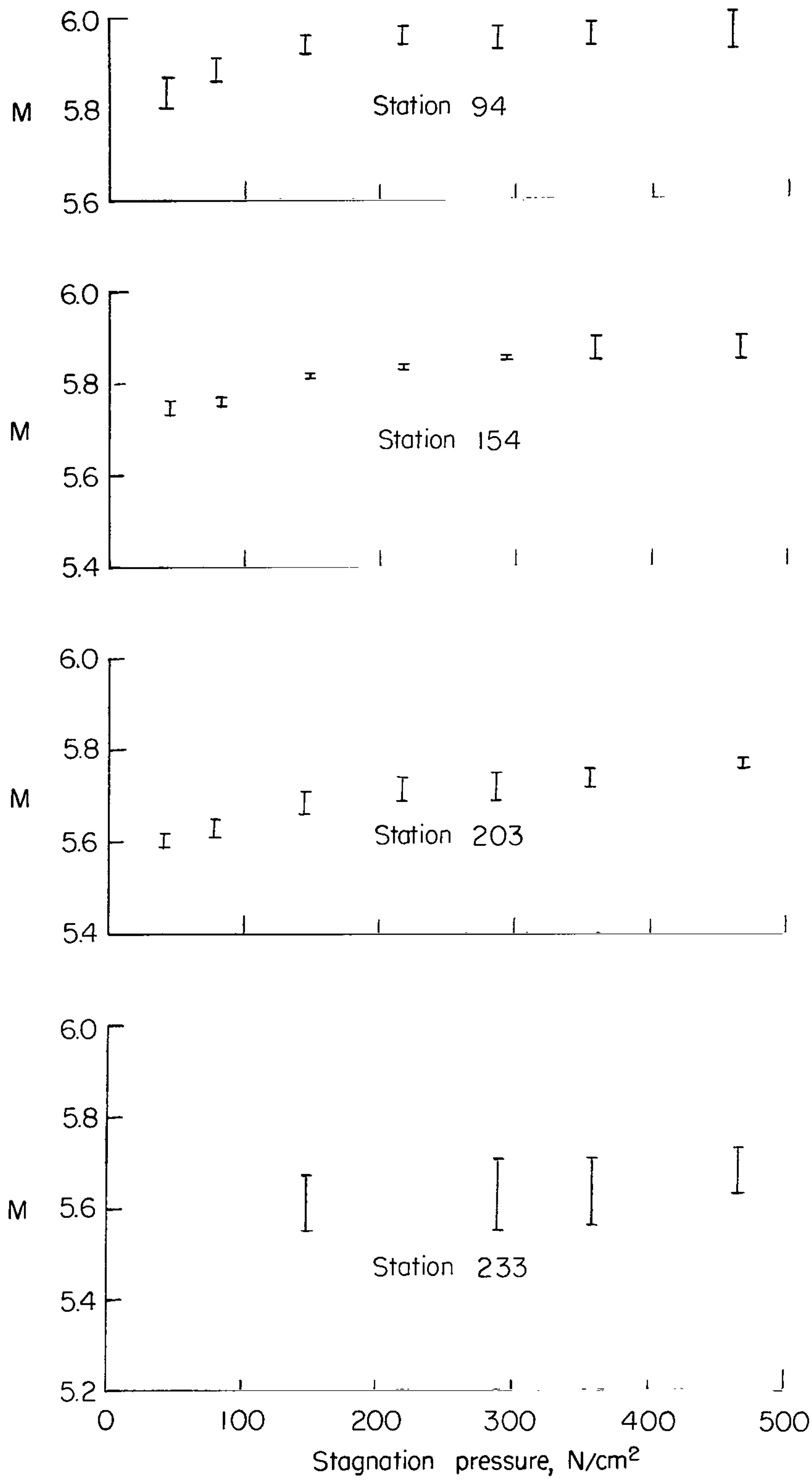

Figure 7.- Free-stream Mach number based on pitot-pressure measurement.

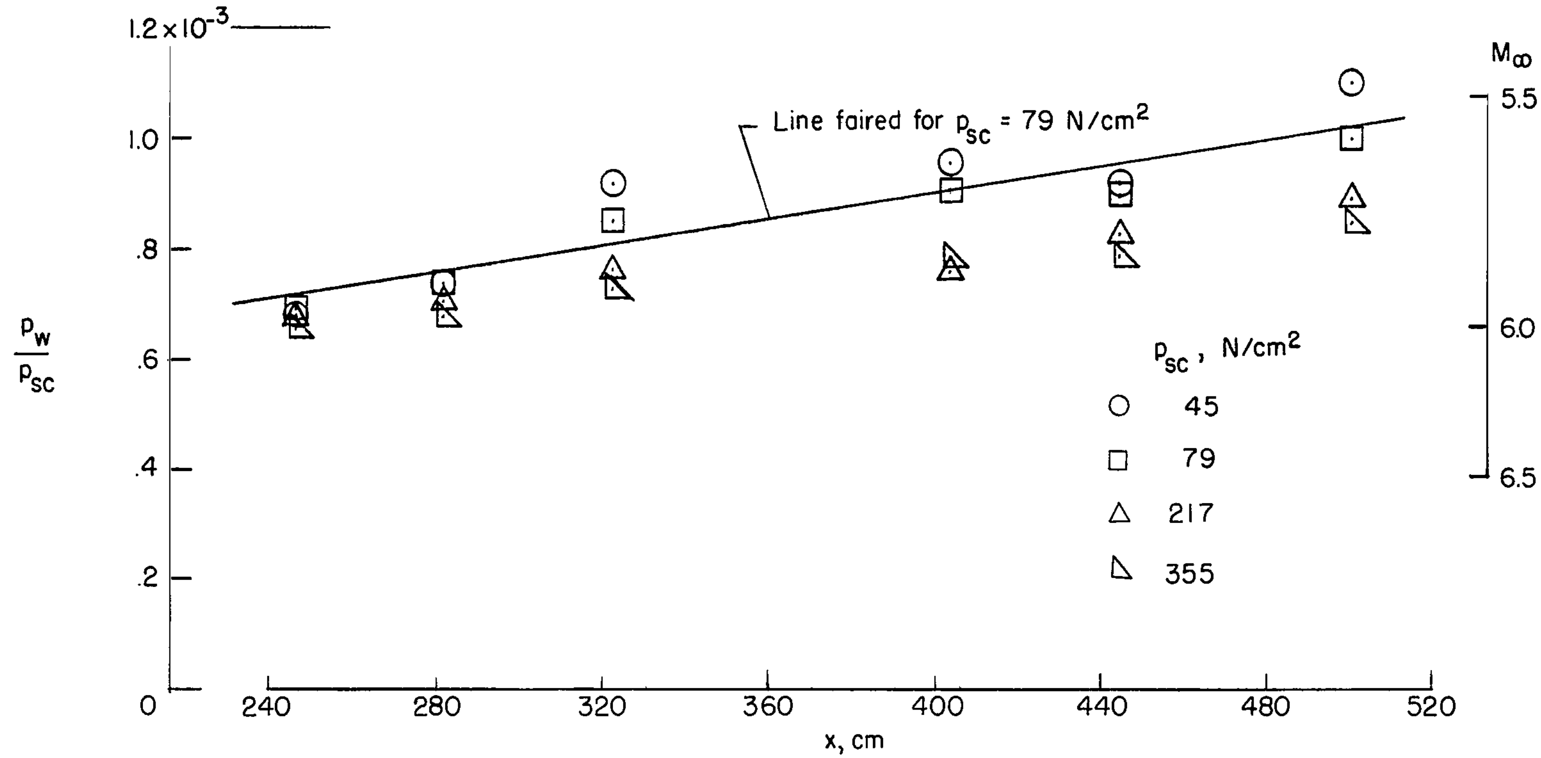

Figure 8.- Wall static pressure.

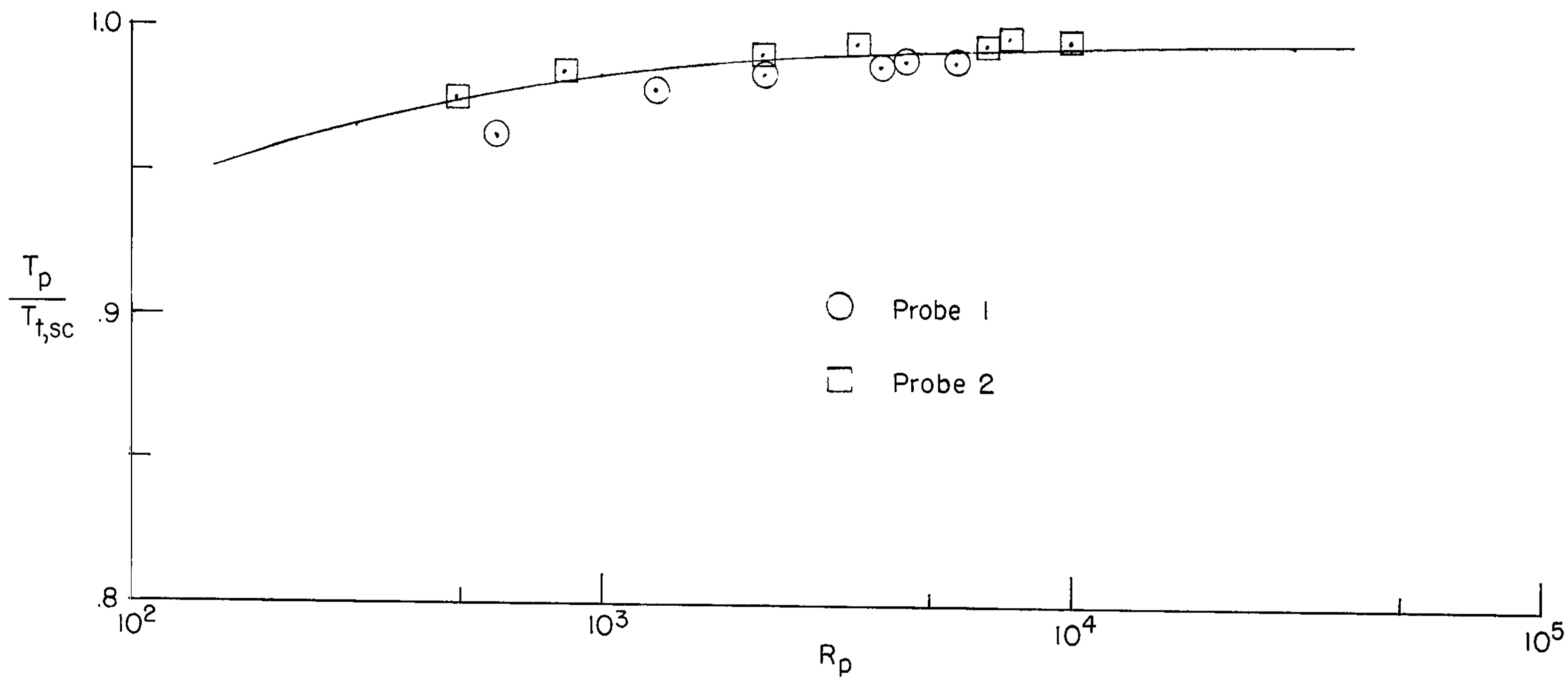

Figure 9.- Probe temperature recovery.

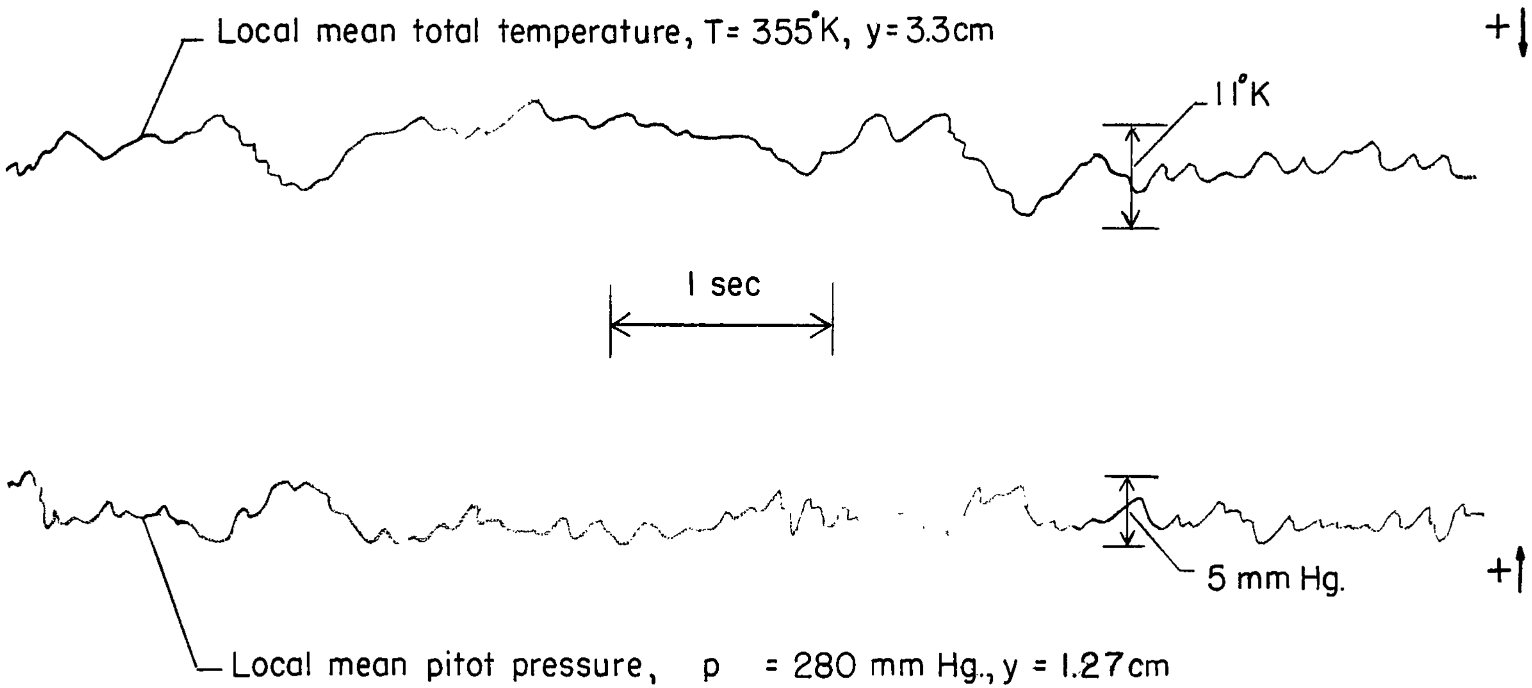

Figure 10.- Temperature and pressure fluctuations in boundary layer at station 172; 505^0 K and 355 N/cm^2.

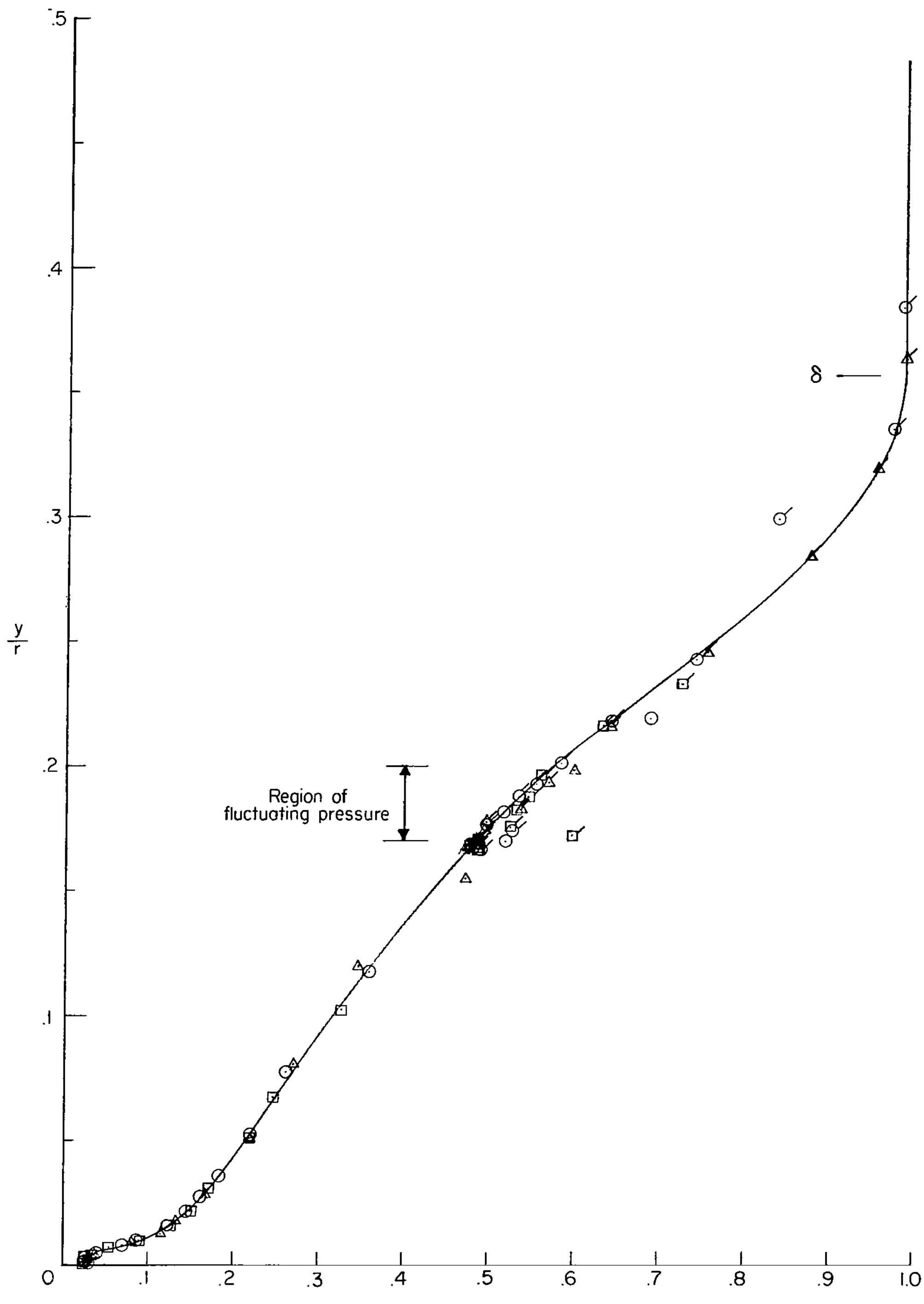

(a) $p_{sc} = 45\ N/cm^2$.

Figure 11.- Total-pressure survey at station 94. Flagged symbols indicate data for probe 2.

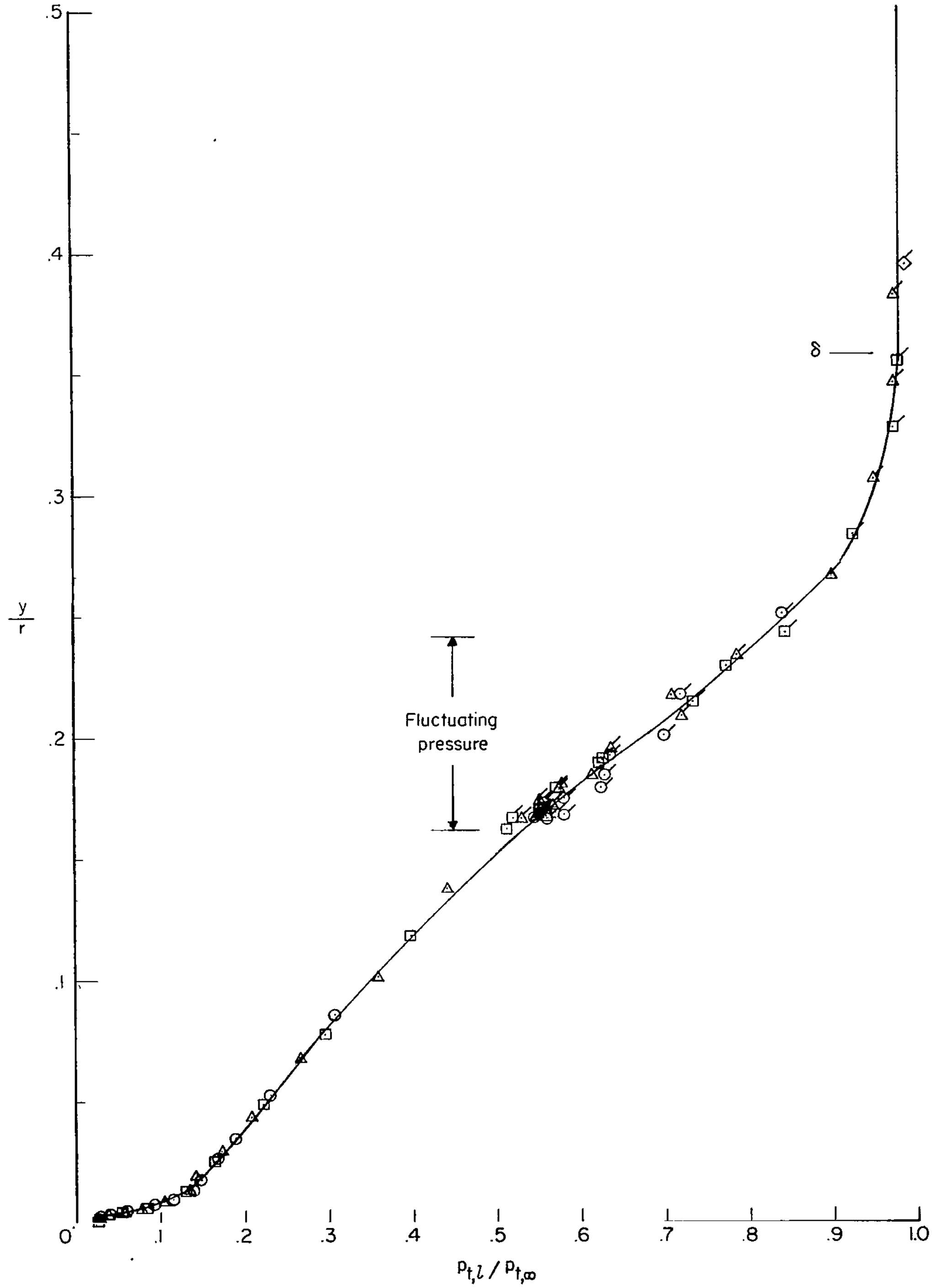

(b) $p_{sc} = 79\ N/cm^2$.

Figure 11.- Continued.

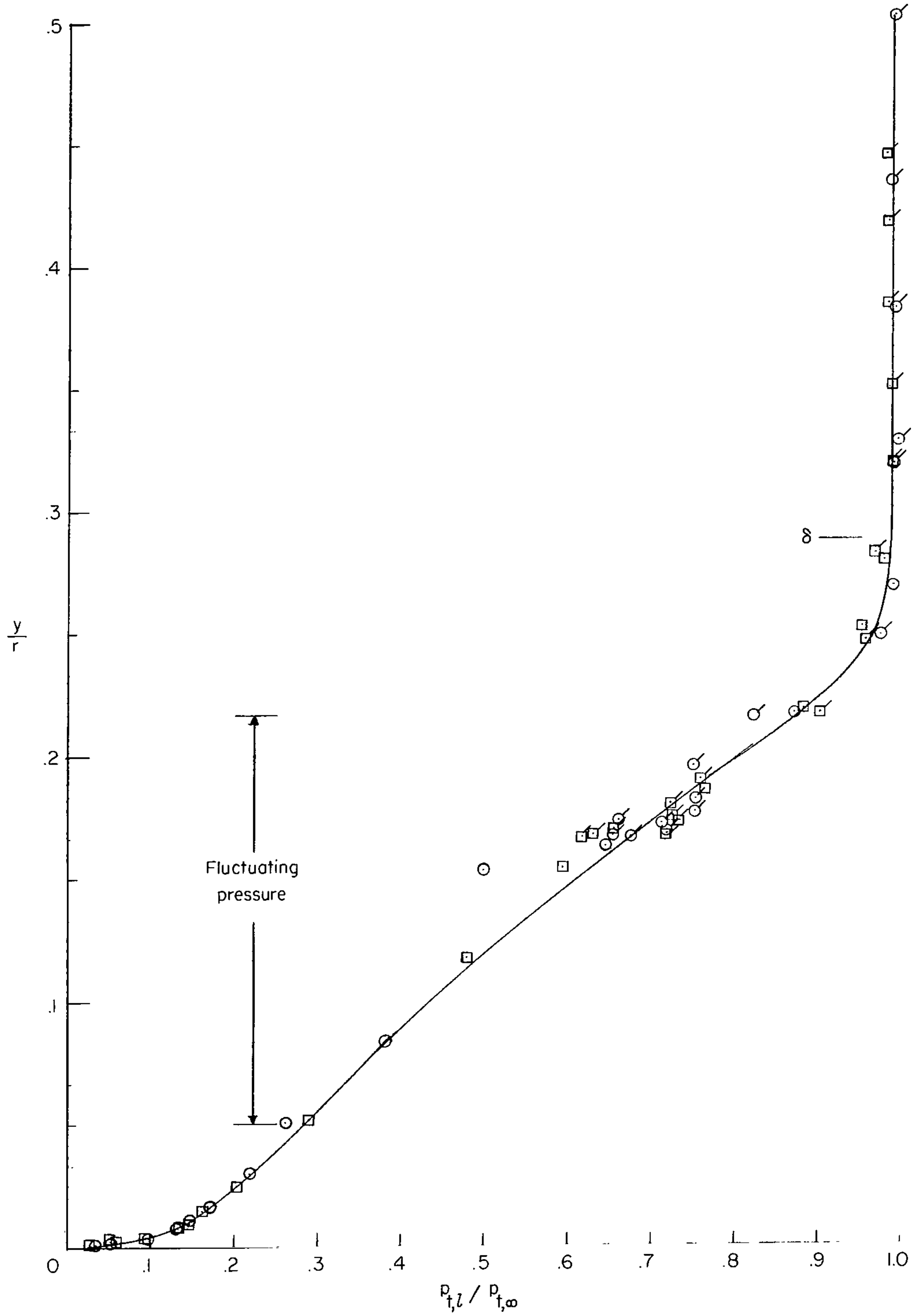

(c) p_{sc} = 217 N/cm^2.

Figure 11.- Continued.

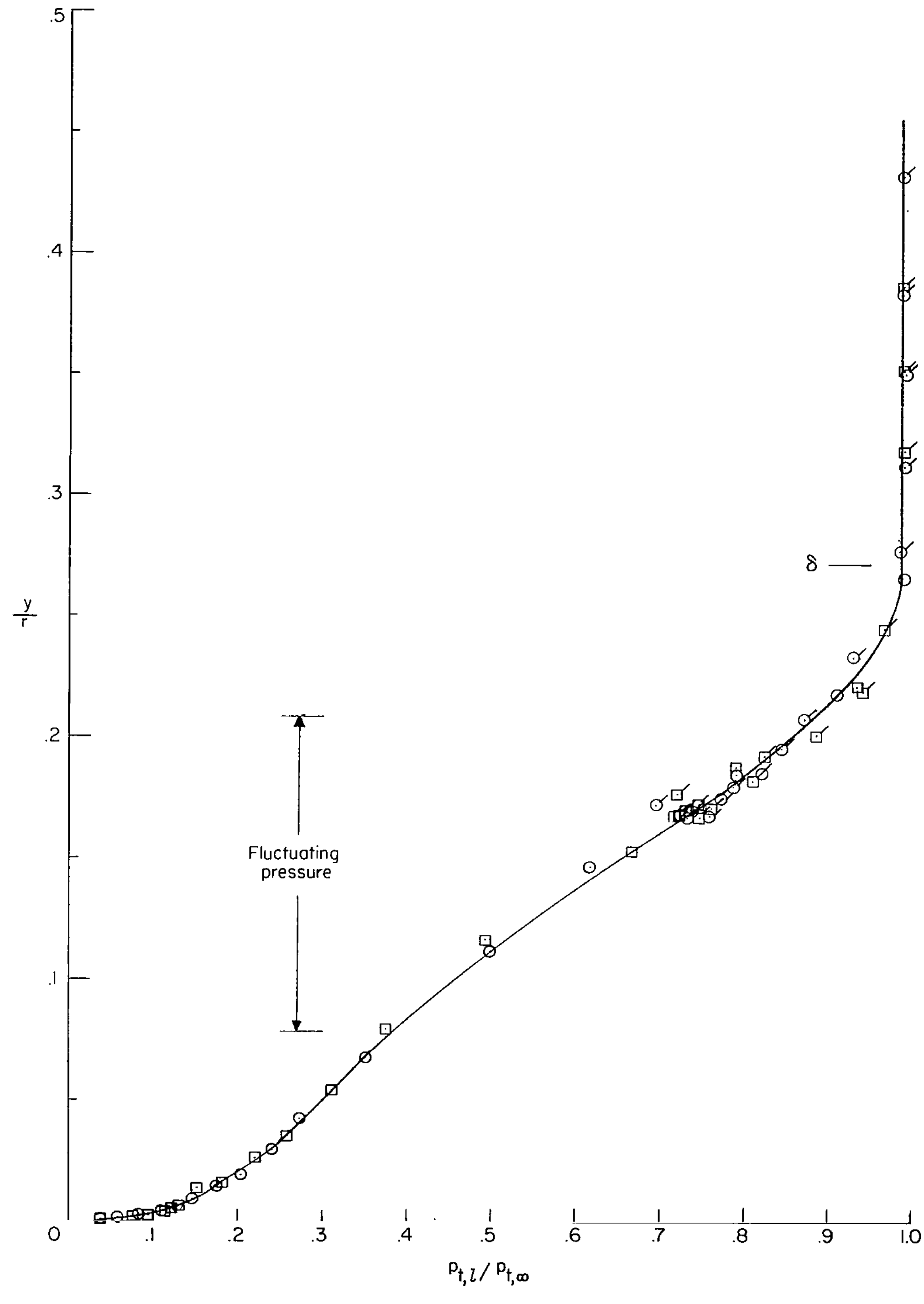

(d) p_{sc} = 424 N/cm^2.

Figure 11.- Concluded.

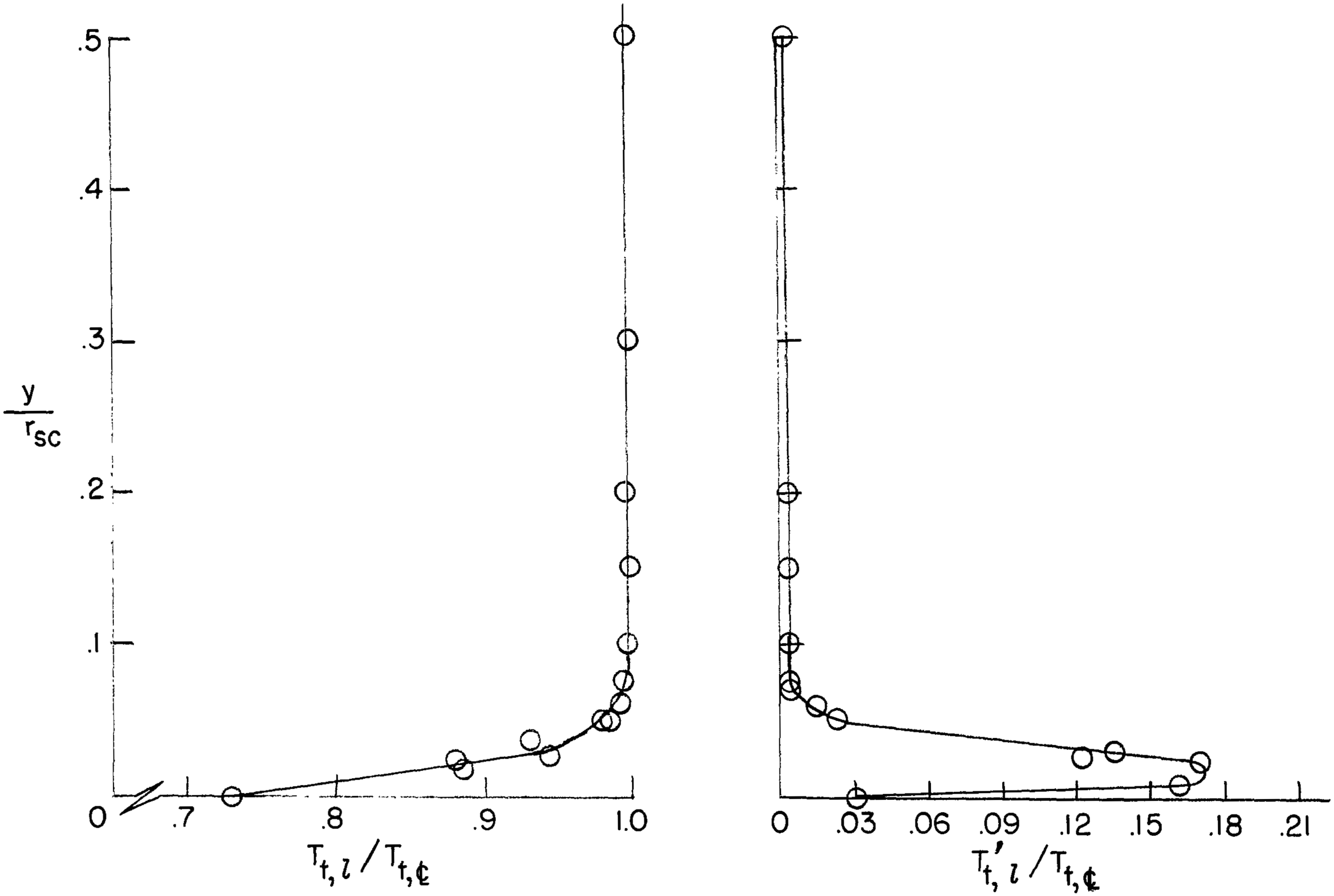

(a) Time-average temperature.

(b) Temperature fluctuations.

Figure 12.- Stagnation-chamber surveys.

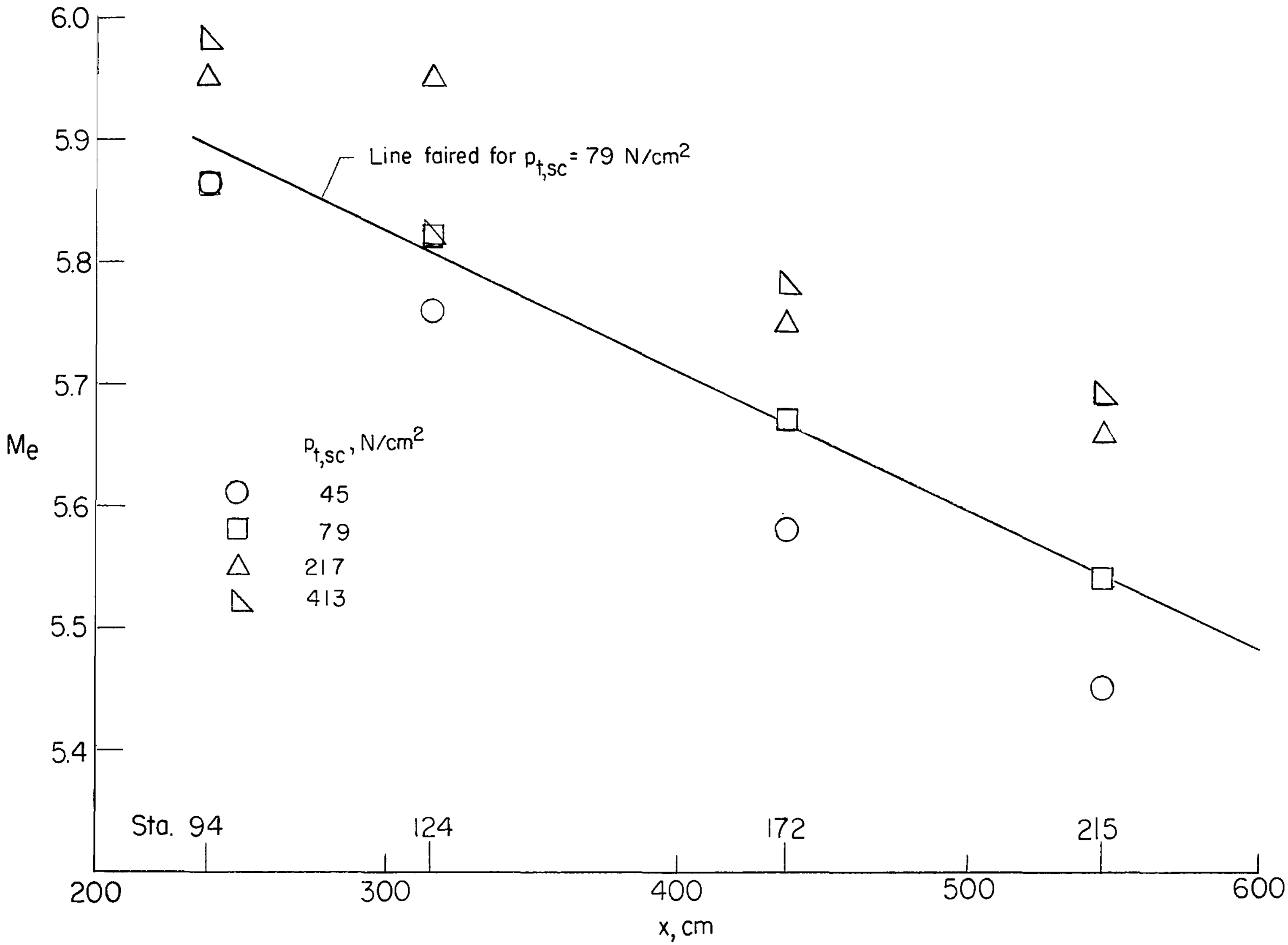

Figure 13.- Mach number at edge of boundary layer.

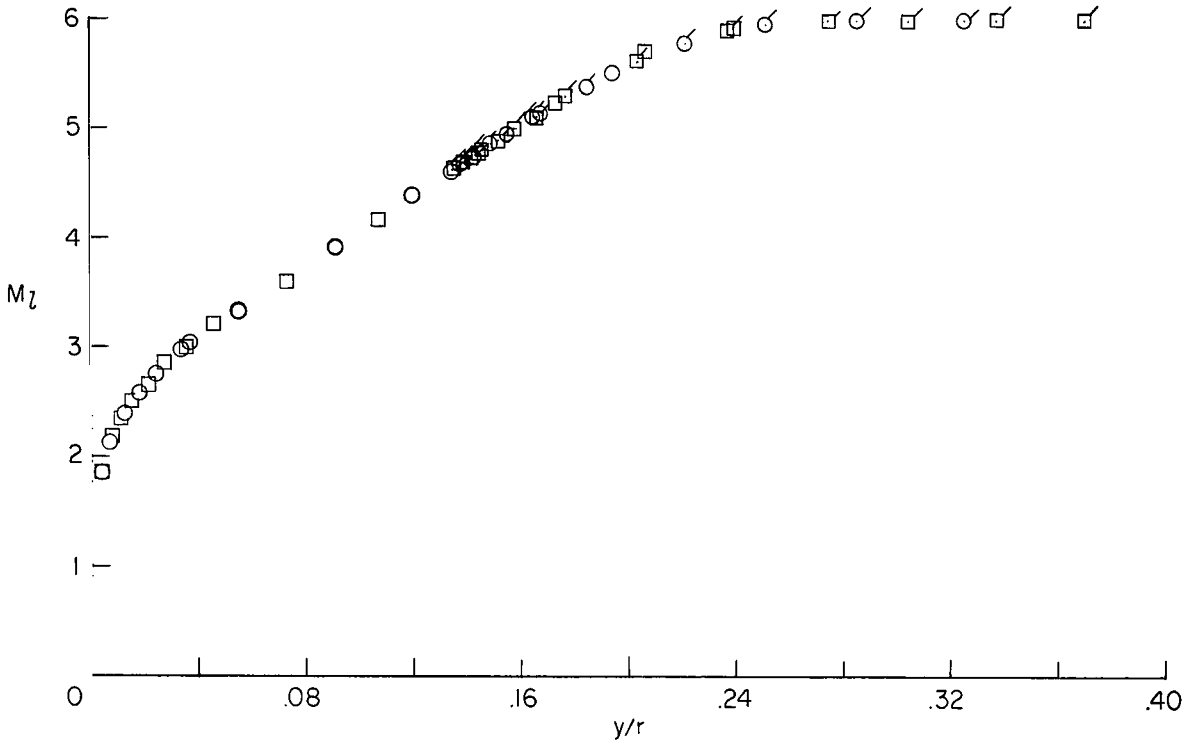

(a) p_{sc} = 424 N/cm^2.

Figure 14.- Local Mach number in boundary layer at station 94.

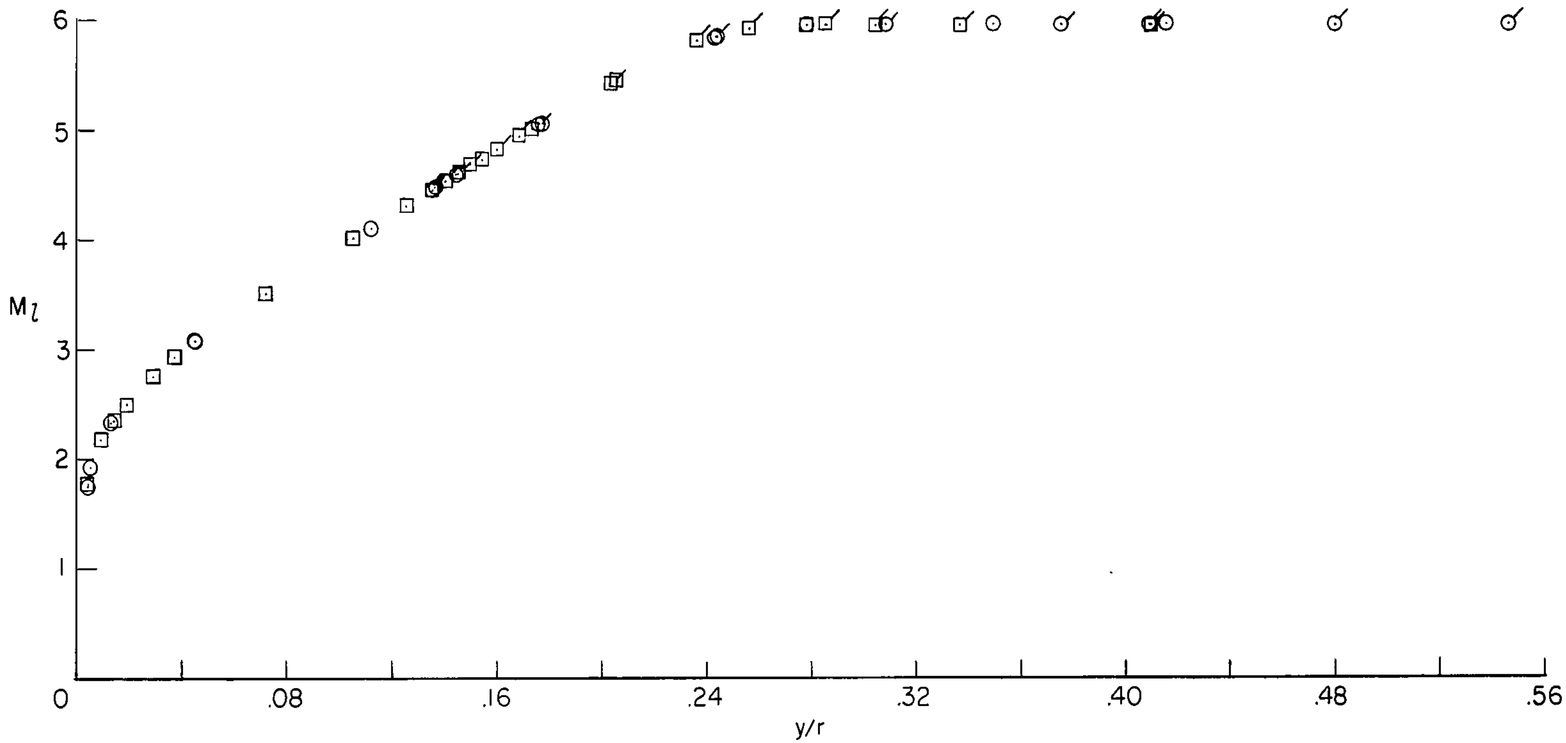

(b) p_{sc} = 217 N/cm^2.

Figure 14.- Continued.

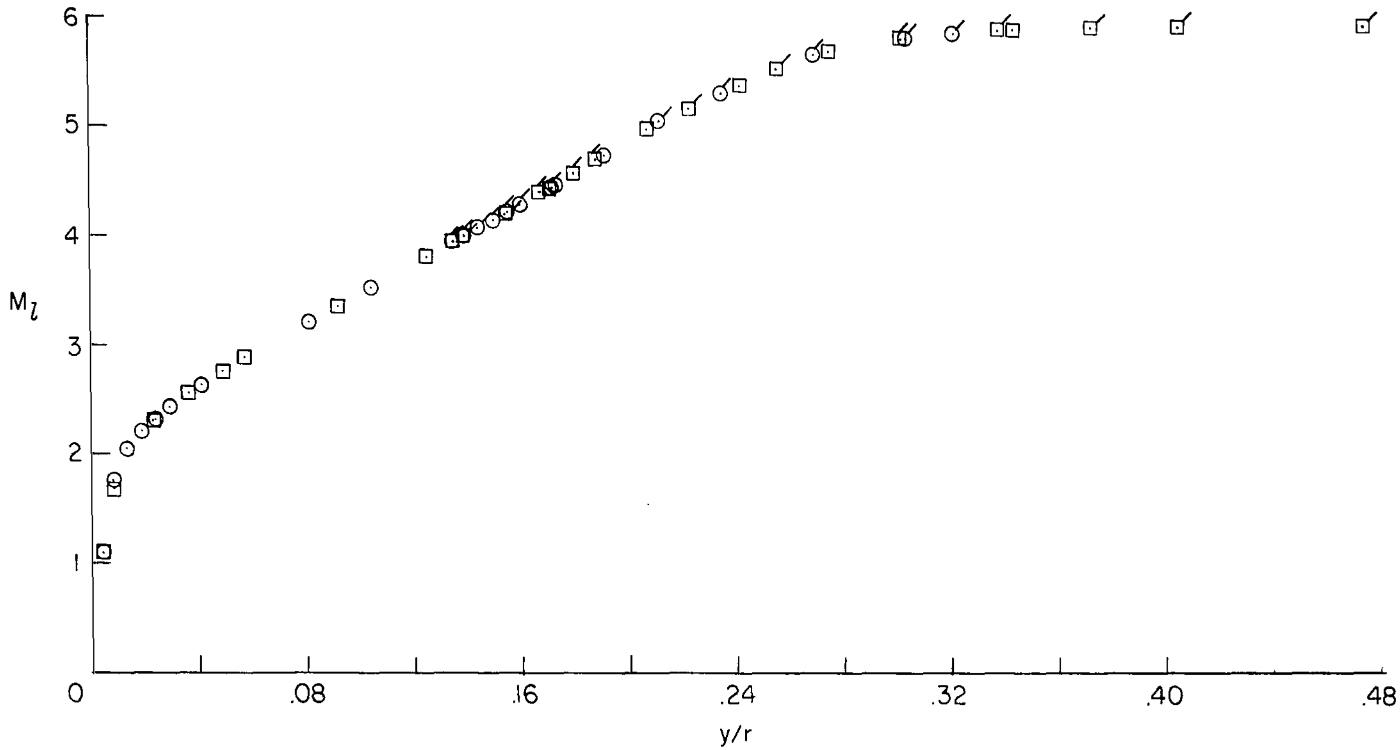

(c) $p_{sc} = 79\ N/cm^2$.

Figure 14.- Continued.

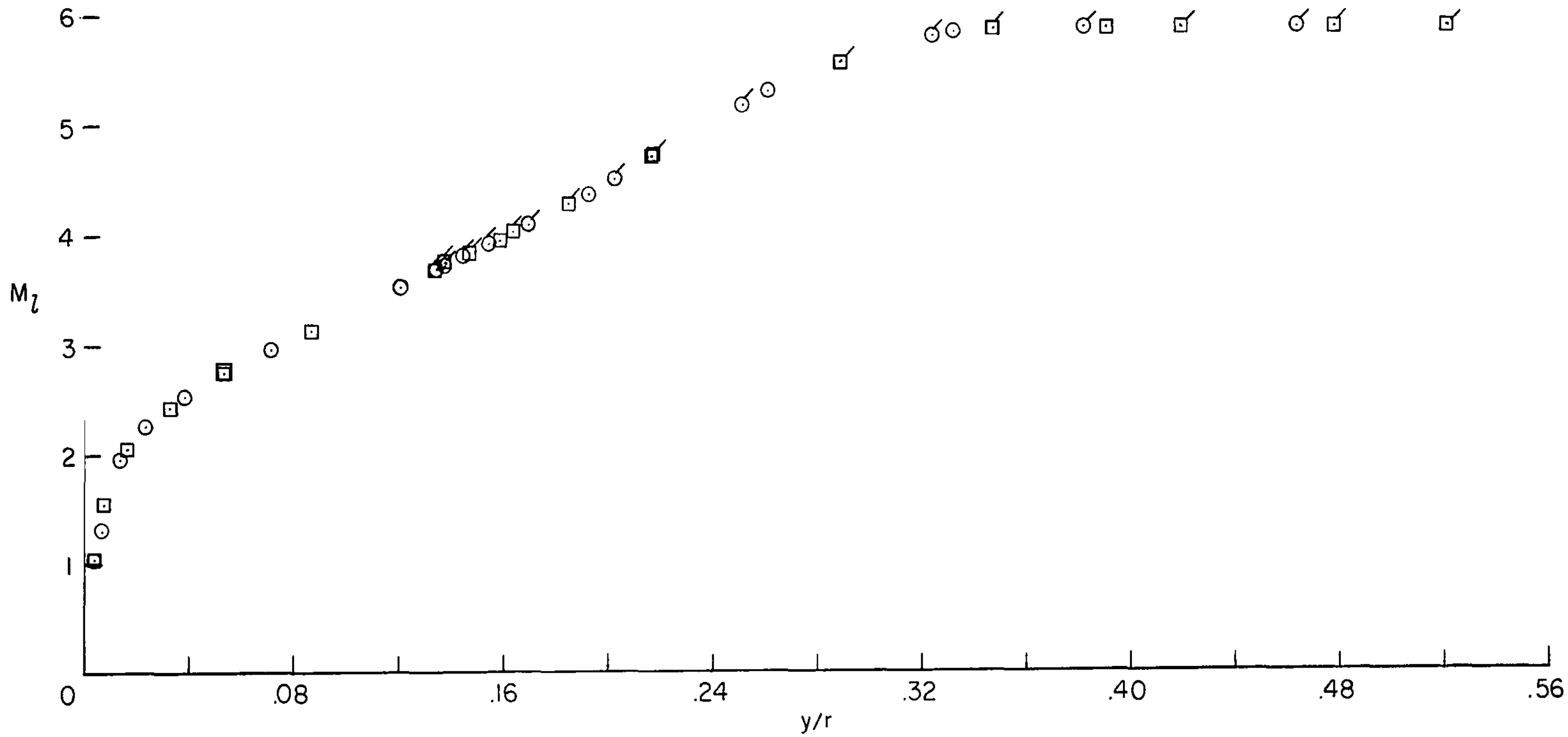

(d) $p_{sc} = 45\ N/cm^2$.

Figure 14.- Concluded.

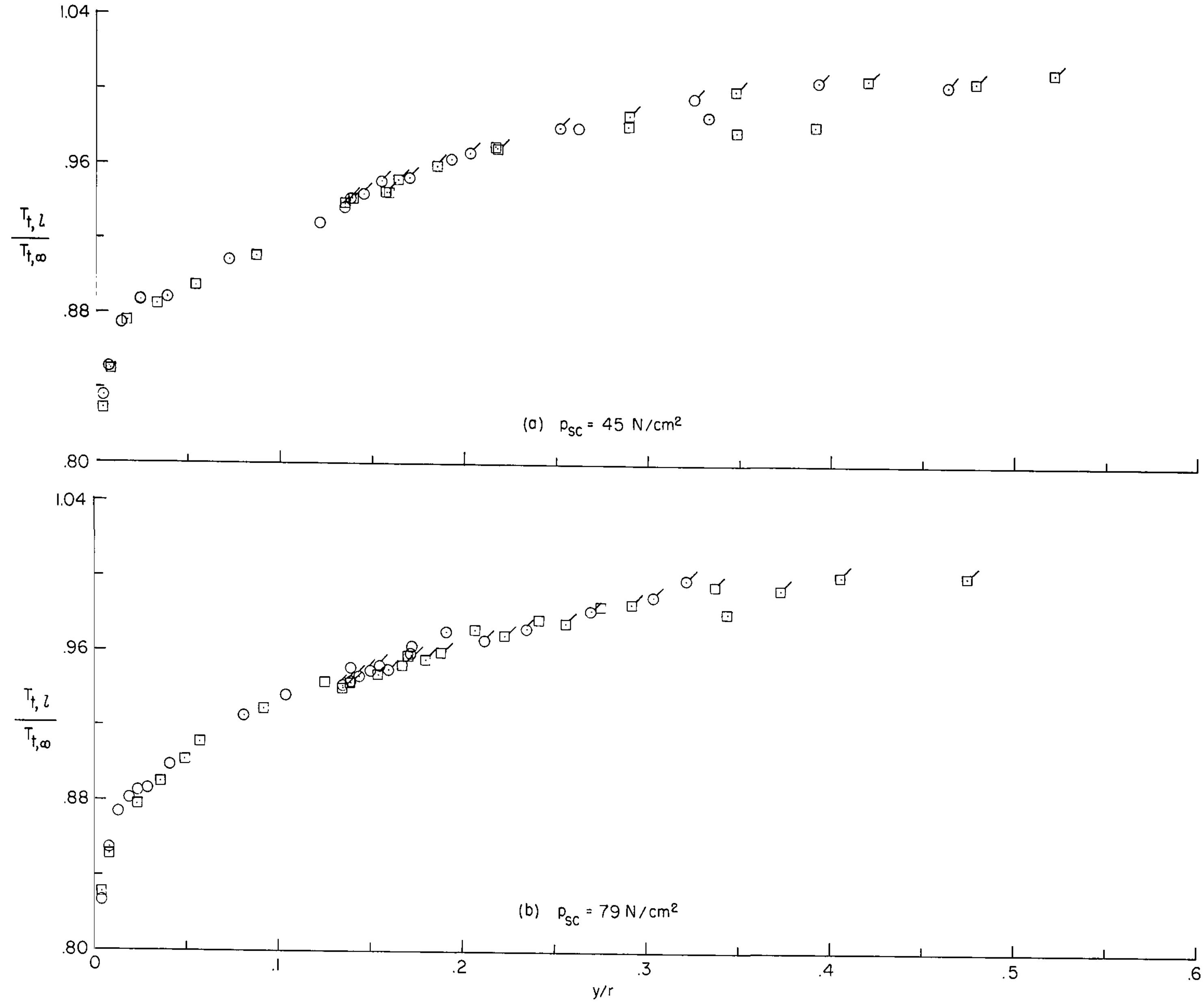

Figure 15.- Temperature profiles at station 94.

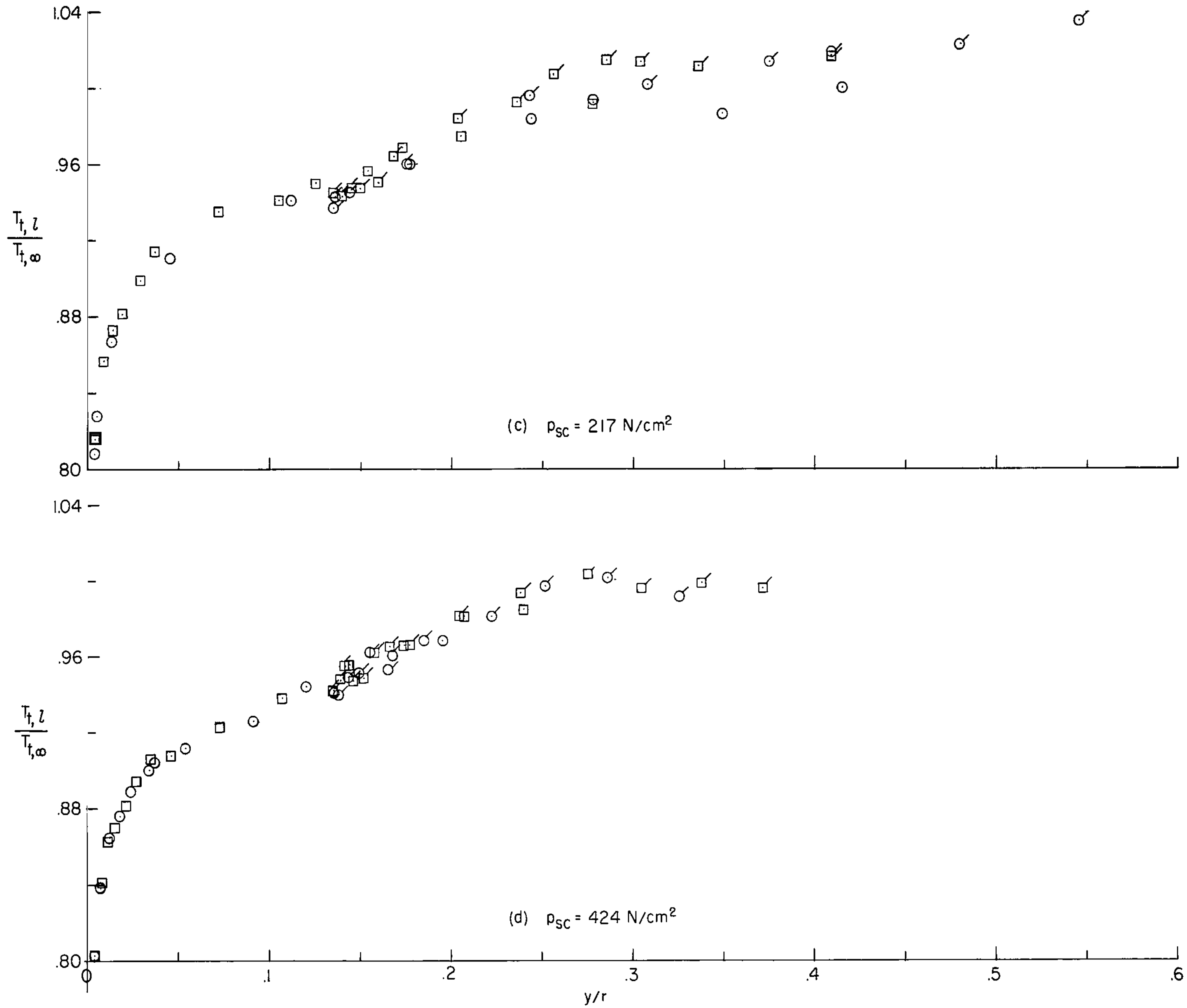

Figure 15.- Concluded.

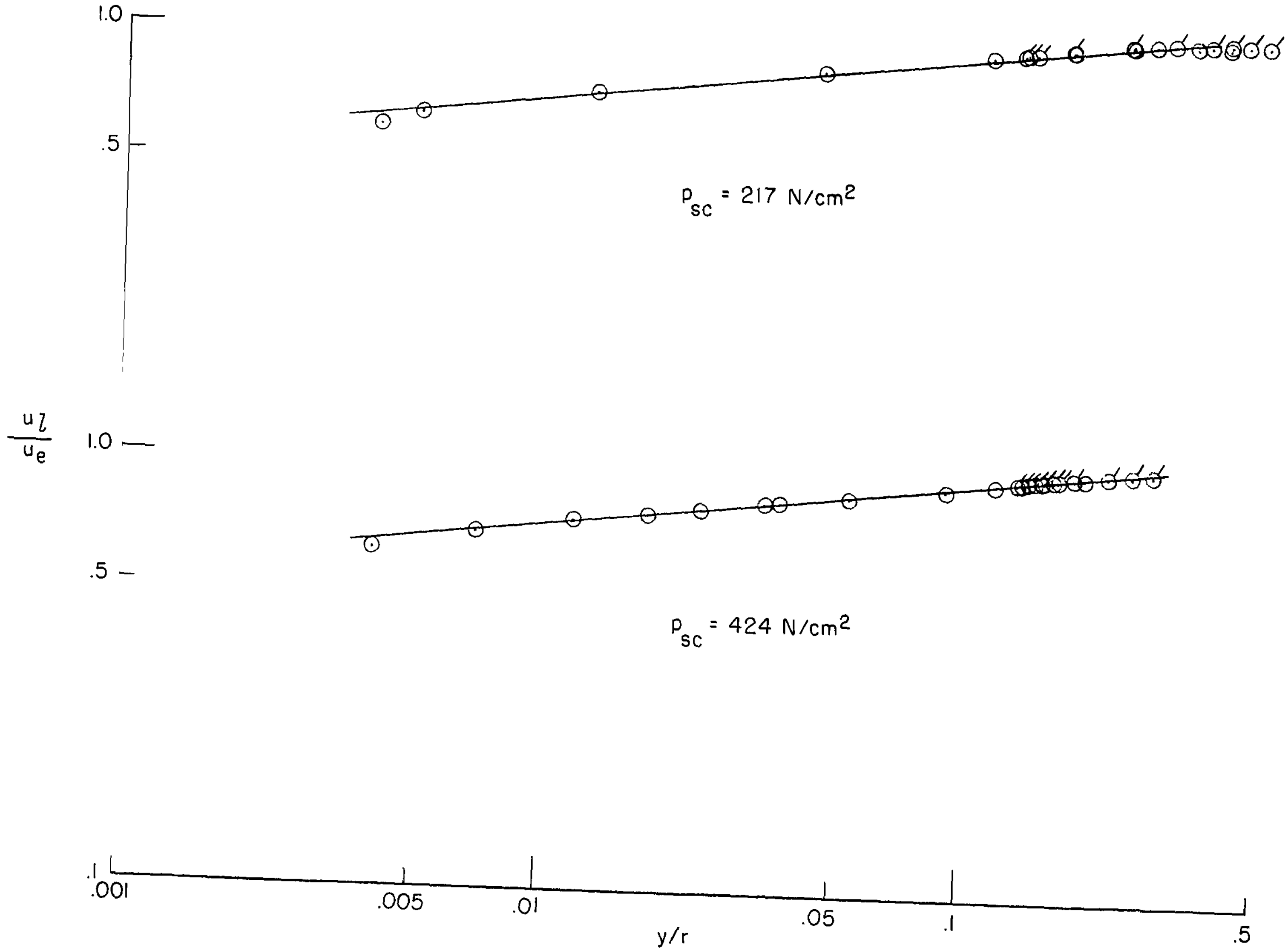

(a) p_{sc} = 424 and 217 N/cm^2.

Figure 16.- Velocity profile at station 94.

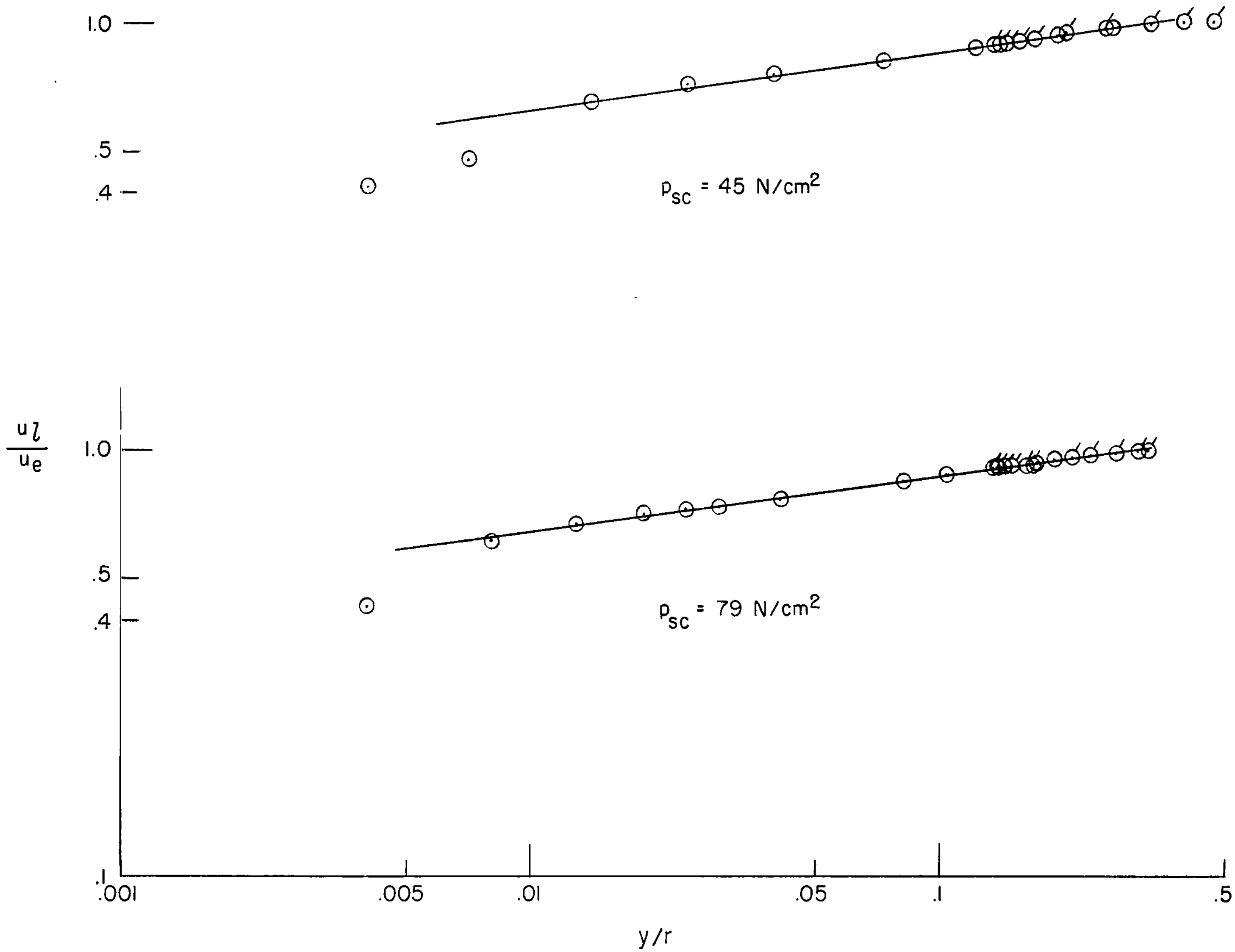

(b) p_{sc} = 79 and 45 N/cm^2.

Figure 16.- Concluded.

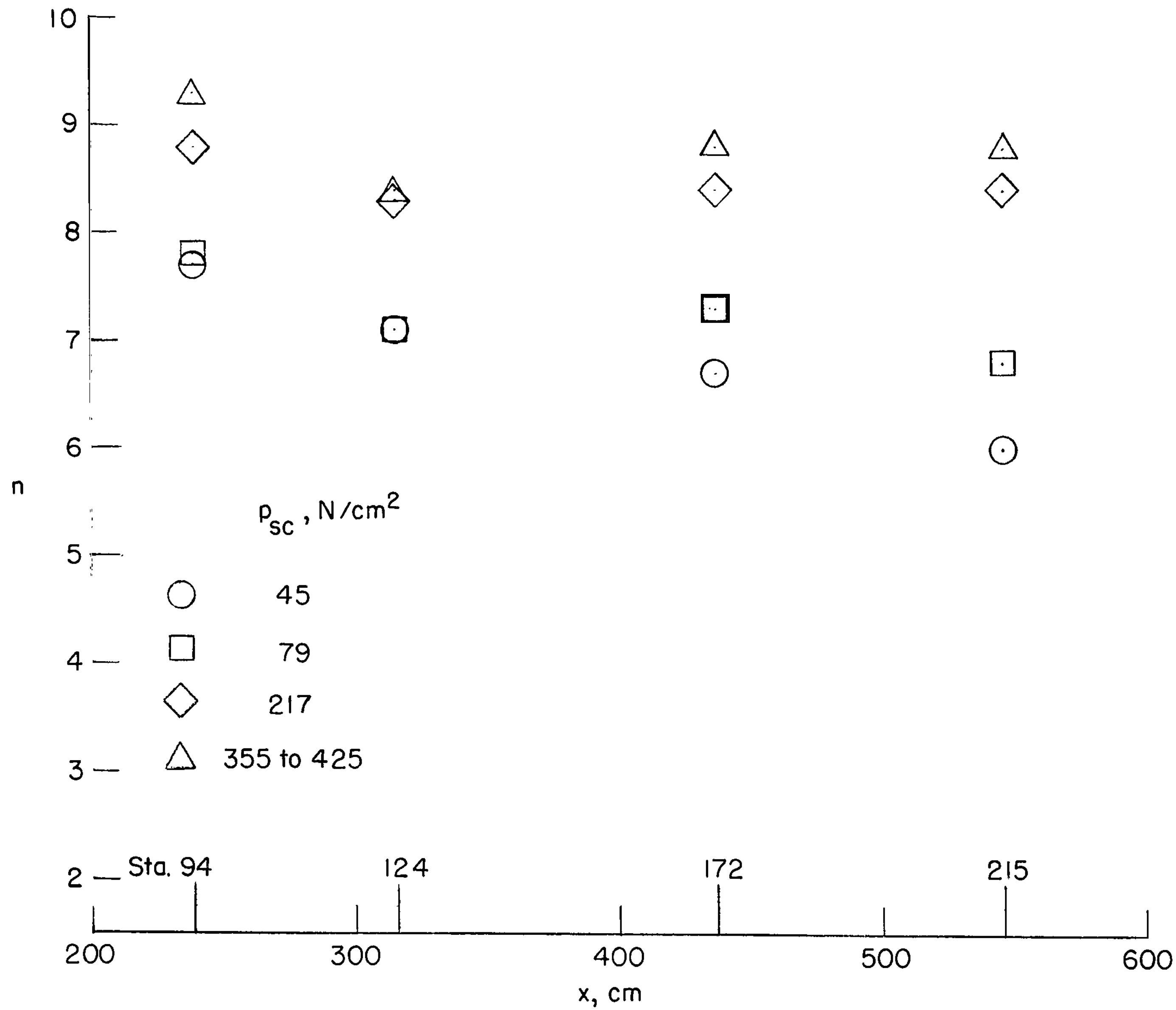

Figure 17.- Variation of n with x.

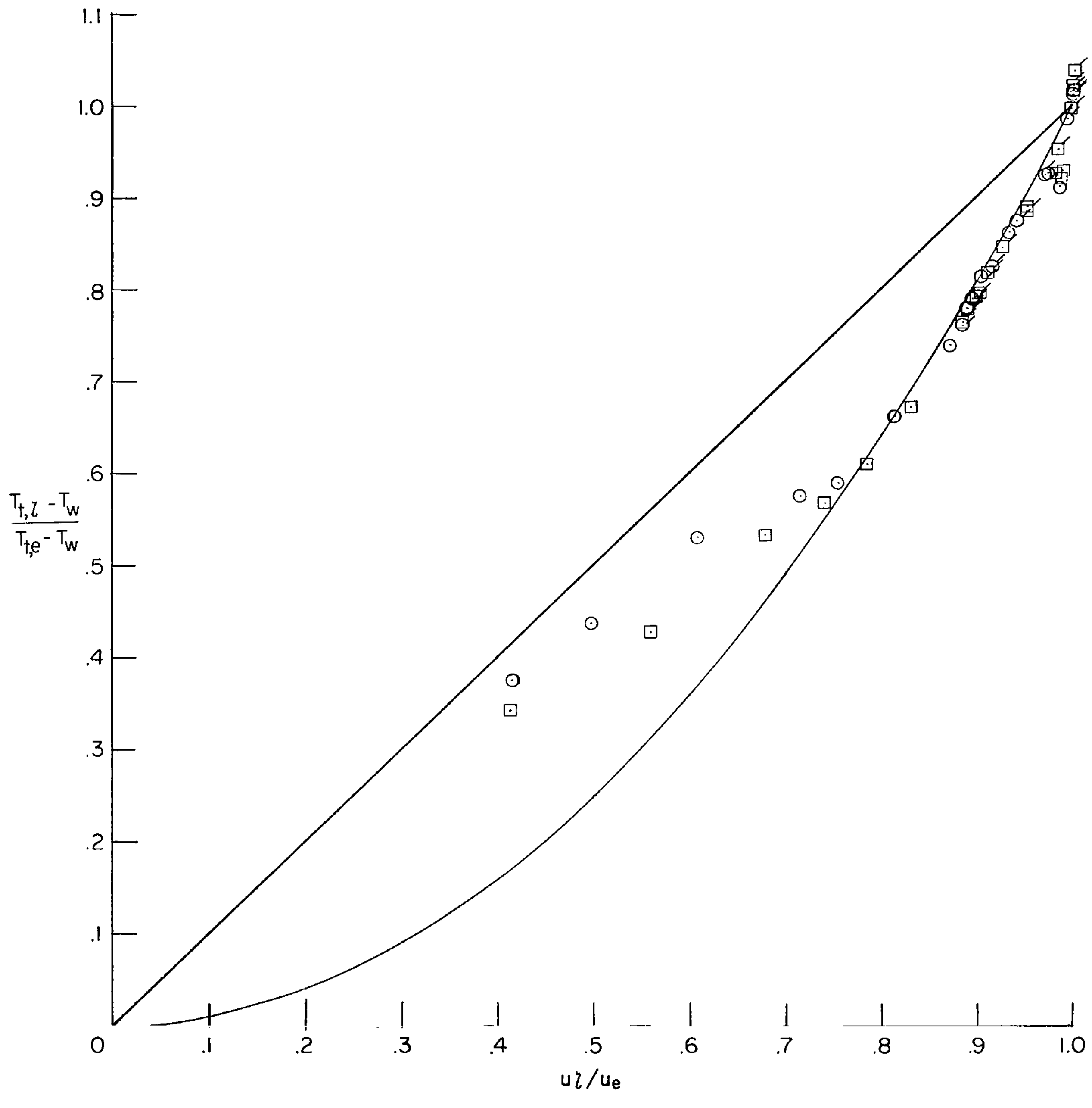

(a) $p_{sc} = 45\ N/cm^2$.

Figure 18.- Temperature-velocity relation.

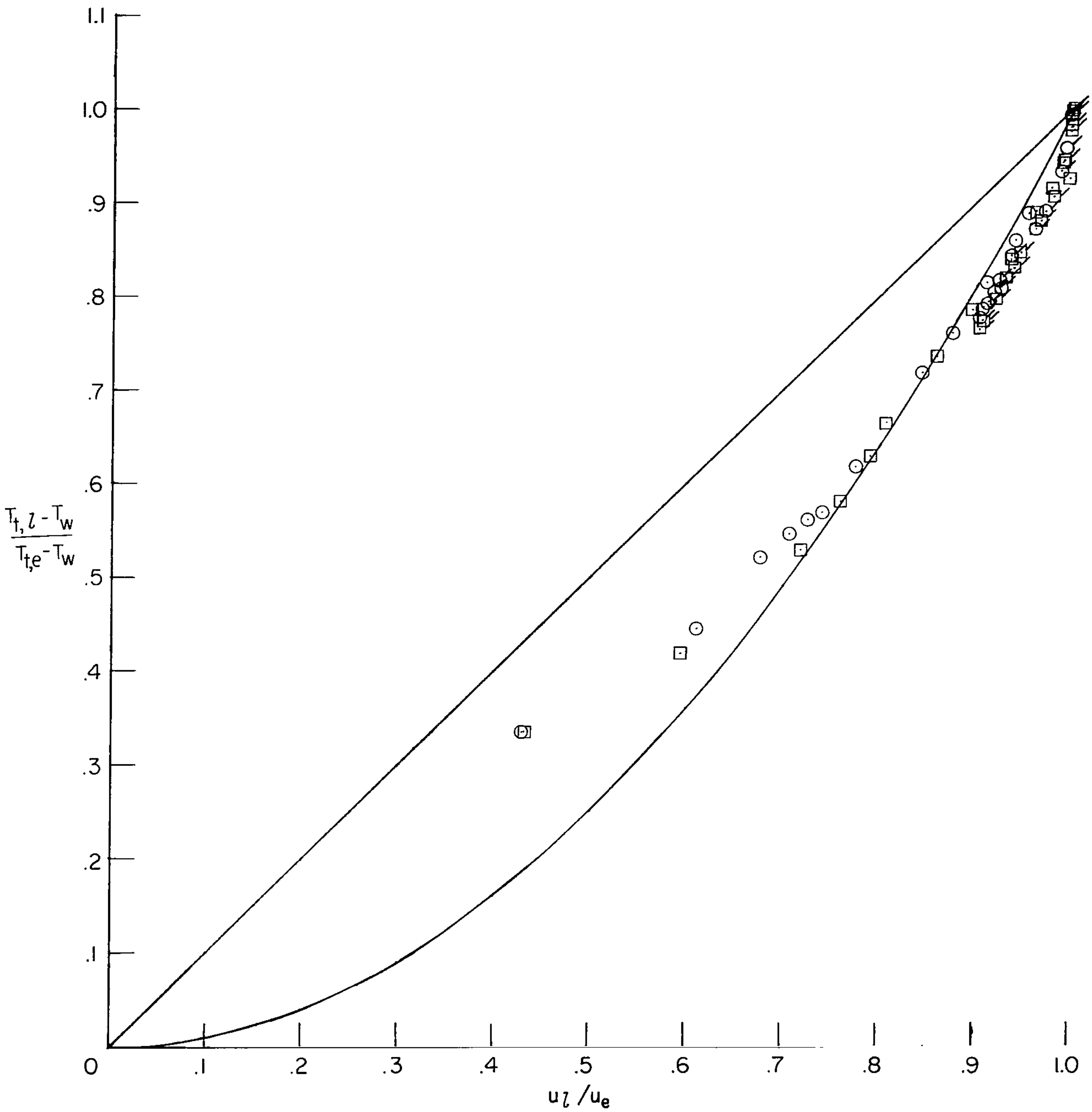

(b) $p_{sc} = 79\ N/cm^2$.

Figure 18.- Continued.

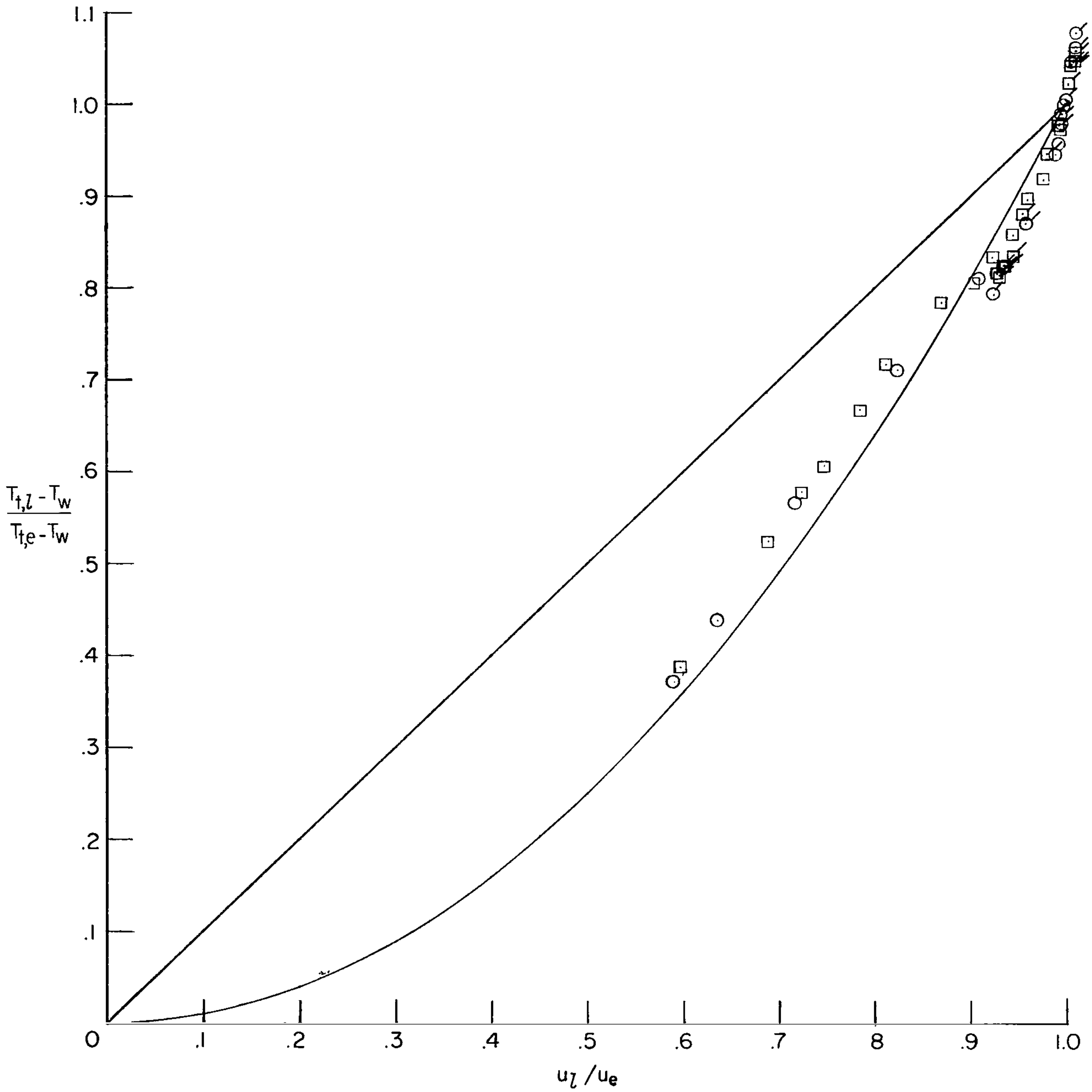

(c) p_{sc} = 217 N/cm^2.

Figure 18.- Continued.

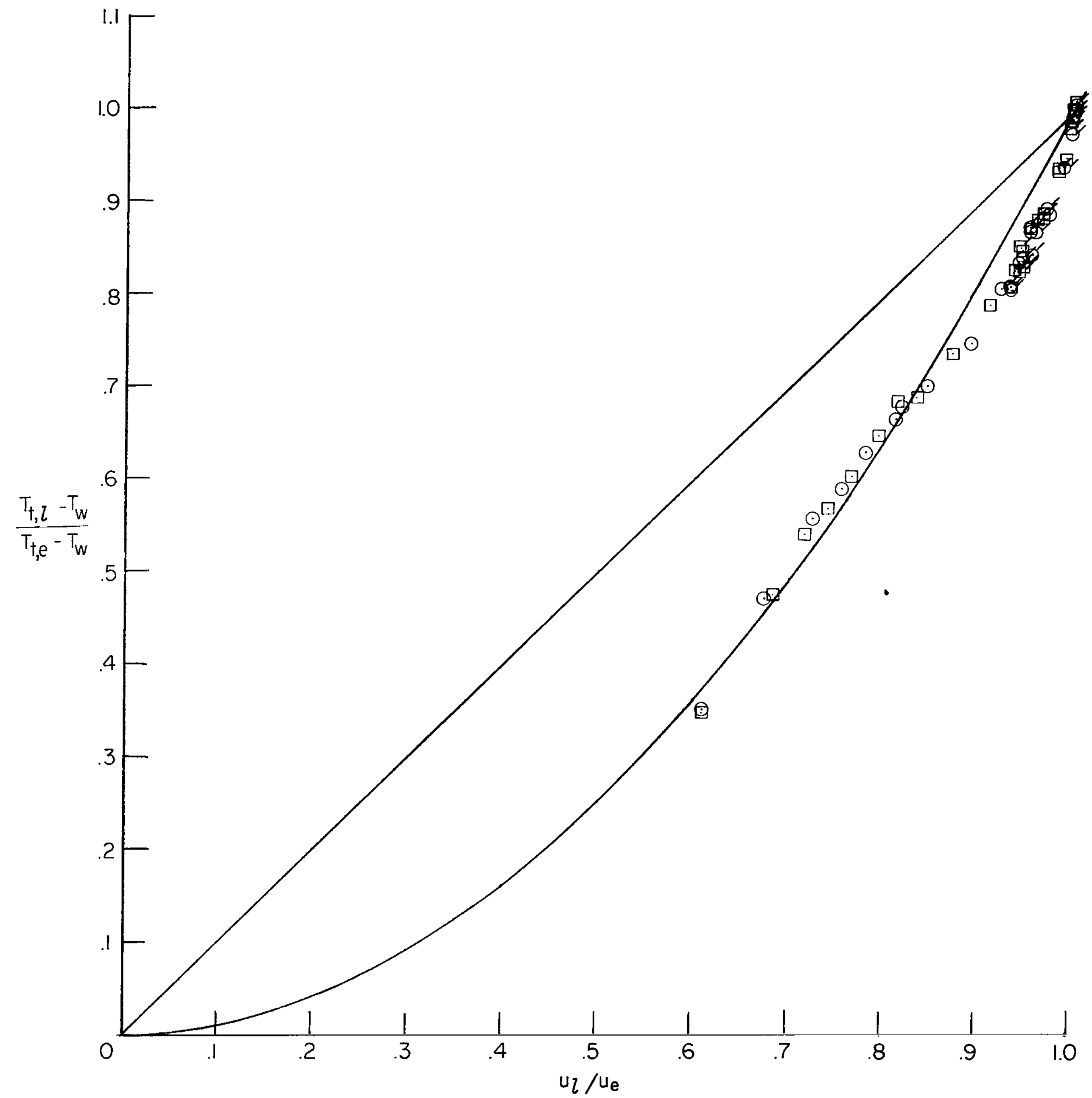

(d) $p_{sc} = 424\ N/cm^2$.

Figure 18.- Concluded.

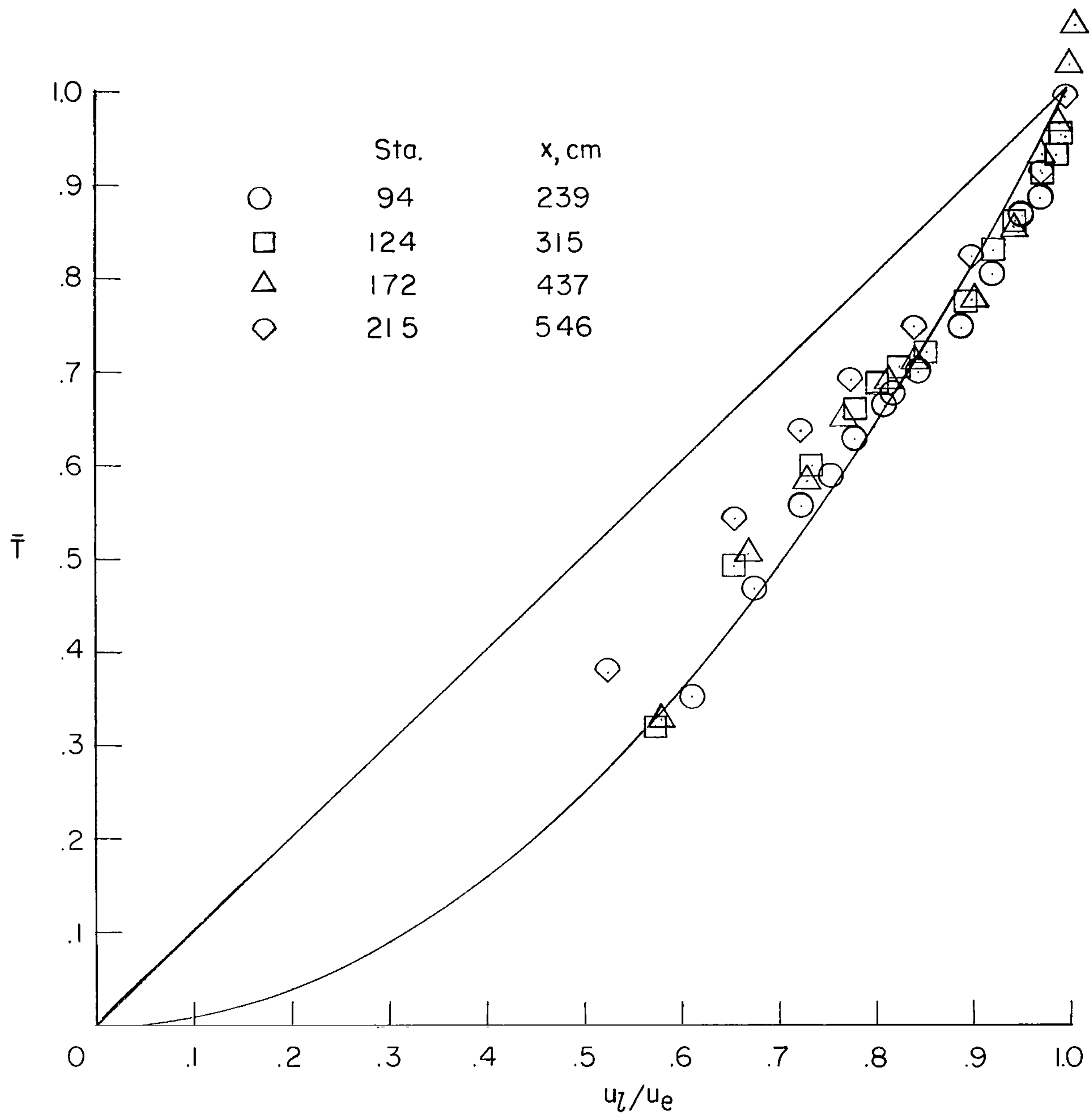

Figure 19.- Comparison of temperature-velocity profiles for different stations at highest Reynolds number.

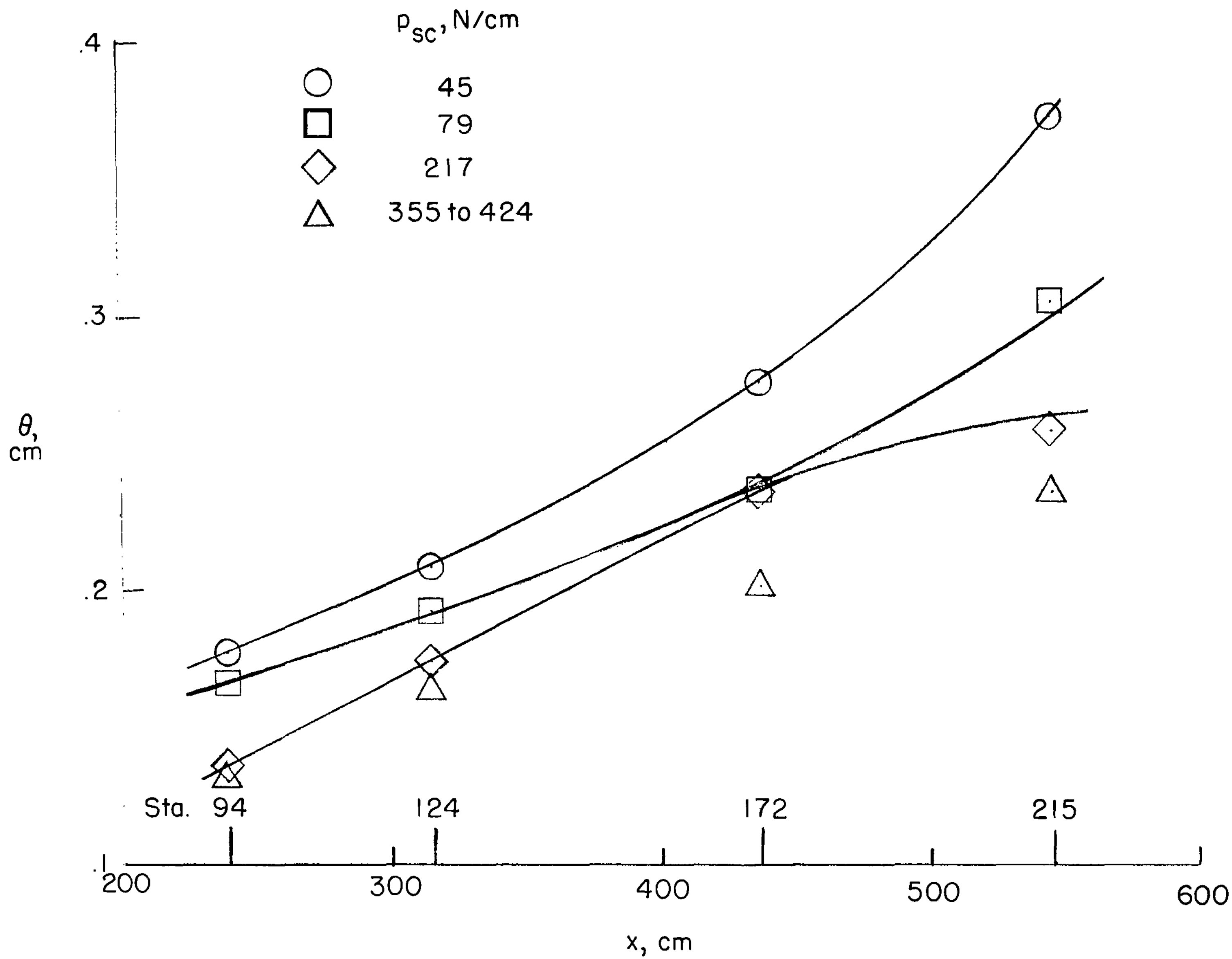

Figure 20.- Momentum thickness.

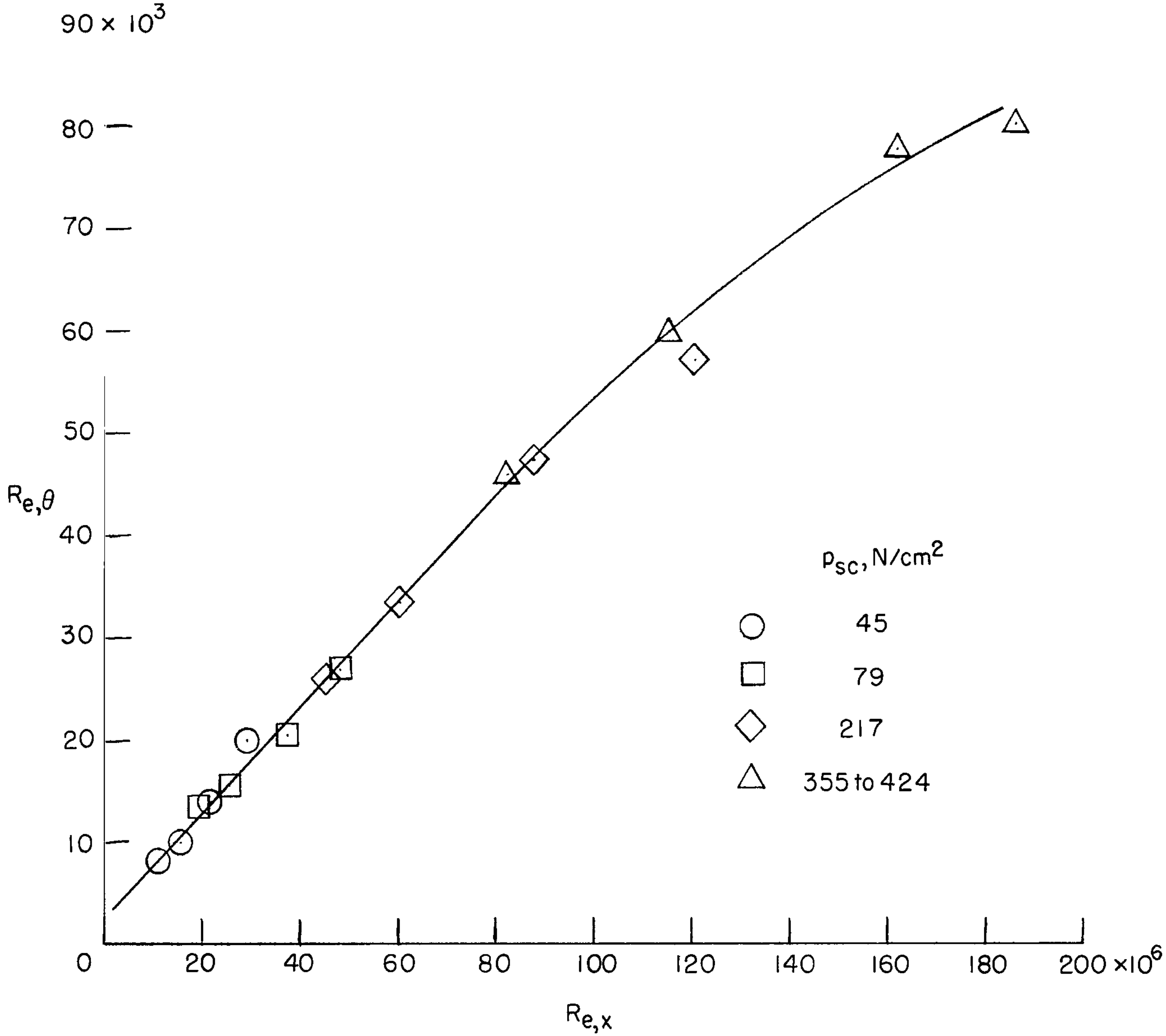

Figure 21.- Momentum-thickness Reynolds number.

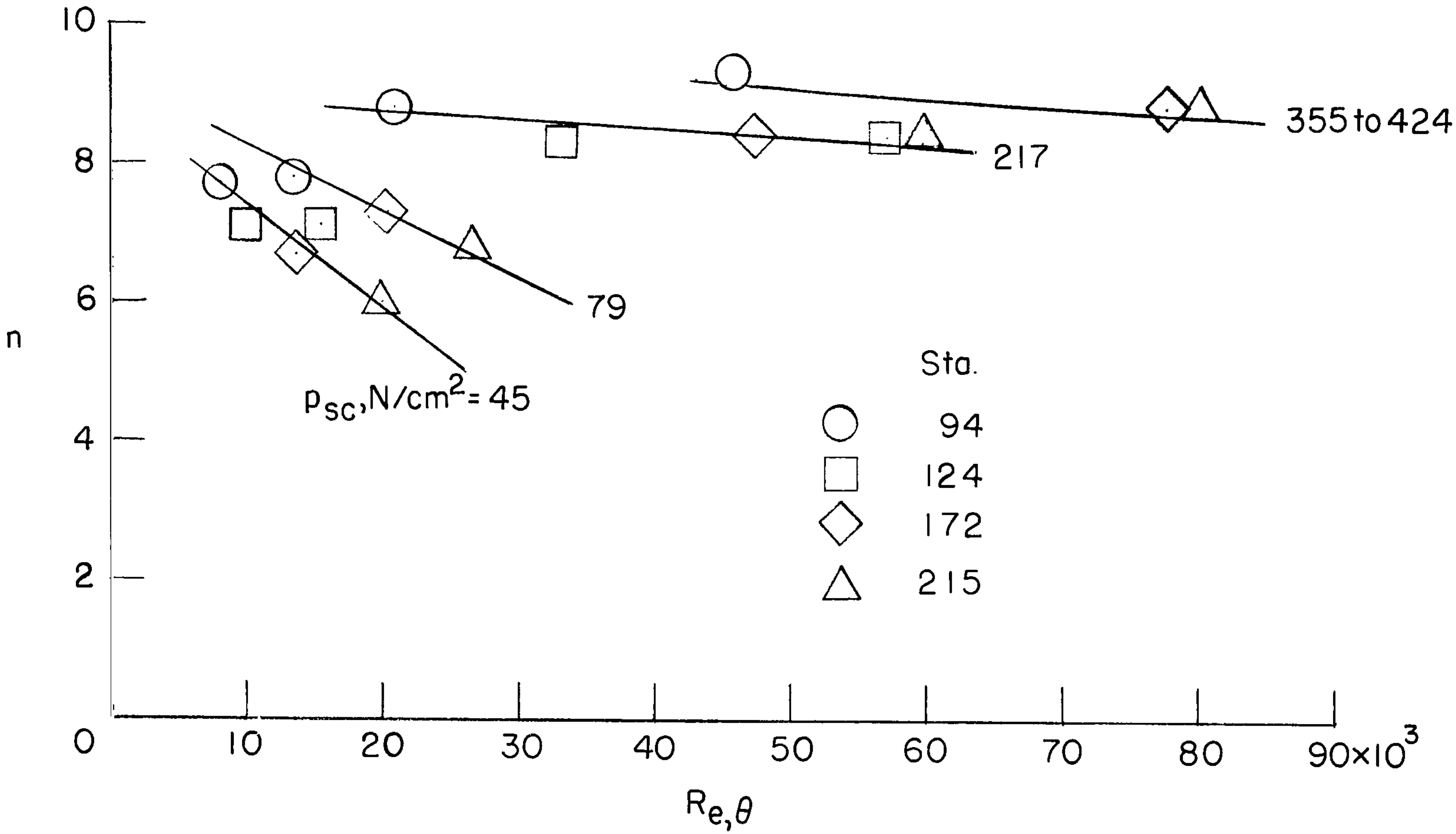

Figure 22.- Variation of n with $R_{e,\theta}$.

NASA-Langley, 1970 — 12 L-6697

NATIONAL AERONAUTICS AND SPACE ADMINISTRATION
WASHINGTON, D. C. 20546

OFFICIAL BUSINESS

FIRST CLASS MAIL

POSTAGE AND FEES PAID
TIONAL AERONAUTICS AND
SPACE ADMINISTRATION

08U 001 36 51 3DS 70033 00903
AIR FORCE WEAPONS LABORATORY /WLOL/
KIRTLAND AFB, NEW MEXICO 87117

ATT E. LOU BOWMAN, CHIEF,TECH. LIBRARY

POSTMASTER: If Undeliverable (Section 158 Postal Manual) Do Not Return

"The aeronautical and space activities of the United States shall be conducted so as to contribute . . . to the expansion of human knowledge of phenomena in the atmosphere and space. The Administration shall provide for the widest practicable and appropriate dissemination of information concerning its activities and the results thereof."

— NATIONAL AERONAUTICS AND SPACE ACT OF 1958

NASA SCIENTIFIC AND TECHNICAL PUBLICATIONS

TECHNICAL REPORTS: Scientific and technical information considered important, complete, and a lasting contribution to existing knowledge.

TECHNICAL NOTES: Information less broad in scope but nevertheless of importance as a contribution to existing knowledge.

TECHNICAL MEMORANDUMS: Information receiving limited distribution because of preliminary data, security classification, or other reasons.

CONTRACTOR REPORTS: Scientific and technical information generated under a NASA contract or grant and considered an important contribution to existing knowledge.

TECHNICAL TRANSLATIONS: Information published in a foreign language considered to merit NASA distribution in English.

SPECIAL PUBLICATIONS: Information derived from or of value to NASA activities. Publications include conference proceedings, monographs, data compilations, handbooks, sourcebooks, and special bibliographies.

TECHNOLOGY UTILIZATION PUBLICATIONS: Information on technology used by NASA that may be of particular interest in commercial and other non-aerospace applications. Publications include Tech Briefs, Technology Utilization Reports and Notes, and Technology Surveys.

Details on the availability of these publications may be obtained from:

SCIENTIFIC AND TECHNICAL INFORMATION DIVISION

NATIONAL AERONAUTICS AND SPACE ADMINISTRATION

Washington, D.C. 20546